

Copyright

by

Lindsey Nicole Jackson, M.D.

2008

**The Dissertation Committee for Lindsey Nicole Jackson, M.D., Certifies that this is
the approved version of the following dissertation:**

**PI3K/AKT ACTIVATION IS CRITICAL FOR EARLY HEPATIC
REGENERATION AFTER PARTIAL HEPATECTOMY**

Committee:

B. Mark Evers, M.D., Chair

Kathleen O'Connor, Ph.D.

Frank C. Schmalstieg, M.D., Ph.D.

Cornelis Elferink, Ph.D.

Sundararajah Thevananther, Ph.D.

Carry W. Cooper, Ph.D.

Dean, Graduate School

**PI3K/AKT ACTIVATION IS CRITICAL FOR EARLY HEPATIC
REGENERATION AFTER PARTIAL HEPATECTOMY**

by

Lindsey N. Jackson, M.D.

Dissertation

Presented to the Faculty of the Graduate School of

The University of Texas Medical Branch

in Partial Fulfillment

of the Requirements

for the Degree of

Doctor of Philosophy

The University of Texas Medical Branch

August, 2008

Dedication

To my husband, James Jackson, D.C., for the most amazing patience and support a husband could possibly offer, and for serving as “mom” to our triplets when I was working late, which has been the rule rather than the exception. To our daughters, Lexi, Jolie, and Faith Jackson, along with expected sister, Summer, who have touched our hearts and enriched our lives in ways we never imagined possible. And to my parents, Michael and Janey Herman, who instilled in me an overwhelming desire to learn, and who have always celebrated my accomplishments with unmatched fervor.

Acknowledgements

I would like to thank B. Mark Evers, M.D., for his incredible mentorship and support. His dedication to clinical work and basic science research have served as an immense source of inspiration for me over the years. I would also like to acknowledge members of Dr. Evers' laboratory, including Piotr Rychahou, M.D., Shawn D. Larson, M.D., Andy L. Chen, Ph.D., and Scott R. Silva, who offered technical advice, support, and amazing friendship. Additional thanks to Karen K. Martin for her many years of assistance with figure preparation.

PI3K/AKT ACTIVATION IS CRITICAL FOR EARLY HEPATIC REGENERATION AFTER PARTIAL HEPATECTOMY

Publication No. _____

Lindsey N. Jackson, M.D., Ph.D.

The University of Texas Medical Branch, 2008

Supervisor: B. Mark Evers

Hepatic resection is associated with rapid proliferation and regeneration of the remnant liver. Phosphatidylinositol 3-kinase (PI3K), composed of a p85 α regulatory and a p110 α catalytic subunit, participates in multiple cellular processes, including cell growth and survival; however, the role of PI3K in liver regeneration has not been clearly delineated. In these studies, I used the potent PI3K inhibitor, wortmannin, and small-interfering RNA (siRNA) targeting the p85 α and p110 α subunits to determine if total or selective PI3K inhibition would abrogate the proliferative response of the liver following resection. After partial hepatectomy in mice, there is an increase in PI3K activity; total PI3K blockade with wortmannin, and selective inhibition of p85 α or p110 α with siRNA resulted in a significant decrease in hepatocyte proliferation, especially at the earliest timepoints (ie, 48h and 72h). Fewer macrophages and Kupffer cells were present in the regenerating liver of mice treated with wortmannin or siRNA to p85 α or p110 α , as reflected by a paucity of F4/80+ cells present by

immunohistochemistry (IHC). Additionally, PI3K inhibition led to an aberrant hepatocyte architecture characterized by vacuolization, lipid deposition, and glycogen accumulation. My data demonstrate that PI3K/Akt pathway activation plays a critical role in the early regenerative response of the liver after resection; inhibition of this pathway markedly abrogates the normal hepatic regenerative response, perhaps by inhibiting macrophage infiltration and cytokine elaboration and thus hepatocyte priming for replication.

Table of Contents

List of Figures	xi
CHAPTER 1 INTRODUCTION	1
1.1 Liver regeneration.....	1
1.1.1 Anatomy and physiology of the liver.....	1
a. Historical perspectives of liver anatomy and regeneration	1
b. Gross anatomy	3
c. Microscopic anatomy	5
d. Physiology and function.....	8
1.1.2 Regulation of liver regeneration	10
a. Signals initiating regeneration.....	11
b. Early events following hepatectomy.....	12
c. Cytokine pathways and hepatocyte ‘priming’	14
d. Cell cycle progression.....	16
e. Contributions of various cell types to regeneration	18
f. Signals leading to cessation of regeneration.....	20
1.2 Activation and function of Phosphatidylinositol 3-kinase (PI3K)	21
1.2.1 Identification and characterization.....	22
1.2.2 Structure.....	23
1.2.3 Downstream signaling	25
1.2.4 Biological functions of PI3K	28
a. Cell proliferation and differentiation.....	28
b. Apoptosis and cell survival	29
c. Cell adhesion and invasion.....	30
d. Insulin signaling	31
e. Immune cell function.....	32
f. Regeneration and repair	34
1.3 Rationale for the study... ..	35
1.3.1 Background problem, central hypothesis, and specific aims	35

CHAPTER 2 INHIBITION OF PI3K WITH WORTMANNIN FOLLOWING 70% HEPATECTOMY ABROGATES LIVER REGENERATION	38
2.1 Abstract	38
2.2 Introduction	39
2.3 Materials & methods	40
2.3.1 Materials	40
2.3.2 Animals	41
2.3.3 70% hepatectomy	42
2.3.4 Experimental design	42
2.3.5 BrdU dot blot	43
2.3.6 Tissue processing, staining, and immunohistochemistry	44
2.3.7 Protein preparation & Western immunoblotting	45
2.3.8 Statistical analysis	46
2.4 Results	46
2.4.1 Expression of pAkt following hepatectomy	46
2.4.2 Total PI3K inhibition with wortmannin decreases hepatic regeneration following partial hepatectomy	47
2.4.3 Treatment with wortmannin led to altered architecture of the regenerating liver	51
2.5 Discussion	54
2.6 Conclusions	57

CHAPTER 3 SELECTIVE INHIBITION OF PI3K WITH siRNA TARGETING p85 or p110 FOLLOWING 70% HEPATECTOMY ABROGATES LIVER REGENERATION	58
3.1 Abstract	58
3.2 Introduction	59
3.3 Materials & methods	62
3.3.1 Materials	62
3.3.2 Experimental design	63
3.3.3 BrdU dot blot	64
3.3.4 Tissue processing, staining, and immunohistochemistry	65
3.3.5 Protein preparation and Western immunoblot	66

3.3.6 Tissue cytokine ELISA.....	66
3.3.7 siRNA delivery study with F4/80 colocalization.....	67
3.3.8 Statistical analysis.....	68
3.4 Results.....	68
3.4.1 siRNA directed to the p85 regulatory and p110 catalytic subunits decreases hepatic regeneration following partial hepatectomy.	68
3.4.2 Selective inhibition of the p85 α regulatory or the p110 α catalytic subunit decreases macrophage infiltration and Kupffer cell hyperplasia/hypertrophy	76
3.4.3 Selective inhibition of the p85 α regulatory or the p110 α catalytic subunit led to cellular injury after partial hepatectomy	80
3.5 Discussion.....	85
3.6 Conclusions.....	90
CHAPTER 4 SUMMARY AND FUTURE DIRECTIONS	91
4.1 Summary.....	91
4.2 Future directions	92
Bibliography	95
Vita	105

List of Figures

Fig 1.1: Lobular structure of the liver.....	6
Fig 1.2: Normal mouse liver.....	11
Fig 1.3: The contribution of remnant hepatic lobes to total mass.....	11
Fig 1.4: Chronology of key events occurring at early stages of liver regeneration after partial hepatectomy.....	14
Fig 1.5: Multistep model of liver regeneration	18
Fig 1.6: Signaling interactions between different cell types.....	20
Fig 1.7: Overview of the mechanisms of initiation of liver regeneration.....	21
Fig 1.8: Domain structure of PI3Ks types	25
Fig 1.9: Simplified activation scheme of class I PI3Ks.....	27
Fig 1.10: Signaling pathways downstream of PI3K	27
Fig 2.1: Upregulation of PI3K 12h following hepatectomy	46
Fig 2.2: Upregulation of PI3K activity following hepatectomy at 48h and 72h timepoints.....	47
Fig 2.3: PI3K inhibition leads to decreased liver regeneration.....	48
Fig 2.4: Wortmannin treatment did not have obvious side effects as evidenced by little change in body weight relative to vehicle-treated mice	49
Fig 2.5: Regenerating liver of wortmannin-treated mice demonstrated aberrant architecture.....	52
Fig 2.6: Livers of sham-operated mice treated with wortmannin did not demonstrate alterations in architecture	52
Fig 2.7: Regenerating liver of wortmannin-treated mice demonstrated aberrant glycogen deposition by PAS staining	53
Fig 2.8: Livers of sham-operated mice treated with wortmannin did not demonstrate aberrations in glycogen storage	53

Fig. 3.1: Selective inhibition of the p85 α regulatory subunit leads to decreased regeneration following liver resection	68
Fig. 3.2: Selective inhibition of the p85 α regulatory subunit leads to decreased regeneration as evidenced by decreased BrdU incorporation following liver resection	70
Fig. 3.3: Protein expression profiles following siRNA treatment	71
Fig. 3.4: Selective inhibition of the p85 α regulatory or the p110 α catalytic subunit leads to decreased regeneration following liver resection	72
Fig. 3.5: Selective inhibition of the p85 α regulatory or the p110 α catalytic subunit leads to decreased regeneration as evidenced by decreased BrdU incorporation following liver resection.....	72
Fig. 3.6: Selective inhibition of the p85 α and p110 regulatory subunit leads to decreased regeneration as evidenced by decreased BrdU incorporation following liver resection	73
Fig. 3.7: Protein expression patterns following siRNA treatment.....	74
Fig. 3.8: Treatment with p85 α and p110 siRNA following priming reaction leads to full liver regeneration.....	75
Fig. 3.9: Selective inhibition of the p85 α regulatory subunit decreases macrophage infiltration and Kupffer cell hyperplasia/ hypertrophy	76
Fig. 3.10: Inhibition of the p85 α regulatory or p110 catalytic subunit decreases macrophage infiltration and Kupffer cell hyperplasia/ hypertrophy.....	77
Fig. 3.11: Selective inhibition of the p85 α regulatory or the p110 α catalytic subunit decreases TNF- expression	78
Fig. 3.12: Selective inhibition of the p85 α regulatory or the p110 α catalytic subunit decreases IL-6 expression	79
Fig. 3.13: siRNA uptake within the liver is predominantly by Kupffer cells.....	80
Fig. 3.14: Selective inhibition of the p85 α regulatory or the p110 α catalytic subunit	

onferred a vacuolar appearance to the regenerating liver.....	82
Fig. 3.15: Selective inhibition of the p85 α regulatory or the p110 α catalytic subunit led to increased glycogen deposition within hepatocytes	82
Fig. 3.16: Selective inhibition of the p85 α regulatory or the p110 α catalytic subunit led to increased lipid deposition within hepatocytes.....	83
Fig. 3.17: Evidence of autophagy within the p85 and p110 siRNA-treated regenerating liver	84
Fig. 3.18: Large vacuoles, abundant mitochondria and accumulation of endoplasmic reticulum (ER) within a hepatocyte of p85 siRNA-treated mouse	84

CHAPTER 1

INTRODUCTION

1.1 LIVER REGENERATION

1.1.1 Anatomy and physiology of the liver

a. Historical perspectives of liver anatomy and regeneration

Our knowledge of liver anatomy dates back to approximately 2000 B.C., with early descriptions first attributed to the Babylonians in the Assyro-Babylonian era (1). Especially interesting is the apparent knowledge of the liver's ability to regenerate by the ancient Greeks, as reflected in the myth of Prometheus. Having been convicted of stealing the secret of fire from the gods, Prometheus was sentenced to having his liver eaten daily by a visiting bird of prey; the liver regenerated nightly, providing the bird with an endless food supply and Prometheus with eternal torture (2). The first known medically relevant anatomical descriptions of the liver emerged between 310 and 280 B.C. by Herophilus and Erasistratus (3). Galen (circa 130-200 B.C.) puzzled over the functions of the liver, as recorded in his treatise, *On the Usefulness of the Parts of the Body*; he stated, "Now, why is the stomach surrounded by the liver? Is it in order that the liver may warm it and it may in turn warm the food? This is indeed the very reason why it is closely clasped by the lobes of the liver, as if by fingers." (4, 5) Galen defined the liver as the most important of human organs, with the spleen and gallbladder its central subsidiaries, the three of which produced and stored three of the four humors of the body: blood, yellow bile, and black bile (4).

There was historically disagreement on the number of lobes of the liver. Ancient and medieval anatomists described five lobes, which is coincidentally the number found in dogs, which were largely studied at the time as surrogates for humans. Renaissance anatomists were increasingly unsure of the number, as an increase in human dissection revealed variations in anatomy as viewed by different dissectors. "It has five lobes, sometimes four and three, sometimes two," wrote Jacopo Berengario da Carpi at the end of the fifteenth century (6). This was later rebutted by Andres de Laguna in 1535, who wrote, "It is very rarely divided into five lobes; more frequently into four most frequently into three." (7) From 1510-1511, Leonardo da Vinci was granted permission to collaborate with a physician, Marcantonio della Torre, to prepare a theoretical work on anatomy for which da Vinci prepared 200 drawings; his work, which was not published until 1680 (161 years after his death), was the first to depict the liver (as well as other organs) without bias and in an anatomically correct fashion (8). In 1654, the English physician Francis Glisson was the first scholar to publish a book devoted exclusively to the *Anatomy of the Liver*, in which he described hepatic vascular anatomy; the fibrous capsule of Glisson bears his name (1, 9).

Earliest descriptions of liver surgery were recorded in the 18th century, with the first known partial hepatectomy attempted by Berta in 1716 to repair a liver laceration resulting from a self-inflicted stab wound; however, surgeons feared working on the organ secondary to its vascularity and propensity to bleed (1, 5). In 1874, the first known successful partial hepatectomy was performed on a 30-year-old woman by Carl A. Langenbuch; he utilized suture ligation followed by removal of the majority of the left lobe of the liver and, despite massive intraoperative bleeding, his patient made an

uneventful recovery (5). Contributions by anatomists and surgeons such as Pringle, Rex, and Cantlie to the definition of vascular planes within the liver in the late 19th century led to innovations in surgical technique allowing for improved intraoperative hemostasis, leading to refinement of human hepatectomy. On April 3, 1963, Thomas E. Starzl attempted the first human liver transplantation for a young boy suffering from biliary atresia; unfortunately, the patient died intraoperatively of massive hemorrhage. Four additional attempts that year were similarly unsuccessful. However, by 1968, Starzl reported seven successful transplantation procedures which patients had survived greater than 6 months post-operatively (3). Since that time, the development of immunosuppression regimens has drastically improved long-term survival of patients receiving liver transplants.

b. Gross anatomy

The liver is the largest solid organ whose mass, approximately 1200-1600g in the adult male, occupies the right upper quadrant of the abdomen. Largely protected by the thoracic cage, the superior surface is convex and molded to the diaphragm, while the inferior surface is concave and encompasses the gallbladder and biliary tree. While historically, the liver was divided into two halves, left and right, by the obvious external landmark of the falciform ligament, the complexity of its vascular anatomy was later realized by anatomists and surgeons, leading to the designation of its segmental anatomy which is applied today. Traditional gross anatomy divided the liver into four lobes; left and right, as noted above, as delineated by the falciform ligament, with an additional two smaller lobes, the caudate and quadrate lobes, which are located on its posterior surface. The lobar anatomy of the liver is now defined by branches of the portal and hepatic veins,

such that a plane running from the gallbladder to the left side of the inferior vena cava (IVC; known as the portal fissure) divides the liver into right and left lobes; further subsegmentalization of the liver into eight segments (I-VIII) is based upon the blood supply of portal triads, composed of portal vein, hepatic artery, and bile duct. The portal vein, which carries largely deoxygenated, post-capillary blood from the spleen, pancreas, stomach, small intestine, and portion of the large intestine, supplies about 75% of the hepatic blood flow and approximately 50-70% of the liver's oxygenation, while the hepatic artery supplies about 25% of hepatic blood flow and 30-50% of its oxygen. Three major hepatic veins then carry deoxygenated blood directly into the IVC(1).

The biliary system, responsible for collecting, storing, and concentrating bile in the gallbladder for later temporal release in relation to meals to aid digestion, is closely associated with the liver. Intrahepatic bile ducts meet to form the main right and left hepatic ducts; the left hepatic duct drains segments II-IV, which constitute the left lobe of the liver, while the right hepatic duct drains the right lobe of the liver, or segments V-VIII. The caudate lobe, segment I, drains into both right and left systems. The two hepatic ducts then join to form the common hepatic duct, which branches to form the cystic duct connecting to the gallbladder, which is firmly attached to the inferior aspect of the liver by fibroconnective tissue band known as the cystic plate. Distal to the site of confluence of the cystic duct and the common hepatic ducts, the common bile duct is formed. Bile formed by the liver is preferentially drained into the gallbladder during periods of fasting for storage and concentration; this is accomplished by contraction of the sphincter of Oddi located distally at the junction of the biliary tree and duodenum,

leading to preferential proximal collection of bile and prevention of reflux of effluent into the biliary tree(1).

c. Microscopic anatomy

The functional microscopic unit of the liver is referred to as the acinus or lobule. The lobule is roughly polygonal in shape, with a terminal hepatic venule located centrally surrounded by four to six terminal portal triads located at its peripheral margins. Each portal triad is composed of microscopic branches of three vessels: the portal vein (bringing post-capillary blood from the intestine), the hepatic artery (bringing highly oxygenated blood), and a bile ductule (carrying bile away from the lobule) (1, 2). Between the portal triads and central venule, hepatocytes are arranged in strands, one cell thick, flanked on each side by blood-filled sinusoids lined by a leaky, fenestrated endothelium. The direction of blood flow is thus from the portal triad, through the sinusoids, to the terminal hepatic venule, to be carried out of the liver. Bile, on the other hand, is formed within the hepatocytes and empties into structures called terminal canaliculi, which ultimately coalesce into bile ductules which carry the bile to the portal triad for clearance (ie, counter to the flow of blood) (Fig. 1.1).

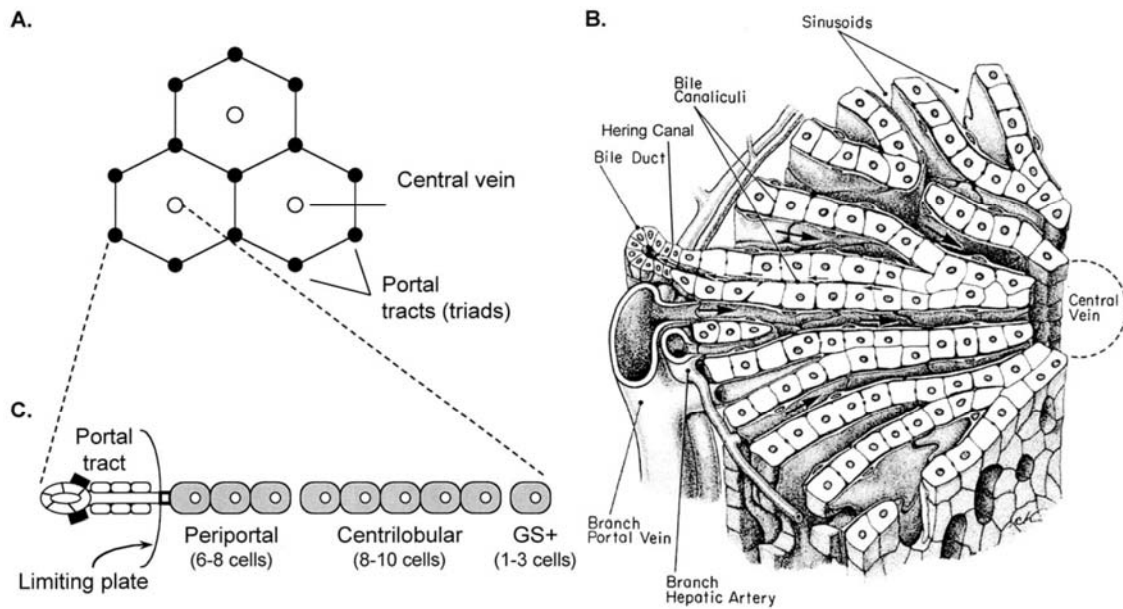


Fig. 1.1 Lobular structure of the liver. Three lobules are shown as hexagonal structures demarcated by portal tracts or triads in the periphery and containing a central vein at the center (A). The histologic structure of the lobule is shown in (B). From Fausto *et al* (2003) (10), used with permission..

Within the hepatic lobule, there are three zones (1-3) varying in exposure to nutrients and oxygenated blood, leading to variations in cellular enzymatic composition. Zone 1, known as the periportal zone, is exposed to an environment which is most rich in nutrients and oxygen, while zones 2 (intermediate) and 3 (perivenular) are exposed to environments increasingly less invested with such nutrients. Therefore, the cells of these zones differ in composition and enzymatic expression and respond differently to exposure to toxins or hypoxia. When exposed the liver becomes hypoxic, for example, during periods of profound hypotension, a phenomenon known as centrilobular necrosis may result, as zone 3 (most centrally located) is the most susceptible to decreases in oxygen delivery (1).

Sinusoidal endothelial cells account for approximately 15-20% of the total number of cells within the liver. They are separated from hepatocytes by the space of

Disse, an extravascular, fluid-filled compartment. Endothelial cells of the liver are unique in their lack of intercellular junctions and basement membrane, leading to the creation of large fenestrae between cells. This allows for maximal contact of hepatocytes with the space of Disse and blood from the sinusoidal space, creating a system promoting free bidirectional movement of both low- and high-molecular weight substances into and out of cells, thus maximizing the liver's filtration capabilities.

Several other cell types are found within the liver. Stellate cells, known as *Ito cells* or *lipocytes*, are located within the space of Disse. These cells normally have a high lipid content and, as their name implies, they express dendritic processes which encompass endothelial cells and contact hepatocytic microvilli. Their major functions include storage of vitamin A and synthesis of extracellular matrix such as collagen. As discussed later, they are activated in disease states and also play an important role in liver regeneration following hepatectomy; they also contribute to the development and progression of hepatic fibrosis. Kupffer cells are specialized phagocytic cells of the macrophage/monocyte cell line. They are irregular stellate-shaped cells lining the sinusoids and interdigitating with endothelial cells. They express histocompatibility complex type II antigens and play a major role in the trapping of foreign substances or organisms; additionally, they play a major role in the hepatic injury response and liver regeneration, as discussed later. Other cells present within the liver include lymphoid cells such as natural killer cells and CD4 and CD8 T cells, which provide the liver with innate immunity (1).

d. Physiology and function

The relatively strategic location of the liver in relationship to the food supply allows it to function as a central regulator of nutritional homeostasis for the body. In addition, the liver plays extremely important roles in the detoxification of potentially hazardous ingested compounds, the storage of vitamins and minerals, the secretion of metabolic breakdown products, and the production of proteins central to coagulation and immunodefense, among others.

The liver is considered the center of carbohydrate metabolism as it is the major regulator of glucose storage and distribution. While both liver and muscle are capable of storing glucose in the form of glycogen, only the liver is able to process glycogen to glucose to provide systemic homeostasis. Following a meal, carbohydrate reaching the liver is converted to its storage form of glycogen, while excess carbohydrate is converted into fatty acids for storage in adipose tissue. Between meals when there is no ingestion of new carbohydrate, the liver becomes the primary source of glucose provision as it breaks down glycogen, releasing glucose into the systemic circulation. After approximately 48 hours of fasting, the liver depletes its supply of glycogen, and shifts from glycogen breakdown to the process of gluconeogenesis, utilizing glycerol from fatty acid and amino acids derived from muscle breakdown to generate glucose; an additional pathway, known as the Cori cycle, utilizes lactate produced largely from muscle during anaerobic metabolism to manufacture glucose molecules. During a prolonged fast, the liver metabolizes fatty acids from adipose tissue to ketone bodies, which become the

primary fuel source for the body. These various processes are tightly hormonally regulated by insulin, glucagon, and catecholamines (1).

In addition to its role in carbohydrate metabolism, the liver synthesizes and catabolizes proteins. Ingested protein is broken down by the liver into amino acids which are utilized by the liver as a fuel source or circulated to the periphery as building blocks for various proteins. When catabolized for energy, the nitrogenous waste byproducts of amino acid degradation are converted by the liver to urea, which is then excreted largely in the urine. The liver also serves to produce proteins involved in such critical functions as coagulation, iron binding, transport, and protease inhibition. Examples include albumin, the predominant serum-binding protein; coagulation factors such as II, VII, IX, and X; α_1 -antitrypsin; and ceruloplasmin, to name a few.

The liver also serves an important role in the metabolism and storage of both fat-soluble vitamins (vitamins A, D, E, and K) and water-soluble vitamins (thiamin, riboflavin, B6, B12, folate, biotin, and pantothenic acid). These products are processed within the liver for distribution to the body, where they act as critical cofactors in enzymatic processes, and are also utilized within the liver, as in the case of vitamin K, which acts as a critical cofactor in the post-translational modification of several hepatically synthesized coagulation factors.

Bilirubin, a compound produced through the breakdown of heme, is cleared by the liver in the form of bile. Circulating bilirubin remains bound to albumin, protecting cells from its potentially toxic effects. The complex enters hepatic sinusoids, where it passes into the space of Disse through endothelial fenestrations, where it is then dissociated. Free bilirubin is taken up by the hepatocyte, conjugated to glucuronic acid,

and secreted into canalicular bile. This is carried to the gallbladder and into the intestine with a meal, where it is eventually deconjugated by intestinal bacteria into urobilinogens. These products are further processed and eventually excreted in the urine or stool.

Lastly, the liver is the central detoxifier of drugs and toxins. The vast majority of ingested medications is processed by the liver into active intermediates, or is degraded by the liver for eventual excretion. The liver is also the first organ to process ingested environmental toxins or organisms, and acts to protect the rest of the body from their potentially harmful effects through amazingly complex and numerous reaction pathways.

1.1.2 Regulation of liver regeneration

The ability of the liver to regenerate has been a subject of curiosity since ancient times, as previously mentioned. However, given its central role in many important processes, such as nutritional homeostasis, detoxification of drugs and poisons, regulation of blood clotting, and clearance of by-products of metabolism such as bilirubin and urea, liver regeneration presumably evolved to protect humans and animals from the potentially catastrophic result of liver loss due to trauma, infection, or intoxication. In both rodents and humans, partial surgical resection of the liver, known as partial hepatectomy, results in the compensatory hypertrophy and hyperplasia of the remaining lobes of the liver to replace the loss of functional mass. In a mouse model of 70% hepatectomy, original liver mass is restored approximately 7-10 days following resection with a peak in DNA synthesis at approximately 42h, while in humans following lobectomy, restoration of mass is complete in approximately 3 months, with a peak in DNA synthesis at 7-10 days (11-14). In rodents, the cell type responsible for this

proliferation is almost exclusively hepatocytes; in humans, a two-tier system composed of hepatocytes and progenitor (stem) cells contribute to the gain in mass (11, 13). A complex network of signaling pathways leads to successful liver regeneration: a cytokine pathway, responsible for hepatocyte priming; a growth factor pathway, responsible for cell cycle progression; and poorly understood pathways linking metabolic signals with DNA replication (13). The remainder of this section will address the regeneration of the rat liver, as most experimental data on the regulation of liver regeneration centers on this model.

a. Signals initiating regeneration

During partial hepatectomy in the mouse or rat, three liver lobes are surgically removed without disruption of the remaining lobes; this results not in regeneration of those lobes removed, but a compensatory hypertrophy and hyperplasia of the remaining lobes to restore the liver's original mass and functional capacity (Fig. 1.2, 1.3). Although there was no structural damage to

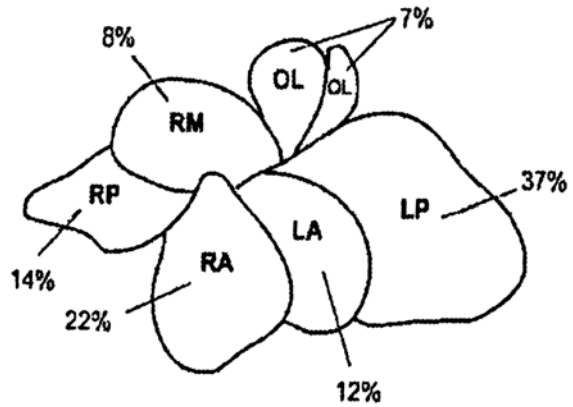


Fig. 1.2 Normal mouse liver consisting of seven lobes with contribution of each lobe to the total hepatic mass. LP, left posterior; LA, left anterior; RA, right anterior; RP, right posterior; RM, right middle; and two OL, omental lobes. From Nikfarjam *et al* (2004) (15), used with permission.

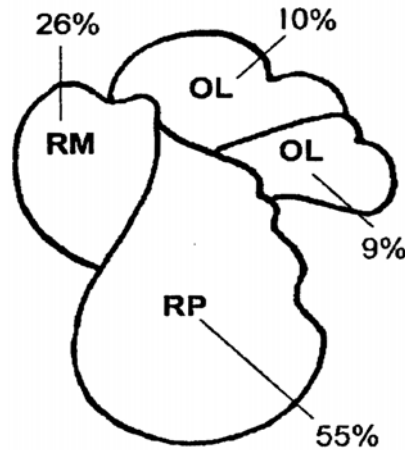


Fig. 1.3 The contribution of remnant hepatic lobes to total mass 21 days following 70% hepatectomy. From Nikfarjam *et al* (2004) (15), used with permission.

the remaining tissue, there are considerable immediate changes in hepatic blood flow. It is now known that following resection, while the portal vein contribution to blood supply per unit of tissue triples, blood supply via the hepatic artery per unit tissue remains constant (16). This is due to the fact that while hepatic arterial blood flow can be easily regulated in response to alterations in hemodynamic pressure, venous outflow from the pancreas, spleen, and intestine must remain constant, leading to the need of this flow to traverse a capillary bed whose total surface area has been immediately reduced by more than 2/3. The net result is a significant decrease in oxygen partial pressure of hepatic blood following hepatectomy, coupled with a tripling of availability of growth factors and cytokines derived by pancreas and intestine. One recent study found that if the pressure of the portal vein is held constant following hepatectomy, there is deficient activation of hepatocyte growth factor (HGF) (17), supporting a central role for hemodynamic changes in the early regenerative response. While these hemodynamic events have only recently been described and remain poorly understood, it is now generally accepted that these changes trigger the subsequent activation of signaling pathways described below.

b. Early events following hepatectomy

Liver resection leads to the rapid induction of more than 100 genes that are not expressed in the quiescent liver (16, 18, 19). One of the earliest observed changes is the increased activation of urokinase plasminogen activator (uPA) throughout the entire remnant liver within 5 minutes of resection (16, 20); it has been demonstrated that mechanical stress resulting from turbulent blood flow, as described above, triggers the release of uPA from endothelial cells (21). Urokinase is a known stimulant of matrix

remodeling, leading to release of locally bound growth factors with signaling capabilities, the most notable of which is HGF, which shares significant sequence homology with plasminogen, the classically recognized target of uPA (20, 22, 23). Release of HGF results in activation of cMet within 30-60 minutes following resection. Other substances activated or released locally immediately following surgery include matrix metalloproteinase 9 (MMP9), hyaluronic acid, and TGF- β 1. Levels of IGFBP1, a plasma protein that binds insulin-like growth factor I (IGF-1) and IGF-II, increases to approximately 100-fold of original levels within 30 minutes of resection (2). Signaling through the epidermal growth factor receptor (EGFR) increases, likely a result of a significantly increased intestinally-derived EGF-to-hepatocyte ratio induced by postsurgical hemodynamic changes (16). Norepinephrine is released following surgery, enhancing the local effects of HGF and EGF receptor activation.

Within 30 minutes of surgical resection, a large number of genes, termed immediate early genes, are activated; these include the protooncogenes c-fos, c-jun, and c-myc, and the transcription factors NF κ B, STAT3, AP-1, and CEBP β (13). While selective inhibition of any one of these signaling molecules does not significantly impede ultimate liver regeneration, leading to some confusion as to the precise role each plays in global liver regeneration, it is obvious that this reflects the existence of multiple redundant pathways which compensate for others' loss (16). Analysis of this complicated gene activation network reveals that the process is dependent upon concurrent activity of both 'priming' events linked to cytokine stimulation in addition to growth factor signaling pathway activation, although growth factor signaling is

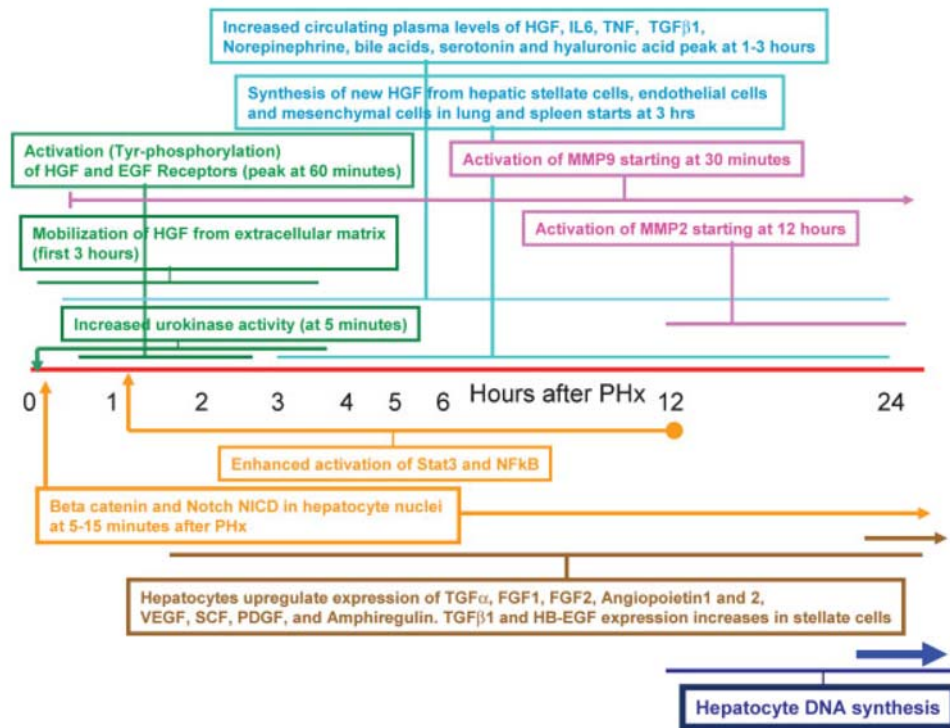


Fig. 1.4 Chronology of key events occurring at the early stages of liver regeneration after partial hepatectomy. Events within similarly colored boxes belong in the same category. The associated horizontal lines for each box delineate the beginning and the duration of each signal. From Michalopoulos (2007) (16), used with permission.

classically thought to occur following an initial priming reaction, as described below (13, 16) (Fig. 1.4).

c. Cytokine pathways and hepatocyte ‘priming’

Cytokines, including tumor necrosis factor-alpha (TNF-α) and interleukin 6 (IL-6), are elaborated by non-parenchymal cells such as Kupffer cells (KCs) and sinusoidal epithelial cells following hepatectomy (13, 24). They are responsible for the initial priming of hepatocytes, with the transition of quiescent hepatocytes from the G₀ to G₁ stage of the cell cycle. In the absence of cytokines, hepatocytes are minimally responsive to growth factor stimulation, illustrating the importance of this initial priming reaction (13).

Interestingly, TNF- α , production of which is stimulated by endotoxin produced by intestinal bacteria following hepatectomy, can have differential effects on cell regulation depending on the activation status of NF κ B; under conditions favoring NF κ B activation, TNF- α enhances concurrent growth factor signaling, while in the absence of NF κ B activation, TNF- α elicits an apoptotic reaction (25, 26). The importance of TNF- α signaling to liver regeneration has been illustrated by knockout experiments and via administration of TNF antibody; while the livers of mice with defective or absent TNF- α signaling eventually regenerate, the process is significantly impeded, with the restoration of mass occurring far later (16, 27-30). In recent studies, treatment with TNF- α antibodies prior to hepatectomy resulted in decreased DNA synthesis and decreases in Jun kinase, c-jun mRNA, and nuclear AP1 activity, while treatment with compounds known to increase TNF- α release from Kupffer cells enhanced induction of IL-6, c-jun, CEBP β , and AP1 (29, 31, 32). Mice with a deficiency in TNF- α receptor type I fail to demonstrate expected increases in STAT3 and NF κ B; these defects were corrected following administration of IL-6, suggesting that TNF- α also plays an important role in the regulation of IL-6, and that these compounds act synergistically to prime hepatocytes for replication.

Similarly, IL-6, elaborated by hepatic macrophages in response to TNF- α signaling, is associated with hepatocyte priming following resection. IL-6 activation of its soluble receptor and gp130 leads to STAT3 activation and downstream signaling central to stimulation of acute phase protein synthesis. Previous reports have found that deficiency of IL-6 leads to decreased activation of STAT3, AP1, Myc, and cyclin D1, with a resultant delay in liver regeneration, while overexpression leads to the

development of periportal hepatocytic hyperplasia (16, 33-35). While neither TNF- α nor IL-6 have direct mitogenic effects on hepatocytes (despite a known direct mitogenic effect of IL-6 on bile duct epithelial cells), both are viewed as optimizing the processes of early liver regeneration and preparing hepatocytes for cell cycle entry following further growth factor signaling.

d. Cell cycle progression

Upon priming of hepatocytes by cytokine pathways as described above, growth factor stimulation leads to G₁ to S phase transition and cell cycle progression. Three factors of major importance are hepatocyte growth factor (HGF), produced by nonparenchymal cells of the liver (13); transforming growth factor- α (TGF- α), produced by hepatocytes (13, 14); and epidermal growth factor (EGF), the major source of which is the salivary glands in rodents and the Brunner's glands of the duodenum in humans (14). HGF, TGF- α , and EGF signaling occurs through receptor tyrosine kinases which, in the activated state, associate with cytosolic proteins rich in Src-homologies (SH-2 and SH-3), such as phosphatidylinositol 3-kinase (PI3K) (14, 36). Downstream signaling leads to the activation of mitogen activated protein kinase (MAPK) cascades, ultimately leading to the regulation of cell cycle and growth (36).

HGF is sequestered within the liver matrix in large quantities relative to other organs (16, 37). Its receptor, cMet, is expressed on most epithelial and endothelial cells and neurons; in addition to its mitogenic and motogenic effects, Met also binds the apoptotic receptor Fas and prevents it trimerization, leading to an anti-apoptotic effect (16, 38). HGF is known to induce the clonal expansion of hepatocytes in culture (39). Following liver resection, plasma levels of HGF increase 10- to 20-fold, and

interestingly, HGF injection into mice that have not undergone hepatectomy results in hepatocyte proliferation and liver hypertrophy (40, 41). Genetic elimination of cMet from the liver or RNA interference following liver resection results in significantly diminished regeneration and blockade of the cell cycle. Therefore, evidence supporting the role of HGF as the major initiator of liver regeneration is supported by the fact that it can act as a direct mitogen for hepatocytes, activates its receptor within the first several hours following liver resection, in its absence, leads to a significantly retarded regenerative response, and can cause massive hepatic enlargement by administration to rodents with intact liver. HGF has been termed an “irreplaceable contributor” to liver regeneration (16).

Both EGF and TGF α signal through EGF receptors, and both are known to activate phosphorylation cascades that culminate in DNA replication (13). Similarly, both are mitogenic to hepatocytes in culture (2). Expression of TGF α mRNA, which is normally very low in the quiescent liver, increases within 2-3 hours, rising to a peak between 12 and 24 hours, and remains elevated for approximately 48 hours following resection, although overall protein levels within the liver increase only twofold (2, 13). While overexpression of TGF α in hepatocytes leads to persistently increased DNA synthesis and eventual tumor formation, deletion of the TGF α gene does not affect ultimate liver regeneration, likely due to redundancy in signaling generated by EGF binding (42). Following 70% liver resection, the amount of EGF available per unit of tissue immediately increases 3-fold due to hemodynamic changes, and catecholamines, such as norepinephrine, are known to further stimulate production of EGF from Brunner’s glands of the human duodenum. All known EGFR ligands are strong mitogens

for hepatocytes in culture, and like HGF, EGF given to intact animals leads to hepatocyte proliferation (16, 43). Although recent data suggests that EGF links the priming and progression phases of liver regeneration (44), the capacity of liver to regenerate following elimination of EGF or EGFR has not yet been tested (16). Therefore, while much is known about the cytokines

responsible for hepatocyte priming, and the growth factors responsible for stimulating cell cycle progression, the complex set of reactions responsible for linking these signaling pathways has yet to be delineated. A summary of the multistep model of regeneration is presented in figure 1.5.

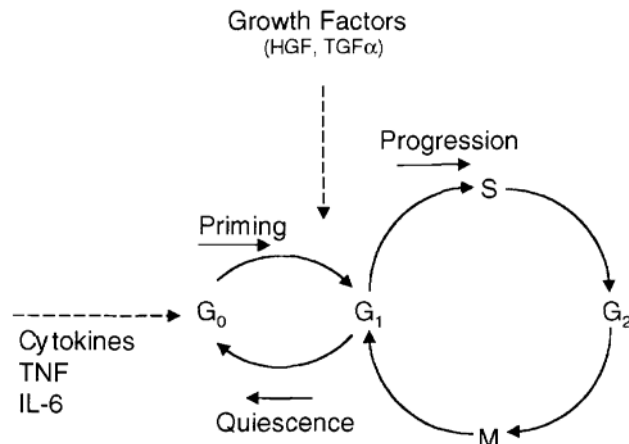


Fig. 1.5 Multistep model of liver regeneration. From Fausto (2000) (45), used with permission.

e. Contributions of various cell types to regeneration

A unique feature of the liver as an organ is the fact that differentiated cells, i.e. hepatocytes, constitute its first line of response following surgical resection, while hepatic “stem” cells, or oval cells, function only as a reserve (13). However, hepatocytes rely upon secondary cell types present within the hepatic parenchyma for stimulation and subsequent division. Circulating macrophages and resident KCs, along with the cytokines they produce, play a critical role in hepatic regeneration following resection. One elegant study utilized a murine model of bone marrow transplantation coupled with 70% hepatectomy to determine the contribution of bone-marrow derived cells to liver

regeneration (46). They found that complete replacement of IL-6^{+/+} bone marrow into IL-6^{-/-} irradiated mice restores regeneration after partial hepatectomy. However, complete replacement of IL-6^{-/-} bone marrow into IL-6^{+/+} irradiated mice significantly inhibits liver regeneration; regeneration can be restored in this case by administration of IL-6. Similarly, experiments utilizing GFP-labeled bone marrow cells have demonstrated an important role for the bone marrow in repopulation of the resected liver, where a majority of cells (70%) commit to an endothelial cell lineage and others (28%) to a Kupffer cell lineage (47). Other studies have used models of KC depletion (liposome-encapsulated dichloromethylene-diphosphonate (Cl₂MDP), gadolinium chloride (GdCl₃), or pentoxifylline) to demonstrate that a >90% reduction in KCs leads to significantly impaired liver regeneration following 70% hepatectomy in mice or rats; this response is attributed to a significant decrease in TNF α production (48-50). Additionally, utilizing the GdCl₃ model of KC depletion, another group confirmed that KC depletion significantly decreases liver regeneration and abolishes hepatic expression of IL-6, HGF, and TNF- α (51); similarly, the administration of TNF- α antibody to mice following hepatectomy significantly inhibits regeneration (27). Given the known importance of IL-6 and TNF- α to the priming of quiescent hepatocytes to enter the cell cycle, it is clear that macrophages and KC are central to the early regenerative response of the liver, and that the bone marrow does contribute, in part, to the increase in KC number following hepatectomy. A summary of the contributions of various cell types to liver regeneration is presented in figure 1.6.

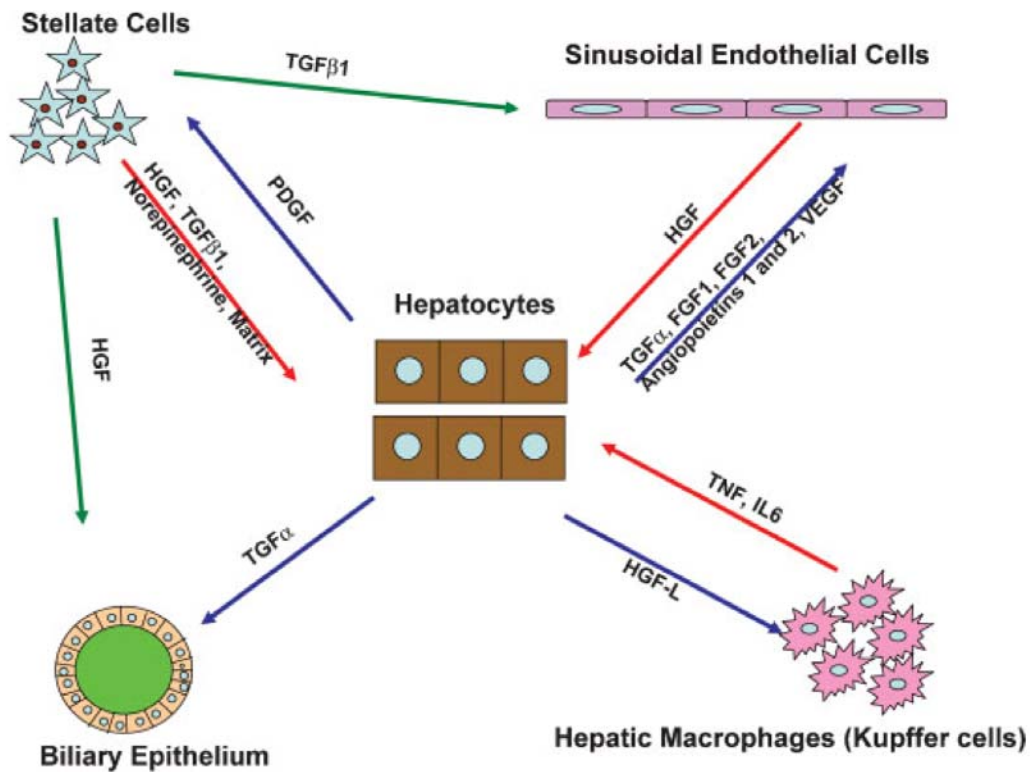


Fig. 1.6. Signaling interactions between different hepatic cell types during liver regeneration. From Michalopoulos (2007) (16), used with permission.

f. Signals leading to cessation of regeneration

It is amazing that following resection, the mass of the fully-regenerated remnant lobes becomes almost identical to the original pre-operative liver weight, although this process is poorly understood. There is evidence that the mass of the regenerating liver might “overshoot” its original mass, such that a small wave of hepatocytic apoptosis occurs at the end of regeneration (16). Additionally, livers from smaller animals transplanted into larger animals increase in size, while conversely, livers from larger animals transplanted into smaller animals decrease in size (52), raising the possibility of the existence of a “hepatostat” control system that ensures liver weight is appropriate to

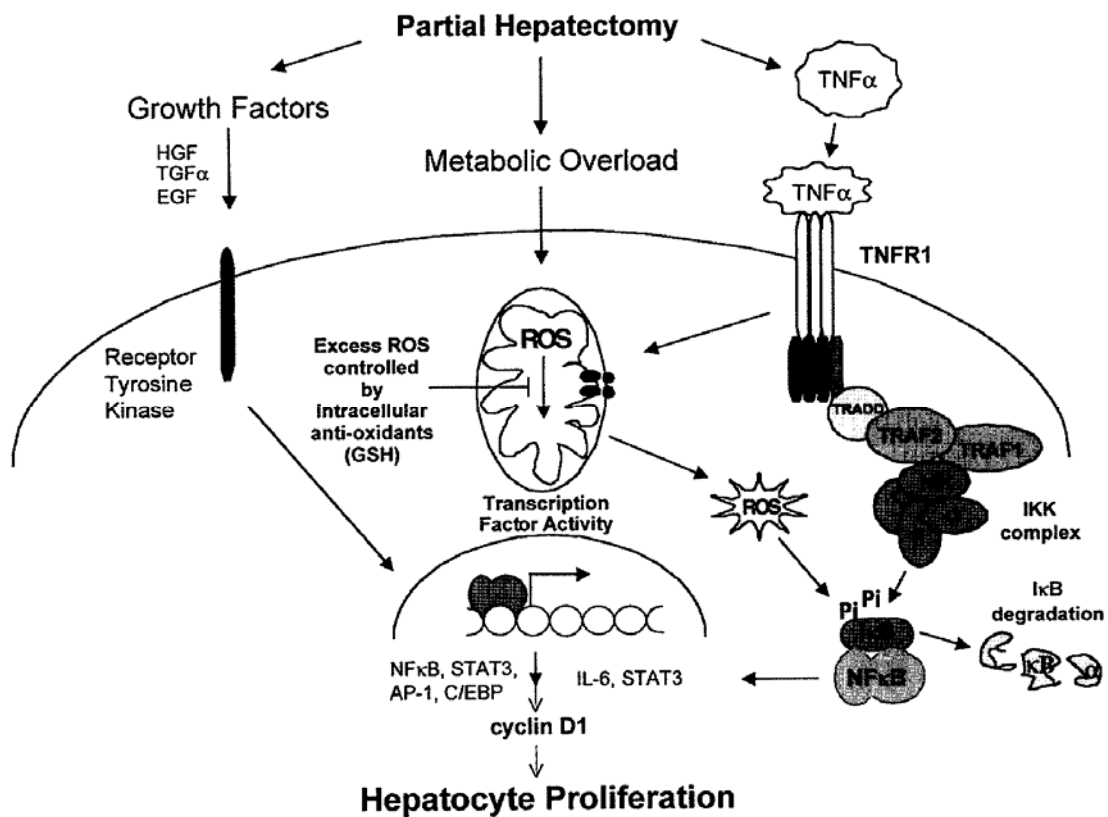


Fig. 1.7 Overview of the mechanisms of initiation of liver regeneration. From Fausto (2000) (45), used with permission.

perform its homeostatic functions (16). Michalopoulos has speculated that the reassembly of the extracellular matrix and the capillary network provides the signaling that aborts the regenerative process, as newly synthesized matrix would again bind and sequester the signaling proteins HGF and TGF β 1 (16). Fausto has suggested that a balance in the elaboration and clearance of reactive oxygen species (ROS) provides signaling that could regulate the ultimate extent of regeneration (Fig. 1.7) (45). However, more research is needed to understand the precise mechanisms switching “off” the regenerative response.

1.2 ACTIVATION AND FUNCTION OF PHOSPHATIDYLINOSITOL 3-KINASE (PI3K)

1.2.1 Identification and characterization

In the mid-1980's, a protein with phosphoinositide kinase activity was discovered that associated with polyoma middle T antigen and anti-phosphotyrosine immunoprecipitates from PDGF-stimulated fibroblasts (53, 54). This protein was found to phosphorylate the D3-hydroxyl group of the inositol moiety of phosphoinositides, resulting in the generation of a previously unknown class of lipids (55, 56). The subsequent observation that increased levels of these 3-phosphorylated phosphoinositides were found in transformed cells implied an involvement of PI3K in oncogenesis (57), and this finding was further supported by the finding that mutants of polyoma middle T, unable to associate with PI3K, failed to transform cells (58). The cloning of two PI3K regulatory subunit isoforms, p85 α and p85 β , occurred in 1991, followed by the identification of p85-associated catalytic subunit isoforms p110 α and p110 β in 1992 (59-61). Since that time, many PI3Ks have been identified and isolated from eukaryotes such as yeast, flies, mold, plants, and mammals; further detail about sequence data and substrate specificity have allowed for the subsequent stratification of PI3Ks into three classes (53). These include class I PI3Ks, heterodimers of approximately 200 kDa, composed of a 50-100 kDa regulatory and 110-120 kDa catalytic subunit, which once activated, catalyze the phosphorylation of PtdIns, PtdIns(4)P, and PtdIns(4,5)P₂ (53). Activation of class I PI3Ks is controlled via receptors with intrinsic protein tyrosine kinase activity, coupled to src-like protein tyrosine kinases, or via G protein linked

receptors (53). Class II PI3Ks, whose substrate specificity includes only PtdIns and PtdIns(4)P, are 170-210 kDa proteins with an additional C-terminal C2 homology domain; the specific signaling functions of this class remain poorly elucidated. Class III PI3Ks, homologues of the *S. cerevisiae* vacuolar protein sorting mutant (Vps34p), phosphorylate exclusively PtdIns and act as major regulators controlling the passage of proteins and membranes through endosomal and lysosomal compartments (53, 62). The remainder of this section will concentrate on the class I PI3Ks.

1.2.2 Structure

Activation of PI3K by ligands involves its translocation to the plasma membrane so as to gain access to lipid substrates. Class I PI3Ks can be divided into two subclasses based upon the adaptor proteins utilized in this process (53). Those able to associate with p85 are directed to phosphorylated tyrosine motifs (class IA), while class IB PI3K, consisting of only one enzyme, PI3K γ , is activated by G-protein coupled receptors (63).

The regulatory subunits of class IA enzymes, collectively referred to as p85, are encoded by three genes in humans--PIK3R1, PIK3R2, and PIK3R3 (63). PIK3R1 encodes p85 α , p55 α , and p50 α via alternative splicing, while PIK3R2 and PIK3R3 encode only one product, p85 β and p55 γ , respectively (63). While p85 α and p85 β are relatively ubiquitous, expressed by most cells of the body, the other isoforms are expressed in only a limited subset of cell types (53, 63). Human cells also express three genes encoding the catalytic subunits of class IA enzymes, PIK3CA, PIK3CB, and PIK3CD, producing the polypeptides p110 α , p110 β , and p110 δ . While p110 α and p110 β are again relatively ubiquitous, p110 δ is expressed primarily in leukocytes.

The p85 polypeptides consist of five major domains; these include an N-terminal SH3 domain, a Rho GTPase-activating protein (GAP) domain, and an N-terminal and C-terminal SH2 domain (nSH2 and cSH2, respectively) separated by an iSH2 domain responsible for binding to the catalytic subunit p110. The p110 subunits also consist of five domains, including an N-terminal adaptor binding domain (ABD) that binds the regulatory p85 polypeptides, a Ras binding domain (RBD), a C2 domain that likely functions to bind cellular membranes, a helical domain of unknown significance, and a kinase catalytic domain. In the quiescent state, the p85 regulatory subunits bind to and inhibit the p110 catalytic subunits; following stimulation, the cSH2 and nSH2 domains bind phosphorylated tyrosines of activated receptors and adaptor proteins, leading to activation of the p110 catalytic subunits, although the heterodimeric state persists during this process (63).

Class IB PI3K consists of only one enzyme, PI3K γ , which interacts with adaptor subunits called p101 and p84/87, but does not need to interact with a regulatory subunit to be enzymatically activated. Instead, it is directly activated by G-protein coupled receptors. The catalytic subunit, p110, is encoded by PIK3CG and expressed only in leukocytes and a small number of other cell types (63). A summary of the domain structures of Class IA and IB PI3Ks are presented in figure 1.8.

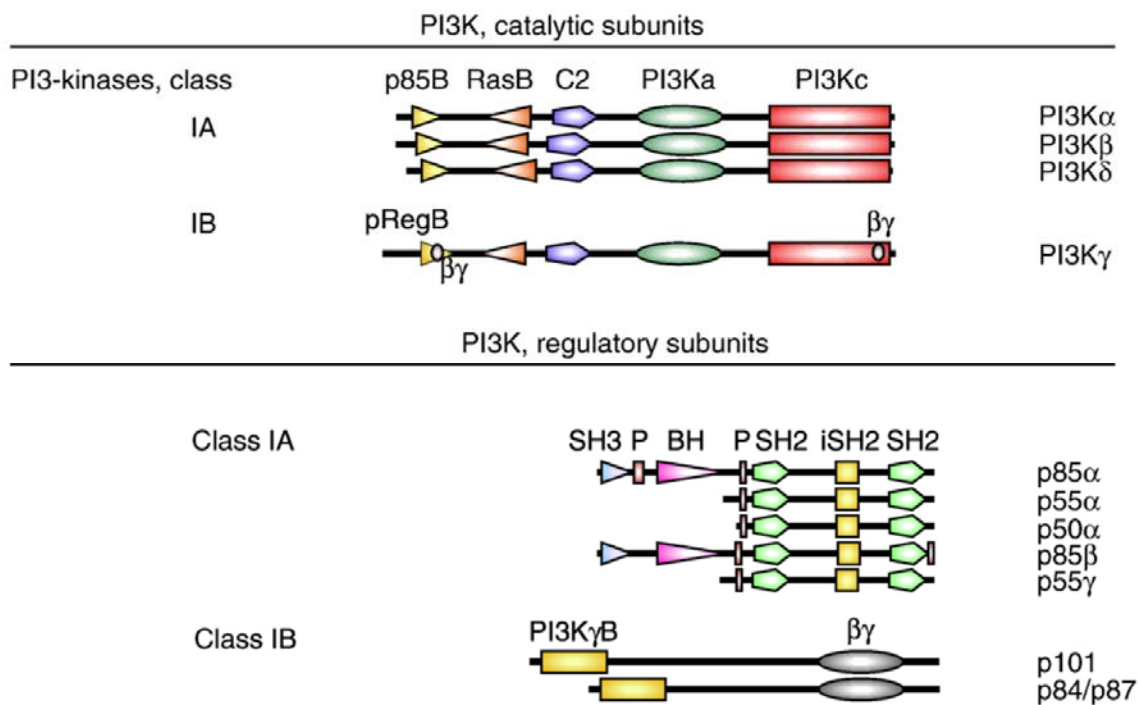


Fig. 1.8 Domain structure of PI3Ks. From Marone *et al* (2008) (64), used with permission.

1.2.3 Downstream signaling

PI3Ks are ubiquitous heterodimeric protein kinases involved in signal transduction through receptor tyrosine kinases or G-protein-coupled receptors as previously described in response to a wide variety of different stimuli including growth factors, inflammatory mediators, hormones, neurotransmitters, immunoglobulins, and antigens. Known PI3K receptor ligands include TNF- α (65, 66), IL-6 (67), HGF (68), EGF (14, 69), and TGF- α (14), among others. Class IA PI3K, discussed in more detail above, is composed of a regulatory p85 (α or β) and a catalytic p110 (α , β , or γ) subunit (69-71). When its receptor is activated by growth factors or cytokines, PI3K catalyzes the production of phosphatidylinositol 4-phosphate and phosphatidylinositol-3,4,5-

triphosphate, yielding PIP₂ and PIP₃. A simplified activation scheme of class I PI3Ks is presented in figure 1.9. The production of PIP₃ leads to the recruitment of a subset of signal proteins with pleckstrin homology (PH) domains to the plasma membrane, ultimately leading to their phosphorylation (70, 72). These proteins include phosphoinositide-dependent kinase 1 (PDK1) and Akt, also known as protein kinase B (PKB) (73). Activated pAkt kinase then phosphorylates another kinase, glycogen synthase kinase-3 (GSK-3), rendering it inactive. Constitutively active GSK-3 is unphosphorylated and responsible for maintaining the cell cycle-activating transcription factors *c-myc*, *c-jun*, *c-myb*, and cyclin D1 in their inactive (ie, phosphorylated) state. Additionally, pAkt phosphorylates the Bcl-2 antagonist of cell death (BAD), caspase 9, and forkhead transcription factor (FKHR), suppressing the pro-apoptotic function of these proteins. Thus, Akt phosphorylation leads to the subsequent phosphorylation of downstream targets that affect cell growth and survival, as well as membrane ruffling, cell migration, and actin cytoskeletal rearrangement important for leukocyte migration and phagocytosis (69, 71). A natural inhibitor of PI3K signaling is the phosphatase and tensin homologue deleted on chromosome 10 (PTEN), a tumor suppressor gene identified on human chromosome 10q23. PTEN dephosphorylates PtdIns(3,4,5)P₃ at the 3' position, effectively reversing the action of PI3K (64). An overview of PI3K signaling is presented in figure 1.10.

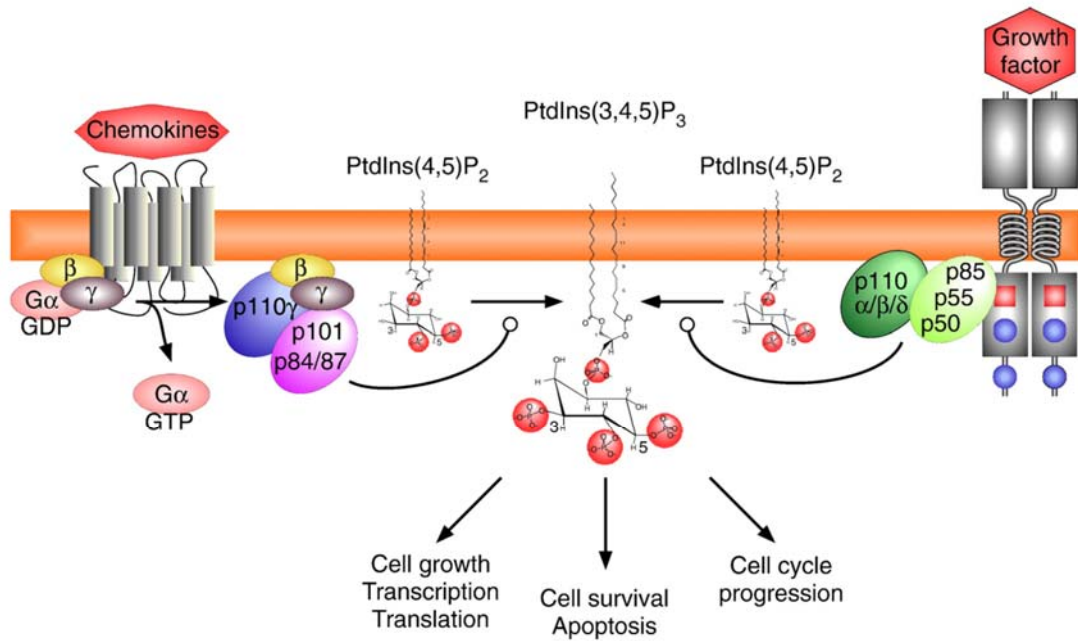


Fig. 1.9 Simplified activation scheme of class I PI3Ks. From Marone *et al* (2008) (64), used with permission.

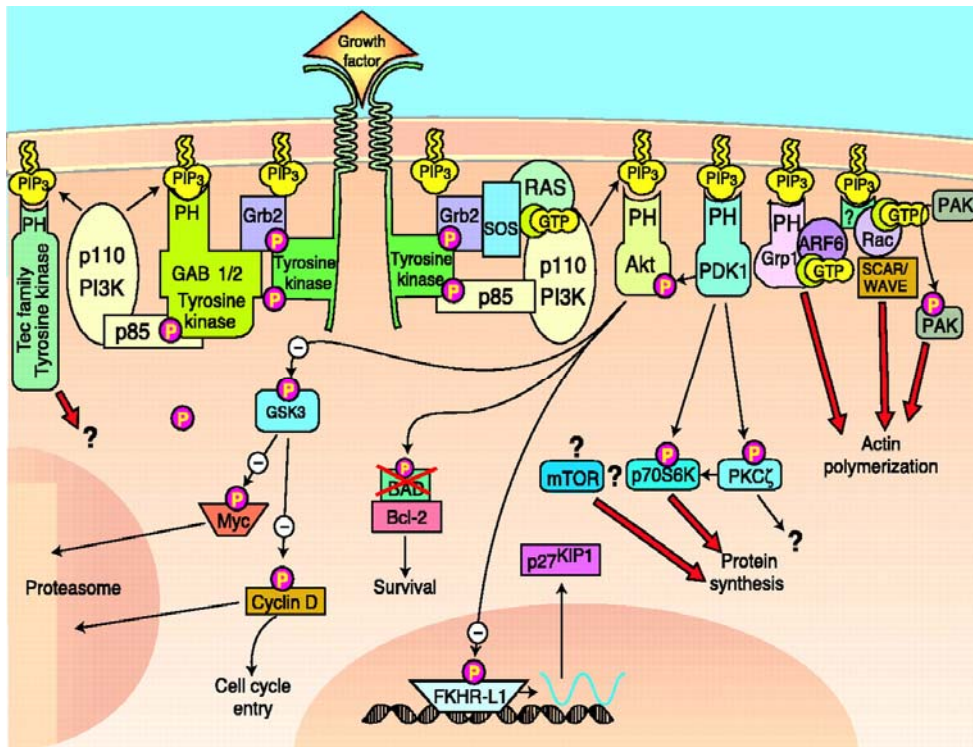


Fig. 1.10 Signaling pathways downstream of PI3K. From Cantley (2002) (71), used with permission.

1.2.4 Biological functions of PI3K

a. Cell proliferation and differentiation

The importance of PI3K in maintenance of cell cycle control is best illustrated by the fact that activating mutations in PI3K α or deactivating mutations in the PI3K inhibitor PTEN, collectively leading to elevated PtdIns(3,4,5)P₃ levels, can be identified in a wide variety of human malignancies. Cowden's disease, characterized by the presence of multiple hamartomas leading to the development of malignancies of the breast, thyroid, or endometrium, is associated with germline mutations of PTEN in approximately 80% of cases. Sporadic PTEN mutations may be found in more than 50% of gliomas, melanomas, prostate, endometrial, and ovarian cancers, while in as many as 50% of leukemias and melanomas, breast, prostate, endometrial, and colorectal cancers, tumor cells down-regulate PTEN via promoter hyper-methylation (64). Similarly, amplification of the PIK3CA gene may be identified in a variety of tumor types, including ovarian, cervical, lung, and colorectal cancers; additionally, mutations, localized mainly to the helical and catalytic domains, can be identified in a large number of solid tumors (64).

Cell cycle progression is tightly controlled by the expression of cyclins and their interactions with cyclin-dependent kinases (CDKs) or CDK inhibitors. Active Akt phosphorylates class O of transcription factors (FOXOs) at three different sites, permitting 14-3-3 protein binding, leading to retention of the FOXO/14-3-3 complex in the cytosol. The absence of FOXO from the nucleus increases the transcription of cyclin D1 and reduces the transcription of the CDK inhibitor p27^{Kip1} (64). Phosphorylated Akt also blocks the activity of GSK3 β , resulting in further accumulation of cyclin D1 and further reduction in p27^{Kip1}, leading to transition from G1 to S phase and cell cycle

progression. Our laboratory has previously confirmed that cyclin D1 levels in intestinal epithelial cells are regulated by the PI3K pathway at both the transcriptional and post-transcriptional levels; cyclin D1 expression was attenuated by treatment with PI3K inhibitors, including the pharmacological inhibitors wortmannin and LY294002 (70).

An additional role has been suggested for PI3K in the differentiation or even de-differentiation of different cell types. For example, PI3K activation has been linked to the differentiation of various cell types, including splenic B cells, osteoclasts, chondrocytes, and adipose cells (74-77). Additionally, our laboratory has found that PI3K activation promotes differentiation of pancreatic duct cells to endocrine cells *in vitro* (78). In contrast, *inhibition* of PI3K induces B16 melanoma cell differentiation in addition to the endocrine differentiation of human fetal stem cells, suggesting an organ-specific role of the PI3K pathway in the maturation and differentiation of tissues.

b. Apoptosis and cell survival

In addition to its role in cell cycle entry, activation of PI3K also confers an anti-apoptotic effect. Phosphorylated Akt phosphorylates and inhibits caspase-9, a critical protease central in the initiation of the apoptotic cascade. Additionally, pAkt phosphorylates the death promoter BAD at Ser 136, releasing the anti-apoptotic proteins Bcl-2 and Bcl-X_L, and phosphorylates and activates I- κ B kinase, which inactivates the inhibitor I- κ B, releasing the transcription factor NF- κ B. NF- κ B may then enter the nucleus, activating transcription of anti-apoptotic proteins such as Bcl-2 and Bcl-X_L. Inactivation and cytosolic retention of FOXO, as previously mentioned, also contributes to a block in FasL transcription, preventing ligand-induced apoptosis (64). Our laboratory has found that treatment of the colon cancer cell line KM20 with the PI3K

inhibitors wortmannin or LY294002, in combination with treatment with sodium butyrate (NaBT), increased activation of caspase-9 and caspase-3 and the subsequent cleavage of PARP; inhibition also increased sensitivity of this cell line to the chemotherapeutic agents gemcitabine and 5-FU, supporting a role for PI3K in the inhibition of apoptosis and subsequent cell survival (79).

c. Cell adhesion and invasion

The PI3K pathway is thought to contribute to tumorigenesis not only secondary to its roles in proliferation and regulation of apoptosis, but also secondary to its contribution to cell adhesion and subsequent invasion. Cancer cell invasion through the extracellular matrix (ECM) and basement membrane is primarily mediated by the degradation of collagen IV, with matrix metalloproteinases (MMPs) playing a critical role in such degradation (80). MMP-2, also known as type IV collagenase or gelatinase A, is a well-described factor associated with tumor cell invasion. Like other secreted MMPs, the latent MMP-2 proenzyme is activated through association with TIMP-2 and cell surface-anchored MT1-MMP; overexpression of MT1-MMP or MMP-2 is associated with tumor formation in a variety of *in vivo* systems (80-82).

IGF-IR signaling is a known regulator of MMP-2 synthesis and activity (83). Activation of the intrinsic type I insulin-like growth factor receptor (IGF-IR) results in phosphorylation of several substrates including the insulin receptor substrates (IRS) 1-4 and Shc, triggering PI3K activation; this leads to elevated levels of MMP-2 in several ways (83). Some evidence suggests that pAkt may directly phosphorylate and activate MMP-2, although this effect may occur indirectly via GSK-3 β inhibition (83). Additionally, the MMP-2 promotor contains several *cis*-acting regulatory elements,

including cyclic AMP responsive element binding, SP1, Ets-1, and AP-2, and Akt is known to up-regulate Ets-2 and cyclic AMP-responsive element (83). Lastly, Akt has been shown to localized to sites of epithelial cell matrix contact, with MMP-2 localizing to the surface of invading tumor and endothelial cells via interactions with $\alpha\text{v}\beta\text{3}$ integrin. Because $\alpha\text{v}\beta\text{3}$ -mediated cell migration of tumor cells has demonstrated a dependence upon Akt activation, Akt and MMP-2 appear to be critically linked to cell adhesion (80).

Directional invasion and migration of tumor cells is also controlled by the establishment of an intracellular gradient of PtdIns(3,4,5)P₃ (PIP₃) and PI(3,4)P₂, which are localized to the leading edge of the cell via activation of Class I PI3K (84). This increased concentration leads to the rapid subcellular relocation and phosphorylation of effector proteins containing pleckstrin homology (PH) domains, such as Akt, as well as the small GTPase protein Cdc42 and GTP-exchange factor (GEF) proteins, implying a network of positive-feedback loops between small GTPases and the PI3K pathway (85, 86). In concert, these proteins initiate and maintain a polarity within migrating cells.

d. Insulin signaling

In addition to its roles in the regulation of proliferation, differentiation, and motility, PI3K plays a central role in insulin signaling. Insulin binding promotes interaction of the insulin receptor substrate (IRS) proteins with Class IA PI3K, increasing activity of the p110 catalytic subunit and recruiting the enzyme to an area rich with its lipid substrates. PIP₃, a major product of PI3K activity, is essential for insulin action, acting as a second messenger and activating downstream kinases such as Akt and atypical protein kinase Cs (87). The regulation of PI3K by IRS proteins illustrates the importance of signal redundancy and diversity. For example, in cell-based assays, IRS-1 (widely

expressed) and IRS-3 (localized only to adipose tissue) activate PI3K more strongly than IRS-2 (also widely expressed), while IRS-4 (localized to thymus, brain, and kidney) barely activates PI3K (88). However, in murine liver, IRS-2 plays a central role in regulating PI3K function (88). In addition to the differences elicited by binding of the various IRS proteins, as previously noted, PI3K itself exists in multiple isoforms, which also contributes to differential signaling which occurs in response to IRS binding; thus, while PI3K plays a central role in insulin signaling, the response is tissue- and organ-specific.

e. Immune cell function

The PI3K pathway plays a critical role in the regulation of immune cell function, including regulation of immune cell development, migration, phagosome formation, cytokine development, and oxidative burst, among others. It has only been through the development of specific PI3K isoform knockout mice that the function of PI3K in immune cell function has been more critically evaluated (89).

Stimulation of immune cell function was one of the first-recognized roles of PI3K signaling in immunity. Cytokines, including interleukin 2 (IL-2), IL-3, IL-6, IL-7, IL-15, granulocyte colony stimulating factor (G-CSF), erythropoietin, and interferons activate class I_A PI3K in many cell types, including T cells and dendritic cells (DCs), via activation of Janus kinase and IRS family proteins. Binding of the T cell receptor, B cell receptor, and immunoglobulin Fc receptors also lead to PI3K activation, as well as signaling through costimulatory receptors such as CD28 on T cells and CD19 on B cells. Toll-like receptors and members of the tumor necrosis factor receptor family also activate

class I_A PI3K in macrophages and DCs, thus illustrating the importance of PI3K in immune cell activation in response to chemical signals (89).

PI3K also plays a central role in immune cell migration. Administration of antibodies against p110 β or p110 δ impairs lamellipodia formation and macrophage migration, while administration of p110 α antibody completely inhibits M-CSF-dependent DNA synthesis in macrophages (69). Class I_B PI3K p110 γ has been shown to be critically involved in chemoattractant-induced neutrophil migration to sites of inflammation *in vivo* (64). Additional studies on endothelial cells have demonstrated that p110 α is required for growth factor-induced migration, while p110 β is required for insulin-dependent migration, such that the involvement of different catalytic subunits of PI3K may be signal- and cell-type dependent (69).

PI3K is also intimately involved in generation of the oxidative burst responsible for phagosome-associated killing. Activation of PI3K by G-protein coupled receptors such as formyl-Met-Leu-Phe (fMLP) induces the assembly of subunits of NADPH oxidase through the binding of PX domains in p40^{phox} and p47^{phox} to PIP and PIP₂, respectively; binding of PIP to p40^{phox} also triggers the production of reactive oxygen species (89). Additionally, macrophages isolated from p85 α knockout mice produce significantly less nitric oxide (NO) than wild-type macrophages following stimulation with interferon- γ and lipopolysaccharide, leaving them more susceptible to bacterial infection (90). The formation of dimers of inducible nitric oxide synthase (iNOS) was significantly decreased in these cells secondary to decreased levels of BH₄, a protein responsible for iNOS dimer stabilization; this, in turn, was associated with a significant decrease in the expression of GTP cyclohydrolase 1 (GCH1), the rate-limiting enzyme

for BH4 synthesis, suggesting the potential etiology for deficiency of NO in these knockout mice (90).

f. Regeneration and repair

There is much evidence to support the role of the PI3K pathway in the regeneration or repair of tissues following injury; its role is not only one of cell proliferation following wounding, but also of restitution via activation of migration of progenitor cells and inflammatory cells to the site of injury. Our lab has previously demonstrated that pancreatic regeneration and acinar cell proliferation is dependent on PI3K/Akt activation (72). This is consistent with findings that PI3K activation is central to regeneration of the epidermis, gastric, intestinal, and colonic mucosa, nerve axons, and even the limbs of *Xenopus* species, among others (91-96). One study found that following ischemia-reperfusion injury to the intestine, EGF treatment significantly improved structural recovery and accelerated functional recovery of the gut barrier; this restitution was preceded by activation of Akt, and PI3K inhibition significantly reduced such restitution (96). Similarly, the administration of HGF to mice with dextran sulfate sodium-induced colitis significantly improved histologic scoring, suggesting improved regeneration of the colonic mucosa; administration of LY294002 or small interfering RNA (siRNA) targeting Akt suppressed cell proliferation in response to HGF therapy (92). Wounding of gastric epithelial cells *in vitro* leads to Akt activation; use of the PI3K inhibitor LY294002 leads to significantly reduced cell migration following injury (94). Another group found that while inactivation of p110 δ in mice did not affect gross neuronal development, it did lead to growth cone collapse, decreased axonal extension, and dampened axonal regeneration following peripheral nerve injury (93).

The importance of the growth factor HGF to liver regeneration has been previously noted. There is evidence that, within the liver, HGF exerts its proliferative effect on cells through PI3K/Akt signaling (68). Following the *in vitro* treatment of rat oval (liver progenitor) cells with HGF, Akt, ERK1/2, and p70^{s6k} were simultaneously upregulated, peaking at 30 min after treatment; when cells were treated with LY294002, the proliferative action of HGF was completely abrogated, implying a central role of this pathway in the biological effect of HGF (68). While preliminary evidence suggests an important role for the PI3K pathway in the regeneration of many tissues, the role of this pathway in liver regeneration has not been clearly explored.

1.3 RATIONALE FOR THE STUDY

1.3.1 Background problem, central hypothesis and specific aims

Liver transplantation is the surgical removal of a diseased liver and replacement by all or part of a donated liver. Sources of donated liver tissue include cadaveric donors (those who have suffered brain death) or living related donors. Liver transplantation is generally employed to treat those at high risk of dying from liver diseases. Such patients undergo pre-transplant evaluation, and are subsequently placed on a waiting list. As of early 2005, 17,000 patients in the US had undergone formal evaluation, were found to be suitable candidates, and were placed on the United Network for Organ Sharing (UNOS) waiting list. However, only 5,000 liver transplants are performed in the US per year; thus, many die of their disease before a suitable donor can be identified.

In the event that a cadaveric donor is not available and a living-related donor can be identified, a volume of graft not below 50% of the required liver volume, estimated as 2% of the body weight of the recipient, will be harvested from the donor. This generally equates to the removal of 50% of the donor's liver. Liver regeneration, both in the recipient and donor, is crucial for the maintenance of homeostasis and survival. A better understanding of pathways which contribute to liver regeneration will hopefully lead to therapeutic agents which augment the regenerative capacity of the injured or transplanted liver.

In an effort to fulfill the knowledge gap in the role of PI3K signaling in liver regeneration, the **central hypothesis** of this proposal is that the PI3K/Akt pathway plays a pivotal role in liver regeneration by regulating growth factor and cytokine signaling through surviving hepatocytes. To examine this hypothesis, a series of experiments were performed with the following **Specific Aims**:

1. To determine if PI3K is activated in the regenerating liver (Chapter 2). In an effort to define the role of PI3K in the regenerating liver, we first sought to establish evidence of PI3K activation following liver resection.

2. To determine if PI3K inhibition abrogates liver regeneration (Chapters 2, 3). After establishing the fact that PI3K is upregulated following liver resection, we next wanted to determine whether inhibition of PI3K would affect liver regeneration.

3. To determine the cell types affected by PI3K inhibition in the regenerating liver, and potential mechanisms of action (Chapter 3). Given the contribution of several cell types to the regenerative response following liver resection, we next attempted to

identify the cell types affected by PI3K inhibition in our animal model in an effort to determine potential mechanisms of action.

The long-term goal of the project is to understand the signal transduction events that mediate the process of liver regeneration such that this knowledge may lead to development of therapeutics that modulate these signaling pathways.

CHAPTER 2

INHIBITION OF PI3K WITH WORTMANNIN FOLLOWING 70% HEPATECTOMY ABROGATES LIVER REGENERATION

2.1 ABSTRACT

Introduction. Hepatectomy is associated with rapid liver regeneration of the remnant; signaling pathways responsible for this process have not been clearly delineated, but macrophages are thought to play an important role. Phosphatidylinositol-3 kinase (PI3K), consisting of a p85 α regulatory and p110 α catalytic subunit, participates in multiple cellular processes, including cell growth/survival and leukocyte migration. The purpose of our study was to determine if there is upregulation of PI3K following 70% hepatectomy in mice. **Methods.** Female Swiss-Webster mice (n=60) underwent 70% hepatectomy or sham operation. Mice were randomized to receive the PI3K inhibitor wortmannin (0.75mg/kg) ip, bid, or vehicle and then sacrificed over a time course. Bromodeoxyuridine (BrdU), a marker of DNA synthesis, was given 1h prior to sacrifice. Livers were harvested, weighed, and DNA and protein extracted; BrdU incorporation was quantitated. **Results.** There was activation of the PI3K pathway, as evidenced by increased Akt phosphorylation, following hepatectomy, especially at the earliest timepoints. Administration of wortmannin significantly decreased early liver regeneration as noted by decreased remnant weight and BrdU incorporation. **Conclusions.** PI3K/Akt pathway activation plays a critical role in early liver regeneration after resection.

2.2 INTRODUCTION

In both rodents and humans, partial hepatectomy results in the compensatory hypertrophy and hyperplasia of the remaining lobes of the liver to replace the loss of functional mass. In a mouse model of 70% hepatectomy, original liver mass is restored approximately 7-10 days following resection with a peak in DNA synthesis at approximately 42h, while in humans following lobectomy, restoration of mass is complete in approximately 3 months, with a peak in DNA synthesis at 7-10 days (11, 12, 14). In rodents, the cell type responsible for this proliferation is almost exclusively hepatocytes; in humans, a two-tier system composed of hepatocytes and progenitor (stem) cells contribute to the gain in mass (11, 13). A complex network of signaling pathways leads to successful liver regeneration: a cytokine pathway, responsible for hepatocyte priming; a growth factor pathway, responsible for cell cycle progression; and poorly understood pathways linking metabolic signals with DNA replication (13).

Phosphatidylinositol 3 (PI3) kinases are ubiquitous heterodimeric protein kinases involved in signal transduction through receptor tyrosine kinases or G-protein-coupled receptors; known PI3K receptor ligands include TNF- α (65, 66), IL-6 (67), HGF (68), EGF (14, 69), and TGF- α (14), among others. Class IA PI3K is composed of a regulatory p85 (α or β) and a catalytic p110 (α , β , or γ) subunit (69-71). When its receptor is activated by growth factors or cytokines, PI3K catalyzes the production of phosphatidylinositol 4-phosphate and phosphatidylinositol-3,4,5-triphosphate, yielding PIP₂ and PIP₃. This leads to recruitment of a subset of signal proteins with pleckstrin homology (PH) domains to the plasma membrane, ultimately leading to their phosphorylation (70, 72). These proteins include phosphoinositides-dependent kinase 1

(PDK1) and Akt, also known as protein kinase B (PKB) (73). Akt phosphorylation leads to the subsequent phosphorylation of downstream targets that affect cell growth and survival, as well as membrane ruffling, cell migration, and actin cytoskeletal rearrangement important for leukocyte migration and phagocytosis (69, 71). While Akt has been shown to play an important role in the compensatory recovery of liver mass following resection by regulating hepatocyte hypertrophy (97), little is known of the contribution of the PI3K to liver regeneration.

Our lab has previously demonstrated that pancreatic regeneration is dependent on PI3K/Akt activation (72). This is consistent with findings that PI3K activation (i) is important for immediate remodeling and cell survival following myocardial infarction (98), (ii) mediates proliferative signals in intestinal epithelial cells *in vitro* and *in vivo* (69), and (iii) modulates vascular regeneration following insult (99). Although PI3K has been shown to be important for the proliferation of various cell types, including intestinal epithelial cells, pancreatic acinar cells, and vascular endothelial cells, and important for leukocyte trafficking, signaling, and phagocytosis, its role in hepatic regeneration is not known.

2.3 MATERIALS & METHODS

2.3.1 Materials

5-0 silk sutures were purchased from Ethicon (Somerville, NJ). DOTAP liposomal transfection reagent was purchased from Roche (Indianapolis, IN). Wortmannin, bromodeoxyuridine (BrdU), phenol-chloroform-isoamylalcohol (25:24:1),

and mouse monoclonal anti-BrdU antibody were purchased from Sigma-Aldrich (St. Louis, MO). Rabbit monoclonal anti-phospho-Akt (Ser473), anti-p110 α , anti-cyclin D1, and anti-p38 MAPK were purchased from Cell Signaling (Beverly, MA). Mouse monoclonal anti-p85 α antibody was purchased from Upstate (Charlottesville, VA). Goat monoclonal anti-cyclophilin B and rabbit monoclonal anti-phospho-Stat3 (Ser727) were purchased from Santa Cruz Biotechnology (Santa Cruz, CA). Immun-Blot polyvinylidene difluoride (PVDF) membranes were from Bio-Rad (Hercules, CA), and X-ray film was purchased from Eastman Kodak (Rochester, NY). The enhanced chemiluminescence (ECL) system for Western immunoblot analysis was from Amersham Biosciences (Arlington Heights, IL).

2.3.2 Animals

Female Swiss-Webster mice, aged 4-6 weeks, weighing approximately 25g, were purchased from Harlan Sprague Dawley (Indianapolis, IN). Mice were housed in an American Association for Accreditation of Laboratory Animal Care-approved facility under a standard 12h light-dark cycle. They were fed standard chow (Formula Chow 5008; Purina Mills, St. Louis, MO) and tap water *ad libitum* and allowed to acclimate for one week. All studies were approved by the Institutional Animal Care and Use Committee of UTMB. Female mice were chosen for study as preliminary studies with male mice housed 5 mice per cage resulted in high mice fatality as a result of cage mate fighting. This altered early serum cytokine analysis.

2.3.3 70% hepatectomy

A model of 70% hepatectomy as originally described by Higgins and Anderson was used in this study (100). After an overnight fast, mice were anesthetized with halothane, placed on a warming blanket in the supine position, and the abdomen was shaven. After disinfection with alcohol, a midline laparotomy was performed. The liver was identified, and the right medial, left medial, and left lateral lobes were removed by carefully passing a 4-0 silk suture around the posterior aspect of each lobe and tying down; each lobe was carefully dissected away after hemostasis was obtained. Care was taken to preserve the gallbladder. After removal of the three lobes, the abdomen was irrigated with warm 0.9 normal saline, and the peritoneum and skin were closed in two layers using a running 4-0 silk suture. The mice were given 0.5cc warm 0.9 normal saline sc in the posterior neck and allowed to recover on the warming blanket before being returned to their cages. Sham-operated mice underwent an identical exposure, and the liver was identified and carefully manipulated. The abdomen was then irrigated with warm 0.9 normal saline, and the peritoneum and skin were closed in two layers using a running 4-0 silk suture. The mice were given 0.5cc warm 0.9 normal saline sc in the posterior neck and allowed to recover on the warming blanket before being returned to their cages. Operating times, and thus halothane exposure, was identical for sham operated and hepatectomized mice.

2.3.4 Experimental design

(i) To confirm that PI3K activity is increased following hepatectomy, female Swiss-Webster mice (n = 9) were randomized to receive either sham operation (n = 3) or 70% hepatectomy (n = 3); an additional 3 mice did not undergo surgery and were considered

controls. Mice were sacrificed at 24 h, liver was extracted for protein, and Western blot analysis of pAkt was performed. To further confirm PI3K activation, the experiment was repeated, and mice were randomized to receive either 70% hepatectomy (n=6) or sham (n=6) operation; mice were sacrificed over a time course (48h, 72h, 7 days), liver was extracted for protein, and Western blot analysis of pAkt was performed. (ii) For the wortmannin treatment study, female Swiss-Webster mice (n=60) were randomized to either 70% hepatectomy or sham operation and then further subdivided to receive either vehicle (5% ethanol ip bid) or wortmannin (0.75 mg/kg in 5% ethanol ip bid), which was administered approximately 6h prior to surgery and every 12h thereafter. To examine for side effects of wortmannin treatment, mice were examined and weighed daily following operation. Mice were sacrificed over a time course (24h, 48h, 72h, 7d) after operation. To measure DNA synthesis, bromodeoxyuridine (BrdU; 50mg/kg body weight) was given ip 3h prior to sacrifice. Livers were harvested for weight (wet and dry); DNA, RNA, and protein extraction; and histology. BrdU was quantitated by a novel dot blot procedure (101).

2.3.5 BrdU dot blot

BrdU dot blot was performed as previously described (101). Briefly, tissues were minced and placed into 4ml of 10mM Tris-HCl (pH 8.0), 10mM EDTA, 0.5% SDS, and 100 µg/ml Proteinase K in 50mM Tris HCl (pH 8.0) and 10mM CaCl₂. After incubation, an equal volume of phenol/chloroform/isoamylalcohol (PCI, 25:24:1) was added, and samples were centrifuged. Supernatant was removed, and an equal volume of PCI was added. Samples were centrifuged, supernatant was removed, and 1/10 volume of 3M

sodium acetate and 2.5x volume of 100% ethanol was added. Samples were centrifuged, supernatant was discarded, and samples were air-dried. 500µl of 10mM Tris-HCl (pH 8.0) and 1mM EDTA were added, and solution was incubated 1 h. 5µl of diluted RNase solution (0.5µl Ribonuclease A in 10mM Tris-HCl (pH 8.0) and 1mM EDTA) was added, and sample was incubated 1 h. An equal volume (500µl) of PCI was added, and samples were centrifuged for 15 m. Supernatant was removed, and 1/10 volume of 3M sodium acetate and 2.5x volume of 100% ethanol was added. DNA was transferred to another tube, and 1ml 100% ethanol was added for rinse. Samples were centrifuged, supernatant discarded, and wash was repeated. Samples were air-dried, and 50µl 10mM Tris-HCl (pH 8.0) in 1mM EDTA was added. DNA concentration was determined by spectrophotometer (OD260), and 2µg of DNA was dissolved in 10µl of 10mM Tris-HCl (pH 8.0) in 1mM EDTA. 100µl of 0.4N NaOH was added, and samples were incubated for 30 m. Samples were placed on ice for 10 m, then 90µl of 1M Tris-HCl (pH 6.8) was added. 5µl of resulting DNA solution was dot-blotted on the nitrocellulose membrane, fixed by UV, and incubated with primary anti-Brd-U antibody (1:2000 in Tris-buffered saline containing 1% nonfat dried milk with 0.05% TWEEN 20). Membrane was washed and incubated with secondary antibody for 1 h. Membrane was washed and visualized by ECL.

2.3.6 Tissue processing, staining, and immunohistochemistry

Upon sacrifice, liver samples were immediately placed in 10% neutral buffered formalin (NBF) for 24 h, followed by 70% EtOH for 24 h. Samples were then paraffin-embedded, sectioned, and stained with hematoxylin and eosin (H&E). IHC was

performed on paraffin-embedded samples as previously described (102, 103). Sections (5 μm) were cut from paraffin blocks, then deparaffinized in xylene and rehydrated in descending ethanol series. Protein staining was performed using DAKO EnVision Kit (Dako Corp., Carpinteria, CA). Sections were incubated overnight at 4°C with monoclonal antibodies diluted in 0.05M Tris-HCL + 1% BSA against F4/80 (1:100), BrdU (1:1000), or PCNA (1:2000). After 3 washes with TBST, the sections were incubated for 30 min with secondary antibody labeled with peroxidase, then washed 3 times with TBST. Lastly, peroxidase substrate DAB was added for staining. All sections were counterstained with hematoxylin and observed by light microscopy. For negative controls, primary antibody was omitted from the above protocol.

2.3.7 Protein preparation and Western immunoblot

Western blotting was performed as previously described (104). Tissues were lysed with 50 mM Tris, 150 mM NaCl, 0.1% Nonidet-P-40 (TNN) lysis buffer using a tissue grinder, then placed on ice for 30 m. Lysates were clarified by centrifugation (10,000 $\times g$ for 30 min at 4°C) and protein concentrations determined using the method of Bradford. Briefly, total protein (60 μg) was resolved on a 10% Nu-PAGE Bis-Tris gel and transferred to PVDF membranes. Filters were incubated overnight at 4°C in blotting solution (Tris-buffered saline containing 5% nonfat dried milk and 0.1% Tween 20), followed by a 1 h incubation with primary antibodies. Filters were washed three times in Tris-buffered saline containing 0.1% Tween 20 and incubated with horseradish peroxidase-conjugated secondary antibodies for 1 h. After three additional washes, the immune complexes were visualized by ECL detection.

2.3.8 Statistical analysis

Remnant liver weight as percent body weight was analyzed using analysis of variance for a two-factor factorial experiment. The two factors were assigned as operation (hepatectomy and sham) and siRNA or wortmannin (present and absent). Effects and interaction were assessed at the 0.05 and the 0.15 confidence levels, respectively, of significance. Fisher's least significant difference procedure was used for multiple comparisons with Bonferroni adjustment for the number of comparisons. All statistical computations were conducted using the SAS[®] system, Release 9.1.

2.4 RESULTS

2.4.1 Expression of pAkt following hepatectomy

To confirm that PI3K activity is increased following hepatectomy, female Swiss-Webster mice (n = 9) were randomized to sham operation or 70% hepatectomy and sacrificed 24 h following operation. Our data indicated a clear increase in PI3K activity, as reflected by an increase in pAkt expression, in 2 of 3 mice undergoing liver resection (Fig. 2.1). To confirm these results, female Swiss-Webster mice (n = 12) were

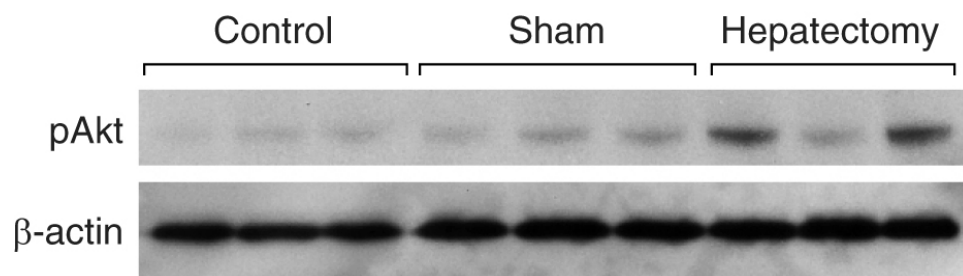


Figure 2.1 Increased PI3K activity 12h following hepatectomy. Mice (n=3 per group) underwent sham operation or hepatectomy. Mice were sacrificed following operation and WB analysis was performed to determine pAkt expression 12 hours following surgery; β-actin served as a loading control. From Jackson et al (2008) (105), used with permission.

randomized to receive either 70% hepatectomy or sham operation. Mice were sacrificed at 48h, 72h, and 7 days, liver was extracted for protein, and Western blot analysis of pAkt was performed (Fig. 2.2). Our data indicated an increase in PI3K activity, as reflected by an increase in pAkt expression at 48h and 72h following operation, with normalization of pAkt expression by day 7.

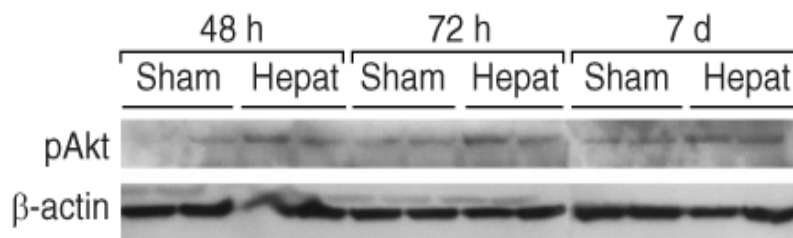


Figure 2.2 Upregulation of PI3K activity following hepatectomy at 48h and 72h timepoints. Mice (n=2 per group) underwent sham operation or hepatectomy. Mice were sacrificed following operation and WB analysis was performed to determine pAkt expression; β -actin served as a loading control.

2.4.2 Total PI3K inhibition with wortmannin decreases hepatic regeneration following PH

To determine the effects of total PI3K blockade on liver regeneration, female Swiss-Webster mice were randomized to receive either 70% partial hepatectomy or sham operation; they were further subdivided to receive the potent PI3K inhibitor, wortmannin, or vehicle via ip injection. They received one “priming” dose of wortmannin or vehicle 6h prior to surgery and every 12h thereafter. Mice were killed 24h, 48h, 72h, and 7d following operation, and wet liver remnant weight was measured and expressed as remnant weight as percent body mass. For sham-operated mice, liver was removed after sacrifice, 70% hepatectomy was performed *ex vivo*, and liver remnant mass was recorded.

Following hepatectomy, mice treated with vehicle demonstrated the expected gradual increase in hepatic remnant wet weight, which increased from approximately 1.8% of body mass at the time of operation, to 2.6% after 24h, 3.2% at 48h, 3.8% at 72h, and 4.2% by day 7 (Fig. 2.3A). Mice treated with wortmannin demonstrated a decrease in liver regeneration relative to vehicle-treated mice, especially at the earliest timepoints. Liver mass in wortmannin-treated mice increased from approximately 1.8% of body mass at the time of operation, to 2.2% at 24h, 2.3% at 48h, 2.7% at 72h, and 4.0% at 7 days. Body mass of mice treated with wortmannin following hepatectomy decreased to a similar extent as mice treated with vehicle; there were no untoward or toxic effects of wortmannin treatment in either sham-operated or hepatectomized mice.

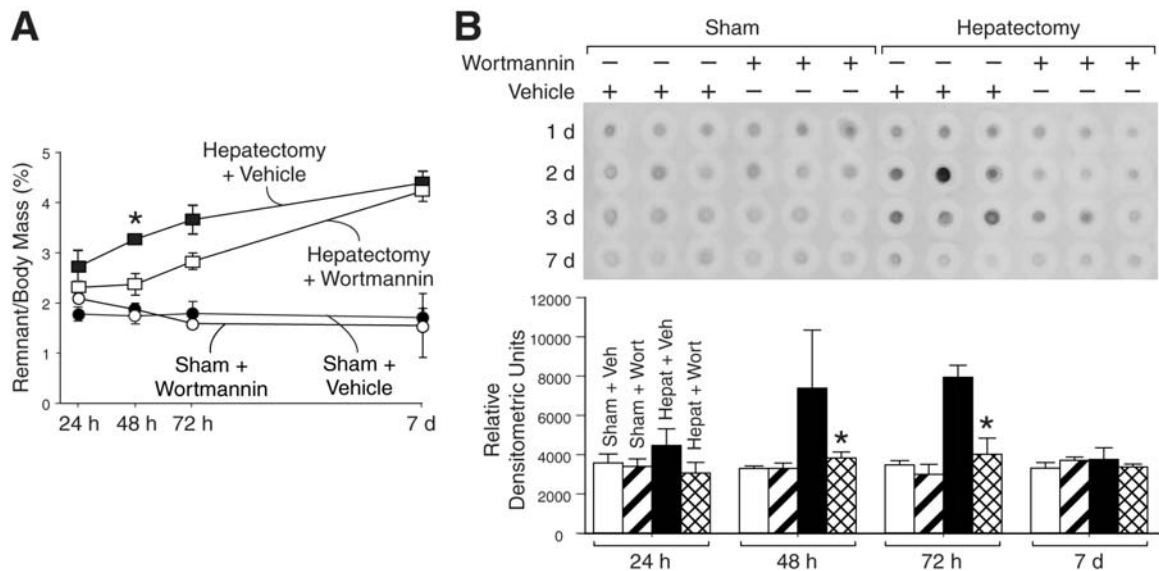


Figure 2.3 PI3K inhibition leads to decreased liver regeneration. (A) Mice (n=60) were randomized to either hepatectomy or sham operation and further subdivided to receive vehicle or wortmannin. Mice were sacrificed over a time course after operation, and wet remnant weight as a percent of body mass was determined. * = p<0.05 vs. wortmannin-treated mice. (B) To measure DNA synthesis, BrdU was given prior to sacrifice, and DNA dot blot was performed with BrdU probe. Densitometry is presented below the blot. * = p<0.05 vs. vehicle-treated mice. From Jackson et al (2008) (105), used with permission.

To further confirm that the decrease in hepatic regeneration is due to reduced hepatocyte proliferation, BrdU incorporation was compared in mice treated with wortmannin or vehicle by DNA dot-blot (Fig. 2.3B). Mice treated with vehicle demonstrated an expected peak in DNA synthesis at 48h and 72h following hepatectomy; mice treated with wortmannin did not experience this peak. However, the peak in DNA synthesis in wortmannin-treated mice may have occurred between 72h and 7 days, as liver mass was recovered in these mice by day 7.

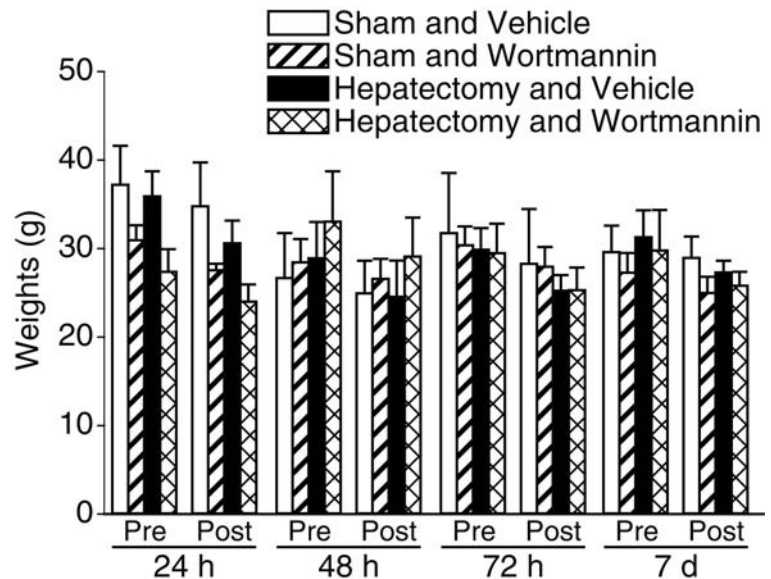


Fig. 2.4 Wortmannin treatment did not have obvious side effects as evidenced by little change in body weight relative to vehicle-treated mice. Mice were weighed daily following liver resection; body weights are presented here as pre- and post-resection.

To confirm that there were no overt side effects of wortmannin treatment, mice in both vehicle-treated and wortmannin-treated groups were examined and weighed daily. We found that weight loss following surgery was similar in both vehicle-treated and wortmannin-treated mice (Fig. 2.4). There were no additional side effects of wortmannin treatment noted, as evidenced by absence of changes in coat texture, grooming, mucus membrane moisture, activity level, or stool caliber or quality.

2.4.3 Treatment with wortmannin led to altered architecture of the regenerating liver

H&E staining was performed on liver samples from mice undergoing sham operation or liver resection treated with vehicle or wortmannin (Fig. 2.5). We identified a widespread vacuolar appearance in the livers of mice undergoing liver resection that had been treated with wortmannin, in contrast to the normal appearance of the regenerating liver in vehicle-treated mice; this appearance has been previously termed panlobular hydropic vacuolization, and has been described in association with inhibition of hepatocyte priming following liver resection (106). Notably, the livers of sham-operated mice treated with wortmannin lacked this histological finding (Fig. 2.6). To further investigate the architectural changes found in these mice, we performed PAS staining for glycogen, and found widespread glycogen deposition throughout the livers of mice undergoing liver resection and treated with wortmannin relative to vehicle-treated mice (Fig. 2.7). Again, we found no change in glycogen deposition in sham-operated mice treated with wortmannin (Fig. 2.8).

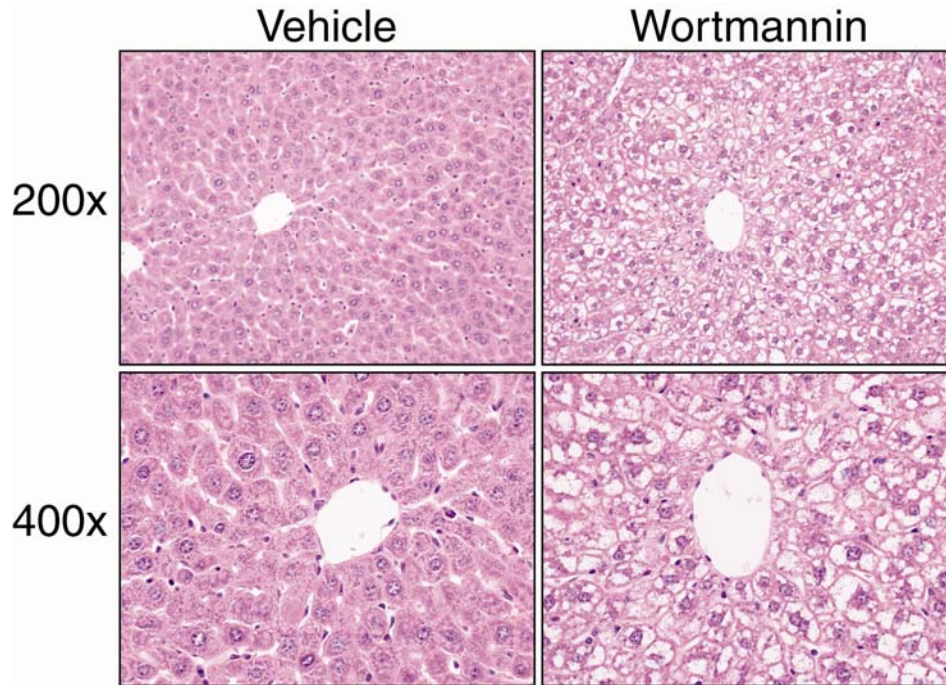


Fig. 2.5 Regenerating liver of wortmannin-treated mice demonstrated aberrant architecture. Liver sections from all timepoints were stained with H&E for histologic evaluation. Liver sample from vehicle-treated mouse on the left; sample from wortmannin-treated mouse 48 h on the right. Representative samples were taken at the 48 h time point for consistency.

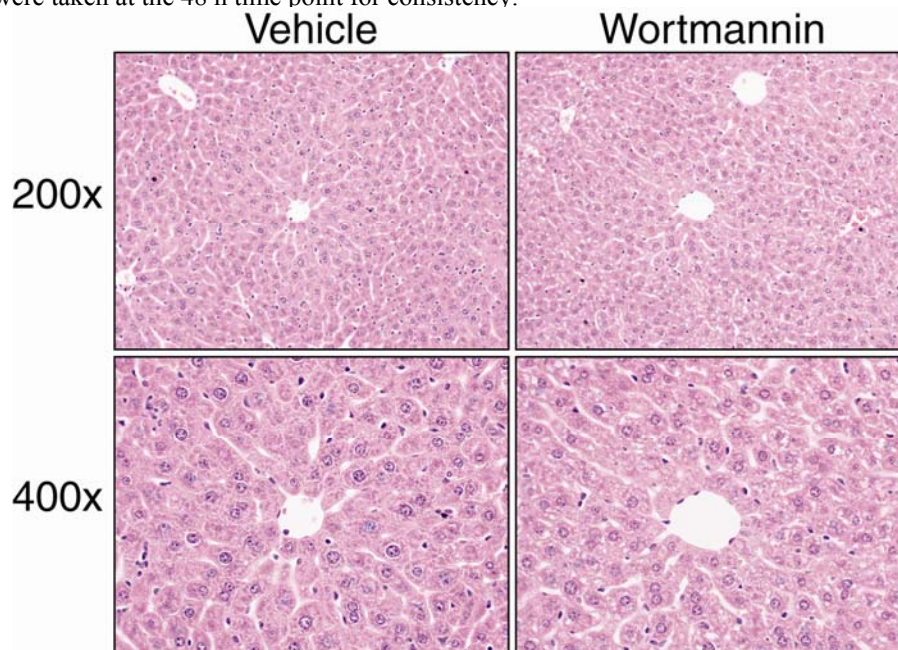


Fig 2.6 Livers of sham-operated mice treated with wortmannin did not demonstrate alterations in architecture. Liver sections were stained with H&E for histologic evaluation. Liver sample from vehicle-treated mouse on the left; sample from wortmannin-treated mouse on the right. Representative samples were taken at the 48 h time point for consistency.

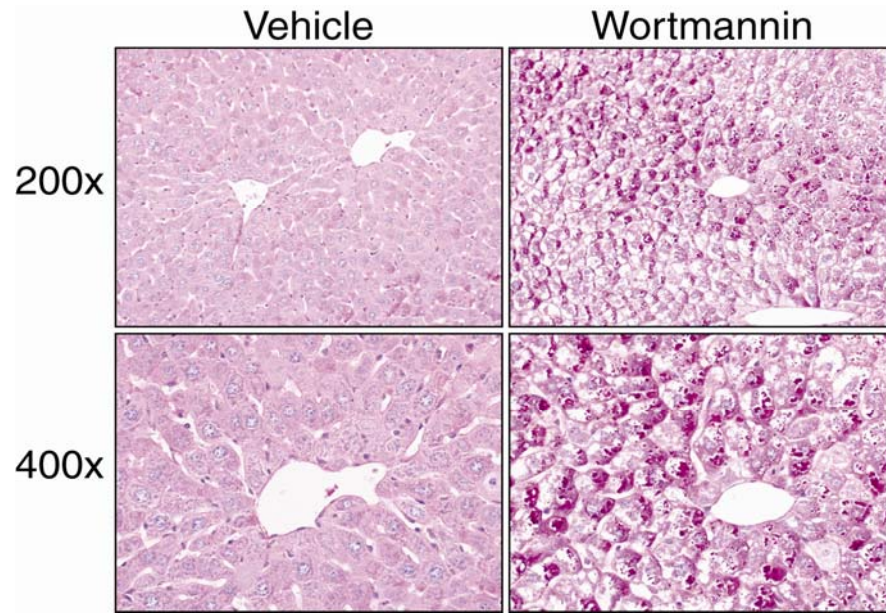


Fig. 2.7 Regenerating liver of wortmannin-treated mice demonstrated aberrant glycogen deposition by PAS staining. Liver sections were stained with PAS to determine distribution of glycogen storage. Liver sample from vehicle-treated mouse on the left; sample from wortmannin-treated mouse on the right. Representative samples were taken at the 48 h time point for consistency.

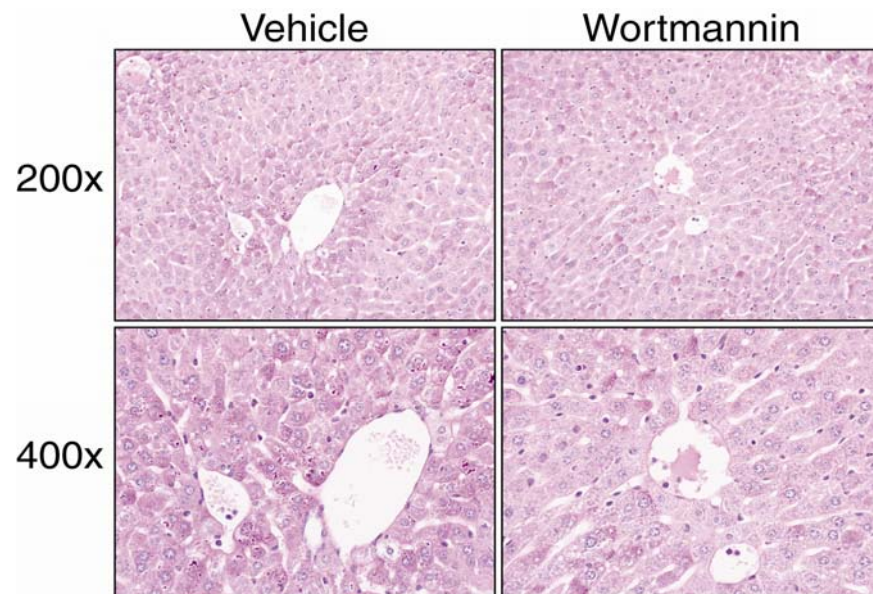


Fig 2.8 Livers of sham-operated mice treated with wortmannin did not demonstrate aberrations in glycogen storage. Liver sections were stained with PAS to determine distribution of glycogen storage. Liver sample from vehicle-treated mouse on the left; sample from wortmannin-treated mouse on the right. Representative samples were taken at the 48 h time point for consistency.

2.5 DISCUSSION

Class I PI3Ks is a heterodimer composed of a regulatory (p85) and catalytic (p110) subunit; the regulatory p85 α subunit is essential for the stability of the p110 α catalytic subunit and for its recruitment to activated receptor tyrosine kinases or G-protein-coupled receptors. Wortmannin, a furanosteroid metabolite of the fungus *Penicillium funiculosum*, displays potency against class I, II, and III PI3Ks. Wortmannin is a potent irreversible inhibitor of PI3K; it is highly soluble with a large volume of distribution and has a short half-life (approximately 10 min *in vitro*) necessitating frequent administration for *in vivo* studies. Although PI3K has been shown to be important for the proliferation of various cell types and regeneration of various tissues following injury, including intestinal epithelial cells, pancreatic acinar cells, and vascular endothelial cells (70, 72, 99), and important for leukocyte trafficking, signaling, and phagocytosis (107), its role in hepatic regeneration is not known. In our present study, we demonstrate 3 major findings: (1) PI3K is activated following partial hepatectomy in mice, especially at the earliest timepoints; (2) total PI3K inhibition with the pharmacologic inhibitor wortmannin markedly decreases the regenerative response of the liver after resection; and (3) PI3K inhibition leads to the development of aberrant architecture within the regenerating liver, with alterations in glycogen deposition noted throughout.

Class I PI3Ks play a central role in cell survival and proliferation; this is well-illustrated by the fact that many cancers display PI3K activating mutations. Stimulation by the growth factors HGF, EGF, and TGF α leads to progression from the G₁ to S phase

of the cell cycle following IL-6 and TNF α -induced cell priming; these proteins signal through receptor tyrosine kinases which, in the activated state, associate with cytosolic proteins rich in Src homologies, such as PI3K (14, 36). Downstream signaling then leads to the activation of MAPK, ultimately leading to cell proliferation. Therefore, our hypothesis in this experiment was that PI3K inhibition would lead to altered growth factor signaling, although alternate pathways would likely compensate over time, such that late liver regeneration would be possible. Given its solubility and wide volume of distribution, treatment with wortmannin is likely to inhibit all cell types present within the liver, altering hepatocyte PI3K response to growth factors and cytokines in addition to action on secondary cell types present within the liver, including endothelial cells, stellate cells, and Kupffer cells, which play supportive roles in liver regeneration. Additionally, wortmannin displays potency against class I, II, and III PI3Ks; it is difficult to speculate whether the findings in the current study can be attributed specifically to its action on class I PI3K. Therefore, future studies will concentrate on the effects of inhibition of specific class I PI3K subunits, p85 α and p110 α , on subsequent liver regeneration.

Some effects of wortmannin on the liver in *in vivo* studies and on hepatocytes in *in vitro* studies have been previously described. One study aimed to identify the effects of wortmannin on bile secretion, cytoskeletal organization, and endotranscytotic pathways in rat liver (108). Following treatment with wortmannin in this study, a 25% reduction in basal bile flow in isolated perfused rat liver was noted, associated with a significant dilatation of the bile canalicular lumen; additionally, they noted decreased biliary excretion of labeled products as well as decreased uptake of a fluid-phase marker, Lucifer yellow, within the liver. Examination of wortmannin-treated rat hepatocyte

couplets revealed a marked disorganization of microfilaments, leading the investigators to conclude that PI3K is involved in the regulation of vesicle trafficking, cytoskeletal organization, and the process of bile formation within the liver (108). Additionally, treatment with wortmannin has been shown to worsen hepatocytic injury in ischemia-reperfusion experiments (109), and has been shown to increase systemic insulin release but impair hepatic glucose metabolism during a rat hyperinsulinemic euglycemic clamp (110). Therefore, known effects of wortmannin-mediated PI3K inhibition within the liver include alteration in cell survival following injury, aberrations in cellular architecture due to alteration of microfilament structure, and derangement of hepatocytic metabolism of glucose. These conclusions are consistent with findings described in our current study.

It was noted that mice that underwent hepatectomy and received wortmannin in our study developed a widespread vacuolar appearance of the regenerating liver. While we initially attributed this to wortmannin toxicity, these changes were not present in sham-operated mice that received wortmannin, nor have they been described in other *in vivo* liver studies in control mice receiving wortmannin (109). In an attempt to determine the composition or content of these vacuoles, liver sections were stained with PAS. We found that there was heavy glycogen deposition within the liver of wortmannin-treated mice following liver resection, but normal glycogen deposition within the livers of sham-operated mice treated with wortmannin. This likely reflects alteration in hepatic insulin signaling as a result of PI3K inhibition. We also noted that on histopathologic examination, the livers of mice undergoing liver resection that were treated with wortmannin appeared to have fewer Kupffer cells present, although macrophage-specific

staining was not performed on these samples. Future studies will thus examine the effects of selective PI3K subunit inhibition on cellular architecture and glycogen and lipid storage, and will also assess for differences in secondary cell types present.

2.6 CONCLUSIONS

Total PI3K inhibition with wortmannin led to significantly decreased liver regeneration and altered architecture of the regenerating liver, especially at the earliest time points. As the PI3K pathway is activated during several critical steps in liver regeneration, for example, following priming and growth factor stimulation, future studies will attempt to determine the specific steps affected by PI3K inhibition. We will also examine the effect of specific PI3K subunit inhibition using small interfering RNA (siRNA) technology.

CHAPTER 3

SELECTIVE INHIBITION OF PI3K WITH siRNA TARGETING p85 α or p110 α FOLLOWING 70% HEPATECTOMY ABROGATES LIVER REGENERATION

3.1 ABSTRACT

Background & Aims. Hepatic resection is associated with rapid proliferation and regeneration of the remnant liver. Phosphatidylinositol 3-kinase (PI3K), composed of a p85 α regulatory and a p110 α catalytic subunit, participates in multiple cellular processes, including cell growth and survival; however, the role of PI3K in liver regeneration has not been clearly delineated. **Methods.** In this study, we used small interfering RNA (siRNA) targeting the p85 α and p110 α subunits to determine if selective PI3K inhibition would abrogate the proliferative response of the liver after partial hepatectomy in mice. Extent of regeneration was assessed by weighing liver remnants, performing immunohistochemical analysis for proliferating cell nuclear antigen (PCNA), and by performing DNA BrdU dot blot. **Results.** Selective inhibition of p85 α or p110 α with siRNA resulted in a significant decrease in hepatocyte proliferation, especially at the earliest timepoints. Fewer macrophages and Kupffer cells were present in the regenerating liver of mice treated with siRNA to p85 α or p110 α , as reflected by a paucity of F4/80-positive cells. Additionally, PI3K inhibition led to an aberrant architecture in the regenerating hepatocytes characterized by vacuolization, lipid deposition, and glycogen accumulation; these changes were not noted in the sham livers. **Conclusions.**

Our data demonstrate that PI3K/Akt pathway activation plays a critical role in the early regenerative response of the liver after resection; inhibition of this pathway markedly abrogates the normal hepatic regenerative response, perhaps by inhibiting macrophage infiltration and cytokine elaboration and thus hepatocyte priming for replication.

3.2 INTRODUCTION

Partial hepatectomy results in the compensatory hypertrophy and hyperplasia of the remaining lobes of the liver to replace the loss of functional mass. In rodents, the cell type responsible for this proliferation is almost exclusively hepatocytes; in humans, a two-tier system composed of hepatocytes and progenitor (stem) cells contribute to the gain in mass (11, 13). A complex network of signaling pathways leads to successful liver regeneration: a cytokine pathway, responsible for hepatocyte priming; a growth factor pathway, responsible for cell cycle progression; and poorly understood pathways linking metabolic signals with DNA replication (13).

Cytokines, including tumor necrosis factor-alpha (TNF- α) and interleukin 6 (IL-6), are elaborated by non-parenchymal cells such as Kupffer cells following hepatectomy (13, 111). They are responsible for the initial priming of hepatocytes, with the transition of quiescent hepatocytes from the G₀ to G₁ stage of the cell cycle. In the absence of cytokines, hepatocytes are minimally responsive to growth factor stimulation, illustrating the importance of this initial priming reaction (13). Upon priming of hepatocytes, growth factor stimulation leads to G₁ to S phase transition and cell cycle progression. Three growth factors of major importance for liver regeneration include hepatocyte growth factor (HGF), transforming growth factor-alpha (TGF- α), and epidermal growth factor

(EGF). These factors signal through receptor tyrosine kinases which, in the activated state, associate with cytosolic proteins such as phosphatidylinositol 3-kinase (PI3K) (14, 36). While much is known about the cytokines responsible for hepatocyte priming and the growth factors responsible for stimulating cell cycle progression, the complex set of reactions responsible for linking these signaling pathways has yet to be delineated.

Class IA PI3K is composed of a regulatory p85 (α or β) and a catalytic p110 (α , β , or γ) subunit (70, 71, 112). When its receptor is activated by growth factors or cytokines (eg, TNF- α or IL-6), PI3K catalyzes the production of phosphatidylinositol-3,4,5-triphosphate, recruiting a subset of signal proteins, such as Akt, to the plasma membrane, ultimately leading to their phosphorylation (70, 72). While Akt has been shown to play an important role in the compensatory recovery of liver mass following resection by regulating hepatocyte hypertrophy (97), little is known regarding the contribution of PI3K subunits to liver regeneration. Interestingly, genetic deletion of all isoforms of p85 α in mice leads to perinatal death secondary to extensive hepatocyte necrosis and chylous ascites (113), suggesting a role for the p85 α subunit in early liver development.

Phosphatidylinositol 3 (PI3) kinases are ubiquitous heterodimeric protein kinases involved in signal transduction through receptor tyrosine kinases or G-protein-coupled receptors; known PI3K receptor ligands include TNF- α (65, 66), IL-6 (67), HGF (68), EGF (14, 69), and TGF- α (14), among others. Class IA PI3K is composed of a regulatory p85 (α or β) and a catalytic p110 (α , β , or γ) subunit (69-71). When its receptor is activated by growth factors or cytokines, PI3K catalyzes the production of

phosphatidylinositol 4-phosphate and phosphatidylinositol-3,4,5-triphosphate, yielding PIP₂ and PIP₃. This leads to recruitment of a subset of signal proteins with pleckstrin homology (PH) domains to the plasma membrane, ultimately leading to their phosphorylation (70, 72). These proteins include phosphoinositides-dependent kinase 1 (PDK1) and Akt, also known as protein kinase B (PKB) (73). Akt phosphorylation leads to the subsequent phosphorylation of downstream targets that affect cell growth and survival, as well as membrane ruffling, cell migration, and actin cytoskeletal rearrangement important for leukocyte migration and phagocytosis (69, 71). While Akt has been shown to play an important role in the compensatory recovery of liver mass following resection by regulating hepatocyte hypertrophy (97), little is known of the contribution of the PI3K to liver regeneration.

We have previously demonstrated that the PI3K pathway is activated following hepatectomy, and that complete inhibition of PI3K with wortmannin significantly inhibited liver regeneration following 70% hepatectomy in mice. Additionally, our laboratory has demonstrated that pancreatic regeneration is dependent on PI3K/Akt activation (72). Given the role of the PI3K pathway in the regeneration of other organs, we hypothesized that PI3K plays an important role in hepatic regeneration following resection. Here, we demonstrate using small interfering RNA (siRNA) directed to the p85 α regulatory or p110 α catalytic subunits that PI3K signaling is required for early hepatic regeneration following hepatectomy.

3.3 MATERIALS & METHODS

3.3.1 Materials

pik3ca (p85 α), *pik3r1* (p110 α), and non-targeting control (NTC) siSTABLE *in vivo* SMARTpool siRNA duplexes and DY547-labeled NTC and p85 α siRNA duplexes were designed and synthesized by Customer SMARTpool siRNA Design from Dharmacon (Lafayette, CO) (102). siSTABLE *in vivo* duplex is chemically modified to extend siRNA stability *in vivo* compared with unmodified siRNA. 5-0 silk sutures were purchased from Ethicon (Somerville, NJ). DOTAP liposomal transfection reagent was purchased from Roche (Indianapolis, IN). bromodeoxyuridine (BrdU), phenol-chloroform-isoamylalcohol (25:24:1), mouse monoclonal anti-BrdU antibody, and Hoescht stain were purchased from Sigma-Aldrich (St. Louis, MO). Rabbit monoclonal anti-phospho-Akt (Ser473), anti-p110 α , anti-cyclin D1, and anti-p38 MAPK were purchased from Cell Signaling (Beverly, MA). Mouse monoclonal anti-p85 α antibody was purchased from Upstate (Charlottesville, VA). Goat monoclonal anti-cyclophilin B and rabbit monoclonal anti-phospho-Stat3 (Ser727) were purchased from Santa Cruz Biotechnology (Santa Cruz, CA). Mouse monoclonal anti-F4/80 antibody was purchased from Abcam (Cambridge, MA). Rabbit anti-LC3 antibody was purchased from MBL International (Woburn, MA). Immun-Blot polyvinylidene difluoride (PVDF) membranes were from Bio-Rad (Hercules, CA), and X-ray film was purchased from Eastman Kodak (Rochester, NY). The enhanced chemiluminescence (ECL) system for Western immunoblot analysis was from Amersham Biosciences (Arlington Heights, IL). TNF α

and IL-6 enzyme-linked immunosorbent assay kits were purchased from R&D Systems (Abingdon, Oxon, UK).

3.3.2 Experimental design

(i) Mice (n=60) were randomized to either 70% hepatectomy or sham operation and then further subdivided to receive either NTC siSTABLE siRNA (20 μ g iv qd; n=30) or p85 α siSTABLE siRNA (20 μ g iv qd; n=30), administered 24 h prior to surgery and every 24 h thereafter; DOTAP liposomal transfection reagent was used for all transfections. Mice were sacrificed over a time course (48h, 72h, 7d) after operation. To measure DNA synthesis, bromodeoxyuridine (BrdU; 50mg/kg body weight) was given ip 3h prior to sacrifice. Livers were harvested for weight (wet and dry); DNA, RNA, and protein extraction; and histology. BrdU was quantitated by a novel dot blot procedure (101). (ii) Mice (n=90) were randomized to either 70% hepatectomy or sham operation and then further subdivided to receive either NTC siSTABLE siRNA (20 μ g iv qd; n=30), p110 α siSTABLE siRNA (20 μ g iv qd; n=30), or p85 α siSTABLE siRNA (20 μ g iv qd; n=30) administered 24 h prior to surgery and every 24h thereafter; DOTAP liposomal transfection reagent was used for all transfections. Mice were sacrificed over a time course (48h, 72h, 7d) after operation. Analysis of tissues was as above. (iii) The study was repeated as in (ii), but mice were not pre-treated with siRNA 24h prior to surgery; instead, to allow priming to occur without alteration, mice were given siRNA 6h following operation, and every 24h thereafter. Mice were sacrificed at 48h and 7d. (iv)

The study was repeated as in (iii), but mice were sacrificed at earlier time points following surgery.

3.3.3 BrdU dot blot

BrdU dot blot was performed as previously described (101). Briefly, tissues were minced and placed into 4ml of 10mM Tris-HCl (pH 8.0), 10mM EDTA, 0.5% SDS, and 100 µg/ml Proteinase K in 50mM Tris HCl (pH 8.0) and 10mM CaCl₂. After incubation, an equal volume of phenol/chloroform/isoamylalcohol (PCI, 25:24:1) was added, and samples were centrifuged. Supernatant was removed, and an equal volume of PCI was added. Samples were centrifuged, supernatant was removed, and 1/10 volume of 3M sodium acetate and 2.5x volume of 100% ethanol was added. Samples were centrifuged, supernatant was discarded, and samples were air-dried. 500µl of 10mM Tris-HCl (pH 8.0) and 1mM EDTA were added, and solution was incubated 1 h. 5µl of diluted RNase solution (0.5µl Ribonuclease A in 10mM Tris-HCl (pH 8.0) and 1mM EDTA) was added, and sample was incubated 1 h. An equal volume (500µl) of PCI was added, and samples were centrifuged for 15 m. Supernatant was removed, and 1/10 volume of 3M sodium acetate and 2.5x volume of 100% ethanol was added. DNA was transferred to another tube, and 1ml 100% ethanol was added for rinse. Samples were centrifuged, supernatant discarded, and wash was repeated. Samples were air-dried, and 50µl 10mM Tris-HCl (pH 8.0) in 1mM EDTA was added. DNA concentration was determined by spectrophotometer (OD260), and 2µg of DNA was dissolved in 10µl of 10mM Tris-HCl (pH 8.0) in 1mM EDTA. 100µl of 0.4N NaOH was added, and samples were incubated for 30 m. Samples were placed on ice for 10 m, then 90µl of 1M Tris-HCl (pH 6.8) was

added. 5µl of resulting DNA solution was dot-blotted on the nitrocellulose membrane, fixed by UV, and incubated with primary anti-Brd-U antibody (1:2000 in Tris-buffered saline containing 1% nonfat dried milk with 0.05% TWEEN 20). Membrane was washed and incubated with secondary antibody for 1 h. Membrane was washed and visualized by ECL.

3.3.4 Tissue processing, staining, and immunohistochemistry

Upon sacrifice, liver samples were immediately placed in 10% neutral buffered formalin (NBF) for 24 h, followed by 70% EtOH for 24 h. Samples were then paraffin-embedded, sectioned, and stained with hematoxylin and eosin (H&E). IHC was performed on paraffin-embedded samples as previously described (102, 103). Sections (5 µm) were cut from paraffin blocks, then deparaffinized in xylene and rehydrated in descending ethanol series. Protein staining was performed using DAKO EnVision Kit (Dako Corp., Carpinteria, CA). Sections were incubated overnight at 4°C with monoclonal antibodies diluted in 0.05M Tris-HCL + 1% BSA against F4/80 (1:100), BrdU (1:1000), or PCNA (1:2000). After 3 washes with TBST, the sections were incubated for 30 min with secondary antibody labeled with peroxidase, then washed 3 times with TBST. Lastly, peroxidase substrate DAB was added for staining. All sections were counterstained with hematoxylin and observed by light microscopy. For negative controls, primary antibody was omitted from the above protocol.

3.3.5 Protein preparation and Western immunoblot

Western blotting was performed as previously described (104). Tissues were lysed with TNN buffer using a tissue grinder, then placed on ice for 30 m. Lysates were clarified by centrifugation ($10,000 \times g$ for 30 min at 4°C) and protein concentrations determined using the method of Bradford. Briefly, total protein ($60 \mu\text{g}$) was resolved on a 10% Nu-PAGE Bis-Tris gel and transferred to PVDF membranes. Filters were incubated overnight at 4°C in blotting solution (Tris-buffered saline containing 5% nonfat dried milk and 0.1% Tween 20), followed by a 1 h incubation with primary antibodies. Filters were washed three times in Tris-buffered saline containing 0.1% Tween 20 and incubated with horseradish peroxidase-conjugated secondary antibodies for 1 h. After three additional washes, the immune complexes were visualized by ECL detection.

3.3.6 Tissue cytokine ELISA

Frozen liver samples were pulverized by mortar and pestle in liquid nitrogen. Protein was then extracted using a method previously described (114, 115). Ice-cold protein extraction buffer, consisting of 0.1% Igepal CA-630 nonionic detergent in PBS with a protease inhibitor cocktail tablet (Complete Mini), was added to pulverized tissue ($50 \mu\text{l}$ to 10 mg of tissue), and vortexed every 10 min for 30 min. The resultant homogenate was transferred to a microcentrifuge tube and centrifuged at 4°C for 10 min at $12 \times g$, and supernatant was collected for use in colorimetric ELISA for TNF- α or IL-6. Briefly, $50 \mu\text{l}$ of supernatant was added to $50 \mu\text{l}$ of assay diluent (1:1 dilution) in a 96-well plate. After a 2 h incubation, wells were aspirated and washed, conjugate was

added, and wells were again aspirated and washed after a 2 h incubation. Substrate solution was added to each well, and the plates were incubated in the dark for 30 min. Stop solution was then added, and optical density determined at 450 nm (with a correction wavelength set at 570 nm). Experiments were performed in duplicate to assure reproducibility.\

3.3.7 siRNA delivery study with F4/80 colocalization

A delivery study utilizing DY547-labeled NTC and p85 α siRNA duplexes was carried out in our laboratory to determine the distribution of labeled siRNA following hydrodynamic and regular tail vein injection, i.p. injection, and intrarectal administration (116). Tissues from this study were utilized to determine siRNA delivery to the liver and bone marrow; to further determine delivery to Kupffer cells and macrophages, additional staining with F4/80 was performed. Tissue samples were frozen sectioned and placed into 90% EtOH for 15 min. Samples were then blocked with 5% BSA in TBST for one hour, washed with TBST, and incubated with primary F4/80 antibody (1:500 dilution) for 1 h. Slides were washed with TBST, incubated with secondary antibody for 30 min, then placed briefly into Hoescht stain (1:10,000 dilution). Tissue samples were then examined with an Olympus BX51 microscope (Olympus, Central Valley, PA) and images were processed using Olympus DP Manager and DP Controller software (Olympus, Central Valley, PA). Three separate images were captured from each field examined, with blue representing nuclear staining, red representing DY547-labeled siRNA, and green representing F4/80 staining. Several representative images were taken from both liver and bone marrow.

3.3.8 Statistical analysis

Remnant liver weight as percent body weight was analyzed using analysis of variance for a two-factor factorial experiment. The two factors were assigned as operation (hepatectomy and sham) and siRNA or wortmannin (present and absent). Effects and interaction were assessed at the 0.05 and the 0.15 levels, respectively, of significance. Fisher's least significant difference procedure was used for multiple comparisons with Bonferroni adjustment for the number of comparisons. All statistical computations were conducted using the SAS[®] system, Release 9.1.

3.4 RESULTS

3.4.1 siRNA directed to the p85 α regulatory and p110 α catalytic subunits decreases hepatic regeneration following partial hepatectomy.

To determine the effects of selective p85 α subunit blockade on liver regeneration, female Swiss-Webster mice were randomized to receive either 70% partial hepatectomy or sham operation and further subdivided to receive either

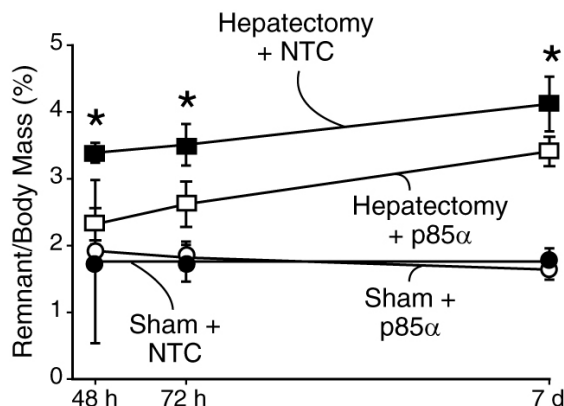


Fig. 3.1 **Selective inhibition of the p85 α regulatory subunit leads to decreased regeneration following liver resection.** Mice were randomized to either 70% hepatectomy or sham operation and then further subdivided to receive either NTC or p85 α siSTABLE siRNA; mice were sacrificed over a time course after operation, and wet remnant weight as a percent of body mass was determined. * = $p < 0.05$ vs. vehicle-treated mice. From Jackson et al (2008) (105), used with permission.

NTC siSTABLE siRNA or p85 α siSTABLE siRNA via hydrodynamic tail vein injection every 24 h. Mice were killed 48 h, 72 h, and 7 d following operation, and wet liver remnant weight was determined (Fig. 3.1). Following hepatectomy, mice treated with NTC siRNA demonstrated the expected increase in hepatic remnant wet weight (1.8% of body mass at the time of operation, 3.3% at 48 h, 3.5% at 72 h, and 4.0% by 7 d). Mice treated with p85 α siRNA demonstrated a significant decrease in liver regeneration relative to vehicle-treated mice at all timepoints. Liver mass in p85 α siRNA-treated mice increased from approximately 1.8% of body mass at the time of operation, to 2.3% at 48 h, 2.6% at 72 h, and 3.2% at 7 d. Body mass of mice treated with p85 α siRNA following hepatectomy decreased to a similar extent as mice treated with NTC siRNA; there were no systemic toxic effects of treatment with p85 α siRNA in mice undergoing sham operation or hepatectomy.

To further confirm that the decrease in hepatic regeneration is due to reduced hepatocyte proliferation, BrdU incorporation was compared in mice treated with NTC or p85 α siRNA by DNA dot blot (Fig. 3.2). Mice treated with NTC siRNA demonstrated an expected increase in DNA synthesis at 48 h and 72 h following hepatectomy; this induction of DNA synthesis was inhibited by p85 α siRNA.

To confirm that treatment with p85 α siRNA led to a decrease in PI3K activation following hepatectomy, Western blot analysis of protein isolates was performed for pAkt with densitometric analysis (Fig. 3.3), as well as other markers of liver regeneration, including pStat3, cyclin D1, and MAPK. Following hepatectomy, mice treated with p85 α siRNA

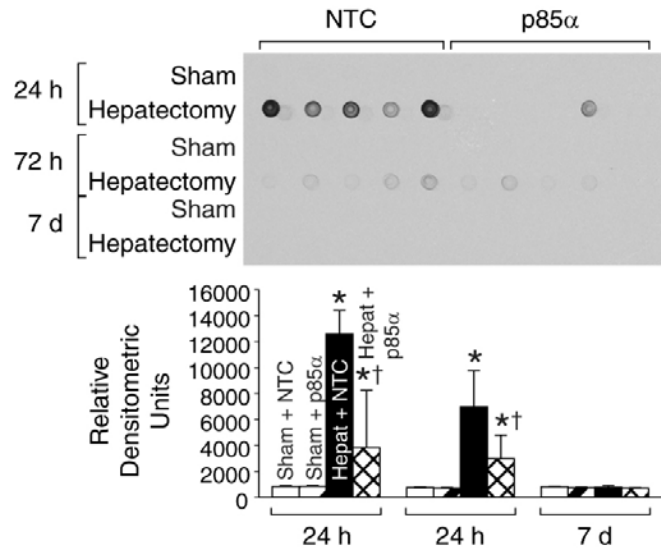


Fig. 3.2 Selective inhibition of the p85 α regulatory subunit leads to decreased regeneration as evidenced by decreased BrdU incorporation following liver resection. To measure DNA synthesis, BrdU was given ip 3h prior to sacrifice, and DNA dot blot with densitometry was performed. * = p<0.05 vs. sham-operated mice; † = p<0.05 vs. NTC siRNA-treated mice. From Jackson et al (2008) (105), used with permission.

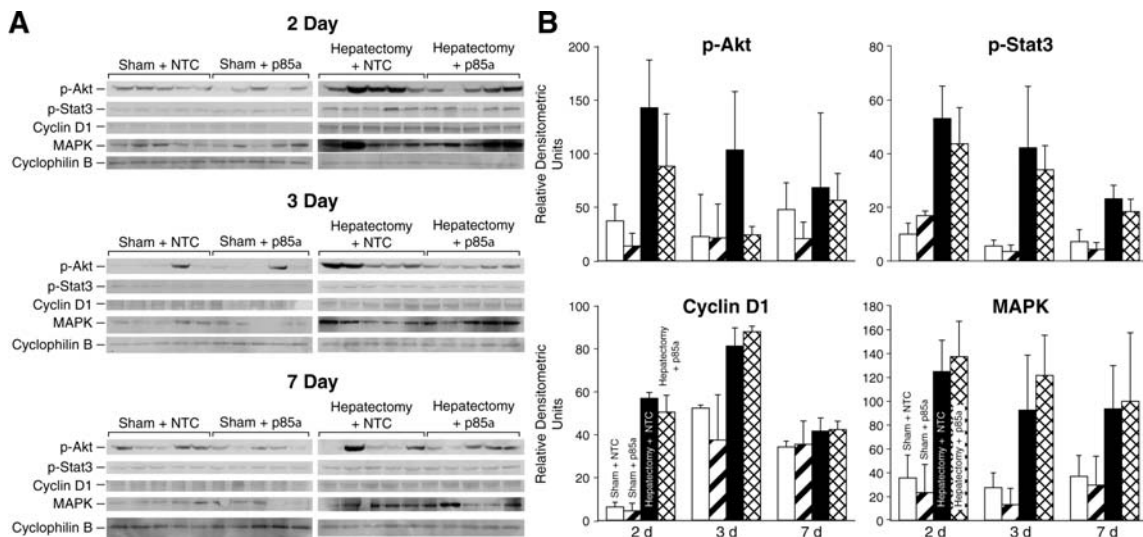


Fig. 3.3 Protein expression profiles following siRNA treatment. Western blot analysis of liver tissue lysates was performed as described in the Materials and Methods to determine pAkt, p-Stat3, cyclin D1, and p38 MAPK expression in mice treated with either NTC or p85 α siRNA who underwent sham operation or hepatectomy, and presented here with densitometry; cyclophilin B served as a loading control. From Jackson et al (2008) (105), used with permission.

showed decreased pAkt expression at 48 h and 72 h relative to mice treated with NTC siRNA. Expression of pStat3, cyclin D1, and p38 MAPK were not statistically significantly different between the two treatment groups.

Next, to determine the effects of selective p110 α subunit blockade on liver regeneration and to confirm our previous results

using p85 α siRNA, female Swiss-Webster mice were randomized to receive either 70% partial hepatectomy or sham operation; they were further subdivided to receive either NTC siSTABLE siRNA, p85 α siSTABLE siRNA, or p110 α siSTABLE siRNA via hydrodynamic tail vein injection every 24 h. Mice were killed 48 h, 72 h, and 7 d following operation, and wet liver remnant weight was measured (Fig. 3.4). As previously described, following hepatectomy, mice treated with NTC siRNA demonstrated the expected gradual increase in hepatic remnant wet weight. However, liver regeneration was significantly inhibited in p110 α siRNA-treated mice. Results for p85 α siRNA were identical to those previously shown.

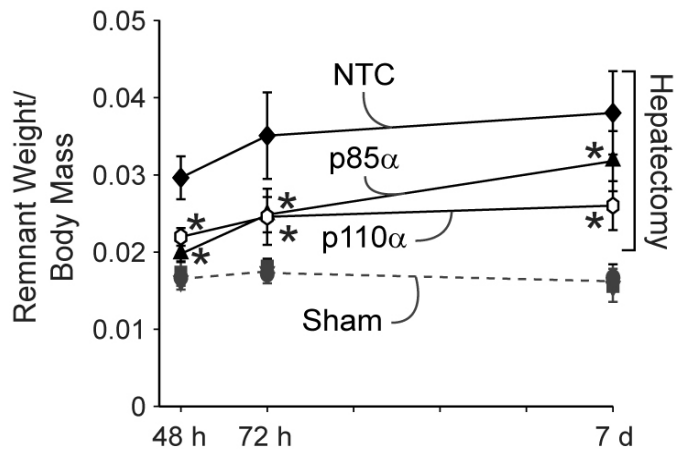


Fig. 3.4 Selective inhibition of the p85 α regulatory or the p110 α catalytic subunit leads to decreased regeneration following liver resection. Mice were randomized to either 70% hepatectomy or sham operation and then further subdivided to receive either NTC, p85 α , or p110 α siSTABLE siRNA; mice were sacrificed over a time course after operation, and wet remnant weight as a percent of body mass was determined. * = p<0.05 vs. NTC siRNA-treated mice. From Jackson et al (2008) (105), used with permission.

To again confirm that the decrease in hepatic regeneration is due to reduced hepatocyte proliferation, BrdU incorporation was

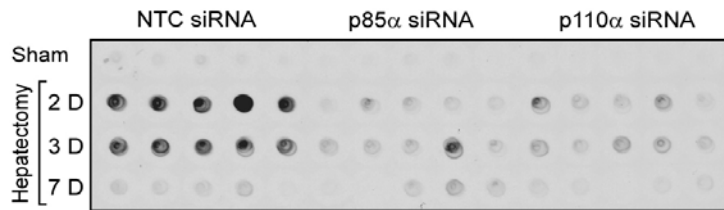


Fig. 3.5 Selective inhibition of the p85 α regulatory or the p110 α catalytic subunit leads to decreased regeneration as evidenced by decreased BrdU incorporation following liver resection. To measure DNA synthesis, BrdU was given ip 3h prior to sacrifice. From Jackson et al (2008) (105), used with permission.

compared by DNA dot blot (Fig. 3.5). Mice treated with NTC siRNA demonstrated an expected increase in DNA synthesis at 48 h and 72 h following hepatectomy, as previously described; however, mice treated with p110 α siRNA did not experience a similar increase. BrdU immunohistochemistry (IHC) was also performed to confirm dot blot results; representative staining patterns are presented in Figure 3.6.

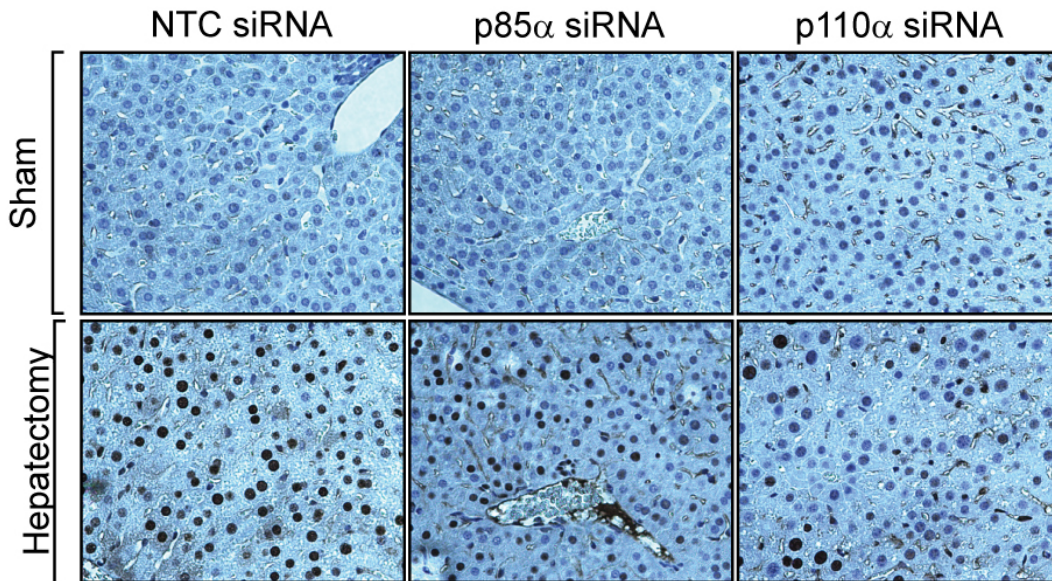


Fig. 3.6 Selective inhibition of the p85 α and p110 α regulatory subunit leads to decreased regeneration as evidenced by decreased BrdU incorporation following liver resection. IHC was performed with anti-BrdU antibody to confirm decreased staining in p85 α - and p110 α -siRNA treated mice relative to NTC-treated mice. Representative samples were taken at the 48 h time point for consistency. From Jackson et al (2008) (105), used with permission.

Western blot analysis of tissues was performed to assess for differences in protein expression between mice treated with p85 α or p110 α siRNA (Fig. 3.7A). While there appeared to be a slight decrease in p85 α expression with p85 α siRNA treatment, and slight decrease in p110 α with p110 α siRNA treatment in mice undergoing hepatectomy, the knockdown did not appear to be significant. Therefore, we performed real time quantitative PCR (RT-PCR) to assess p85 α and p110 α mRNA expression (Fig. 3.7B).

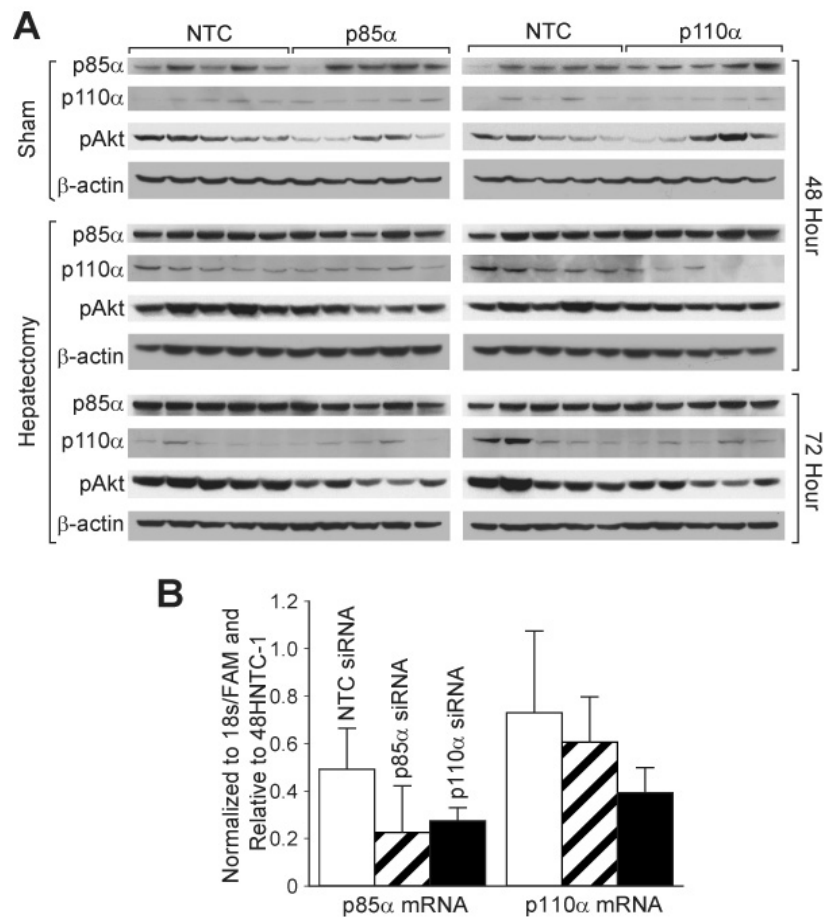


Fig. 3.7 Protein expression patterns following siRNA treatment. A. Western blot analysis of liver tissue lysates was performed as described in the Materials and Methods to determine p85 α , p110 α , and pAkt expression in mice treated with either NTC or p110 α siRNA who underwent sham operation or hepatectomy; β -actin served as a loading control. B. Real time quantitative PCR was performed on RNA isolated from livers at the 48h time point to determine p85 α and p110 α subunit knockdown. Results were normalized to 18s/FAM. From Jackson et al (2008) (105), used with permission.

While there again appeared to be decreased p85 α mRNA in mice treated with p85 α siRNA, and decreased p110 α mRNA in mice treated with p110 α siRNA, this difference was not statistically significant.

Next, to determine if p85 α and p110 α siRNA administration led to decreased liver regeneration by inhibiting the essential priming reaction, we repeated the experiment above without siRNA pre-treatment; instead, mice were given NTC, p85 α , or p110 α siRNA via hydrodynamic tail vein injection 6h following sham operation or hepatectomy to allow for the completion of the priming response. Interestingly, there was no statistically significant difference in liver regeneration between mice treated with

NTC, p85 α , or p110 α siRNA (Fig. 3.8). This suggests an important role for PI3K in the early response to liver resection, including the initiation of the priming response.

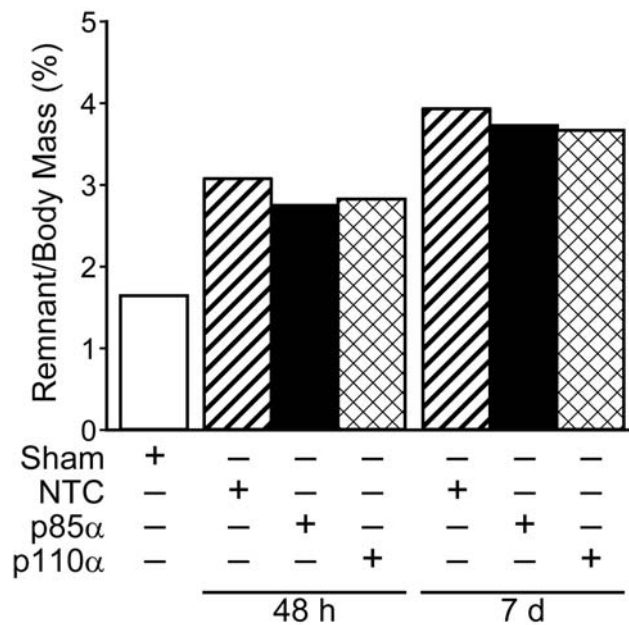


Fig. 3.8 Treatment with p85 α and p110 α siRNA following priming reaction leads to full liver regeneration. Mice were randomized to either 70% hepatectomy or sham operation and then further subdivided to receive either NTC, p85 α , or p110 α siRNA; mice were sacrificed 48h and 7d after operation, and wet remnant weight as a percent of body mass was determined.

3.4.2 Selective inhibition of the p85 α regulatory or the p110 α catalytic subunit decreases macrophage infiltration and Kupffer cell hyperplasia/hypertrophy

Given the known importance of the PI3K pathway in macrophage migration and

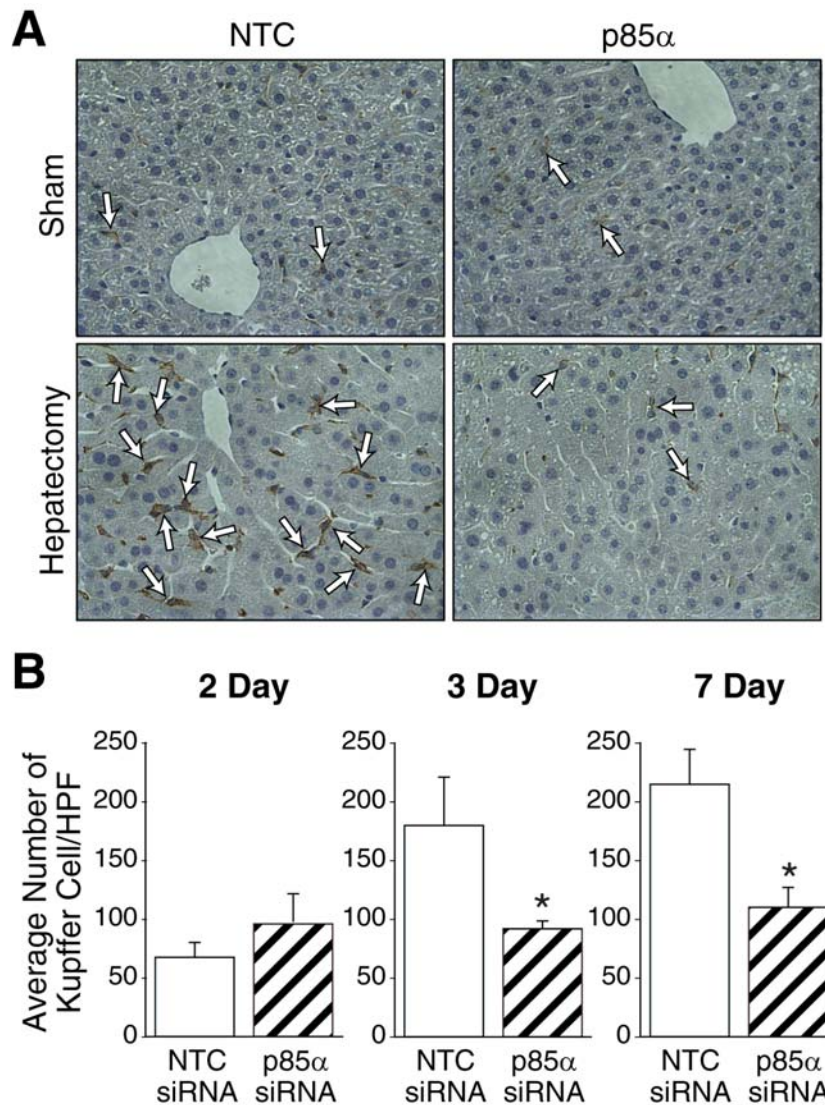


Fig. 3.9 Selective inhibition of the p85 α regulatory subunit decreases macrophage infiltration and Kupffer cell hyperplasia/ hypertrophy. (A) IHC for F4/80 was performed on mice undergoing sham operation or liver resection treated with NTC or p85 α siRNA; representative sections are shown from the 72h timepoint. Arrows indicate F4/80 staining cells. Magnification: x200. (B) Slides stained for F4/80 were presented to a pathologist in a blinded fashion, and number of positive cells per 8 high power fields were counted. Bars represent average and SD of 8 fields; asterisks indicate statistically significant changes. *= $P \leq 0.01$ relative to NTC siRNA-treated mice. From Jackson et al (2008) (105), used with permission.

cytokine production (4, 11, (73), we next performed F4/80 IHC staining on liver samples from mice undergoing sham operation or liver resection treated with NTC- or p85 α siRNA (Fig. 3.9A). Following hepatectomy, mice treated with NTC siRNA demonstrated an increase in F4/80 positive cells (67 ± 13 at 48 h; 180 ± 41 at 72 h; and 214 ± 30 at 7 d) concentrated around the central vein and scattered throughout the parenchyma. However, mice treated with p85 α siRNA showed no increase in F4/80 positive cells (95 ± 25 at 48 h; 92 ± 6 at 72 h; and 109 ± 16 at 7 d) over the same time course (Fig. 3.9B).

To confirm prior findings that macrophage migration and Kupffer cell hyperplasia was decreased in mice treated with PI3K inhibitors, we next performed F4/80 IHC staining on liver samples from mice undergoing sham operation or liver resection treated with NTC, p85 α , or p110 α

siRNA (Fig. 3.10). Following hepatectomy, mice treated with NTC siRNA again demonstrated a gradual increase in F4/80 positive cells concentrated around the central vein and scattered throughout the parenchyma. However, mice treated with p85 α or p110 α siRNA showed no increase in

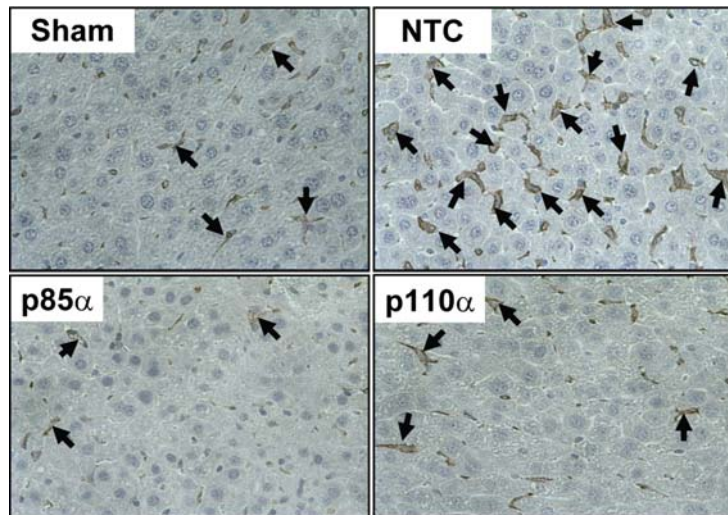


Fig. 3.10 Inhibition of the p85 α regulatory or p110 α catalytic subunit decreases macrophage infiltration and Kupffer cell hyperplasia/ hypertrophy. To confirm our findings, IHC for F4/80 was performed on mice undergoing sham operation or liver resection treated with NTC, p85 α , or p110 α siRNA; representative sections are shown from the 72 h timepoint. Arrows indicate F4/80 staining cells. Magnification: x400. From Jackson et al (2008) (105), used with permission.

F4/80 positive cells over the same time course. To determine whether the decreased number of F4/80 positive cells, coupled with PI3K inhibition, could translate to decreased cytokine expression, we performed tissue cytokine analysis for TNF- α (Fig. 3.11) and IL-6 (Fig. 3.12) on protein lysate from mice undergoing sham operation or hepatectomy and treatment with NTC, p85 α , or p110 α siRNA, with sacrifice at earlier time points (2 h, 4 h, 6 h, and 12 h). As suspected, we found statistically significantly higher levels of both TNF- α and IL-6 in the regenerating livers of mice treated with NTC siRNA at 4 h and 6 h following hepatectomy relative to p85 α and p110 α siRNA treated mice.

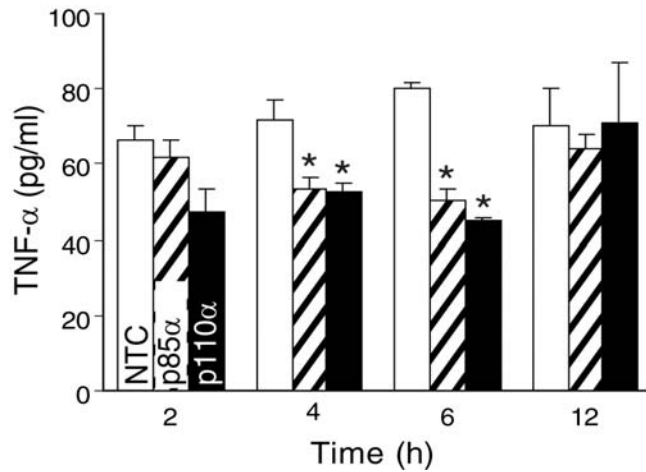


Fig. 3.11 Selective inhibition of the p85 α regulatory or the p110 α catalytic subunit decreases TNF- α expression. To determine if the reduced number of F4/80 staining cells present in liver of p85 α or p110 α siRNA-treated mice translated to decreased tissue cytokine expression, tissue cytokine ELISAs were performed for TNF- α at 2, 4, 6, and 12h time points as described in the Materials and Methods. Results are expressed as pg/ml. *=P \leq 0.01 relative to NTC siRNA-treated mice. From Jackson et al (2008) (105), used with permission.

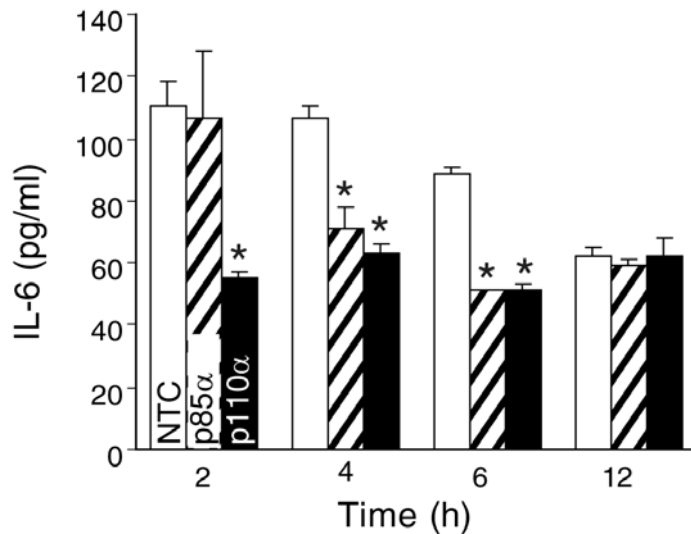


Fig. 3.12 Selective inhibition of the p85 α regulatory or the p110 α catalytic subunit decreases IL-6 expression. To determine if the reduced number of F4/80 staining cells present in liver of p85 α or p110 α siRNA-treated mice translated to decreased tissue cytokine expression, tissue cytokine ELISAs were performed for IL-6 at 2, 4, 6, and 12h time points as described in the Materials and Methods. Results are expressed as pg/ml. *=P \leq 0.01 relative to NTC siRNA-treated mice. From Jackson et al (2008) (105), used with permission.

In an effort to determine whether siRNA was indeed taken up by macrophages, and to determine if siRNA was also delivered to hepatocytes, we performed an siRNA delivery study with DY547-labeled NTC and p85 α siRNA (116). Additionally, we stained with F4/80 to determine if Kupffer cells and macrophages expressed the siRNA. Figure 3.13 represents liver samples harvested from a mouse treated with p85 α DY547-labeled siRNA, delivered via tail vein injection, 24 h following one-time injection. To our surprise, there was very little delivery of siRNA to the hepatocytes, but there appeared to be high concentrations of labeled siRNA within the Kupffer cells and macrophages present within the liver. Similarly, there was significant uptake of siRNA by the bone marrow, including the majority of F4/80 cells present. Therefore, we hypothesize that the lack of significant p85 α and p110 α knockdown as detected by WB and RT-PCR is due to a relatively selective delivery of siRNA to Kupffer cells, which compose the minority of hepatic cellular mass.

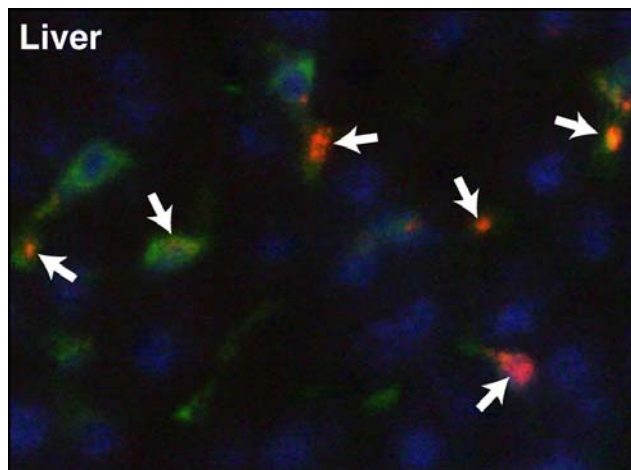


Fig. 3.13 siRNA uptake within the liver is predominantly by Kupffer cells. siRNA delivery to the liver was confirmed by injection of mice with DY547-labeled p85 α siRNA; additional staining with anti-F4/80 antibody was performed to determine colocalization of F4/80 with siRNA. Representative sections are shown for liver from a mouse treated with one-time tail vein injection of labeled siRNA sacrificed 24h following injection. Red = DY547-labeled siRNA; green = F4/80; blue = Hoescht nuclear stain. From Jackson et al (2008) (105), used with permission.

3.4.3 Selective inhibition of the p85 α regulatory or the p110 α catalytic subunit led to cellular injury after partial hepatectomy

H&E staining was performed on liver samples from mice undergoing sham operation or liver resection treated with NTC, p85 α , or p110 α siRNA (Fig. 3.14). We identified a widespread vacuolar appearance in the livers of mice undergoing liver resection that had been treated with p85 α or p110 α siRNA, in contrast to the normal appearance of the regenerating liver in NTC siRNA-treated mice (Fig. 3.14, right panels); this appearance has been previously termed panlobular hydropic vacuolization, and has been described in association with inhibition of hepatocyte priming following liver resection (106). Notably, the liver of sham-operated mice treated with p85 α or p110 α siRNA lacked this histological finding (Fig. 3.14, left panels). To further investigate the architectural changes found in these mice, we performed PAS staining for glycogen (Fig. 3.15) and ORO staining for lipid (Fig. 3.16), and found widespread glycogen and lipid deposition, respectively, throughout the livers of mice undergoing liver resection and treated with p85 α or p110 α siRNA relative to NTC-treated mice (Fig. 3.15 and 3.16, right panels). Again, we found no change in lipid or glycogen deposition in sham-operated mice treated with siRNAs (Fig. 3.15 and 3.16, left panels).

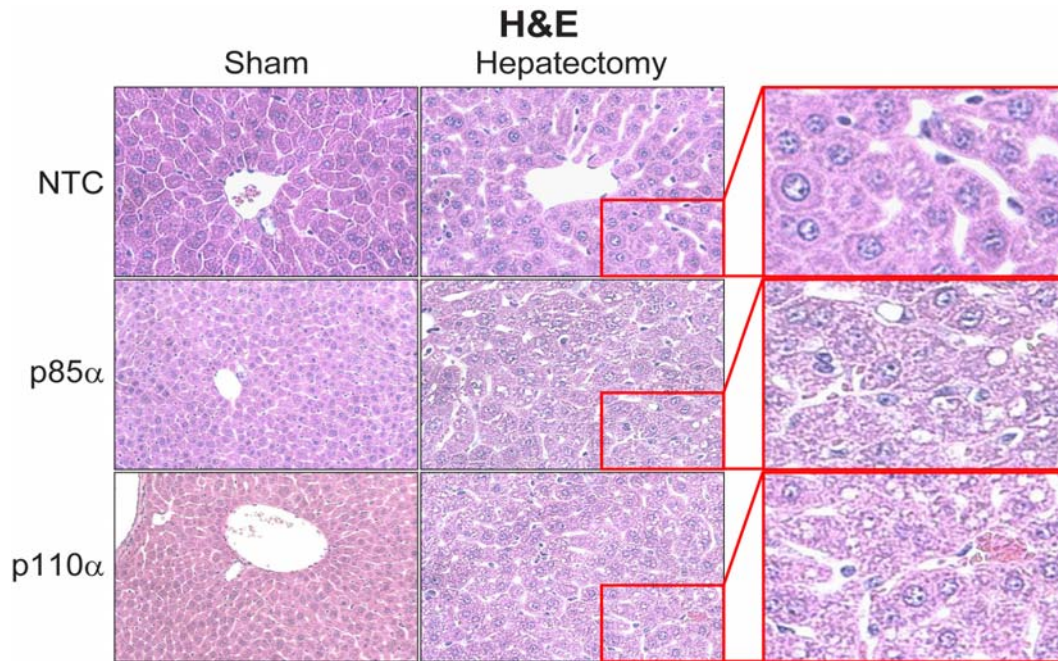


Fig. 3.14 Selective inhibition of the p85 α regulatory or the p110 α catalytic subunit conferred a vacuolar appearance to the regenerating liver. H&E staining was performed on formalin-fixed, paraffin embedded liver samples. Representative sections are shown for NTC-, p85 α -, and p110 α siRNA-treated mice sacrificed at the 48 h time point. From Jackson et al (2008) (105), used with permission.

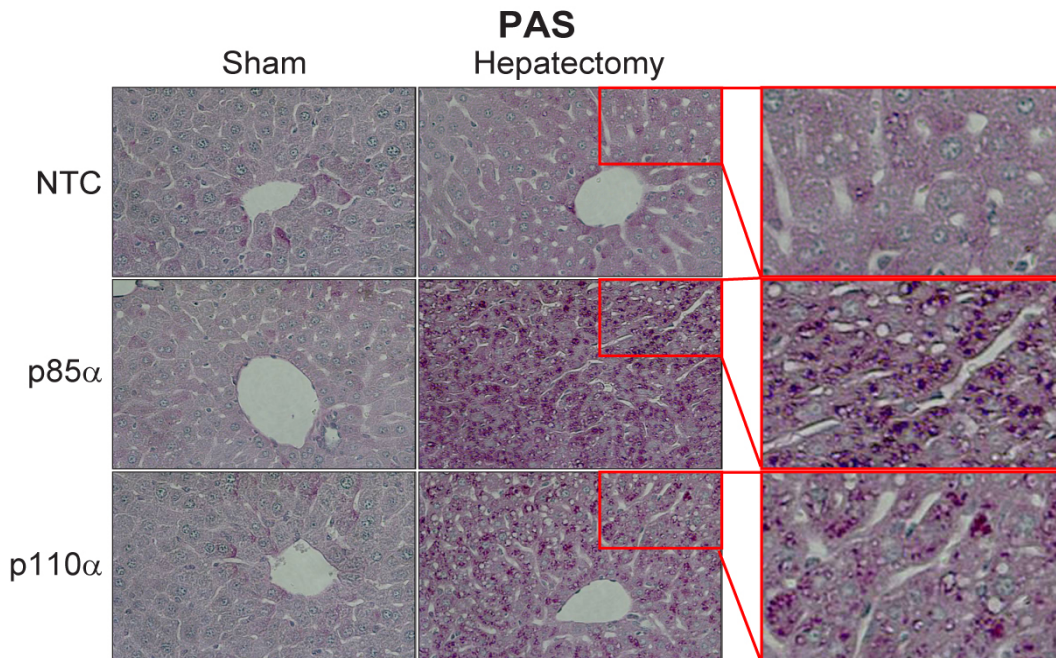


Fig. 3.15 Selective inhibition of the p85 α regulatory or the p110 α catalytic subunit led to increased glycogen deposition within hepatocytes. PAS staining was performed on formalin-fixed, paraffin embedded liver samples. Representative sections are shown for NTC-, p85 α -, and p110 α siRNA-treated mice sacrificed at the 48 h time point. From Jackson et al (2008) (105), used with permission.

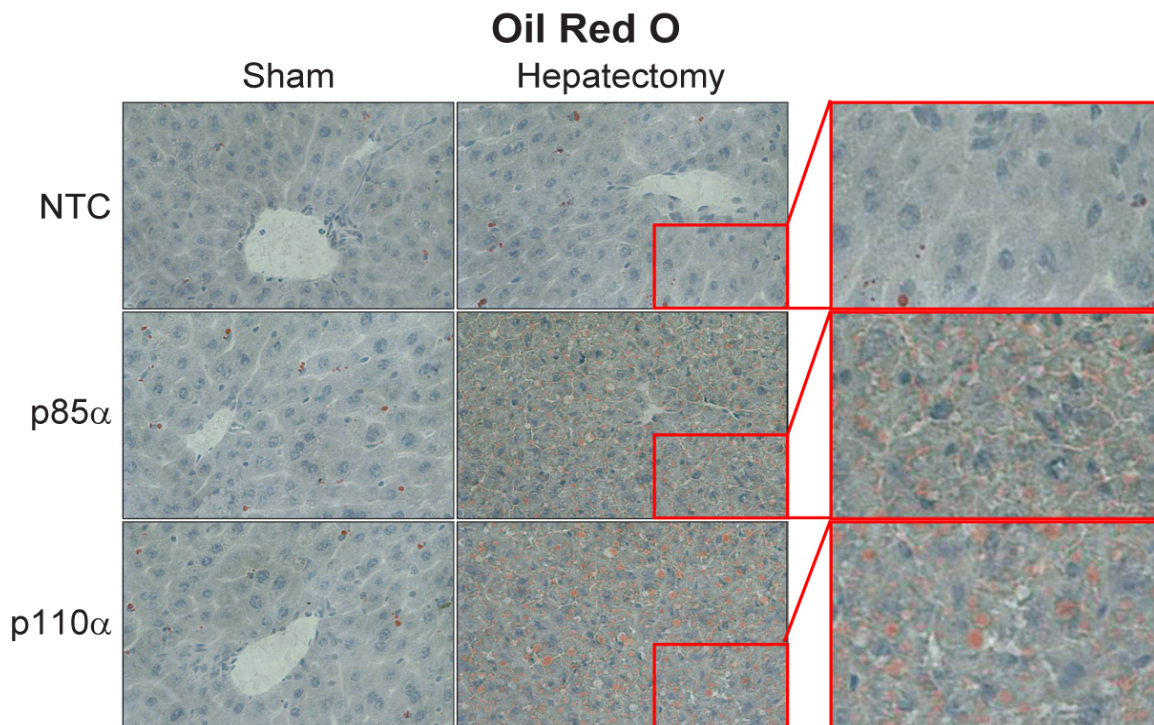


Fig. 3.16 Selective inhibition of the p85 α regulatory or the p110 α catalytic subunit led to increased lipid deposition within hepatocytes. Oil red O staining was performed on frozen-sectioned liver samples. Representative sections are shown for NTC-, p85 α -, and p110 α siRNA-treated mice sacrificed at the 48 h time point. From Jackson et al (2008) (105), used with permission.

Given the importance of autophagy, a regulated degradation process that recycles cellular proteins, nutrients, and organelles through the action of autophagosomes, to hepatocyte survival during periods of nutritional deprivation and cellular stress (117, 118), we next performed IHC for microtubule-associated protein 1 light chain 3 (LC3), a known marker of autophagosomes (117). Fig. 3.17 summarizes the results of LC3 staining within the regenerating livers of mice treated with NTC, p85 α , or p110 α siRNA; there was no LC3 staining noted within the livers of sham-operated mice (data not shown). NTC-treated mice, represented in the left panel, lacked LC3 staining throughout the liver. In contrast, LC3 staining of regenerating liver from p85 α and p110 α siRNA-treated mice demonstrated a heterogenous, patchy nature of LC3 staining; while there were some areas were completely devoid of LC3 positivity, others demonstrated

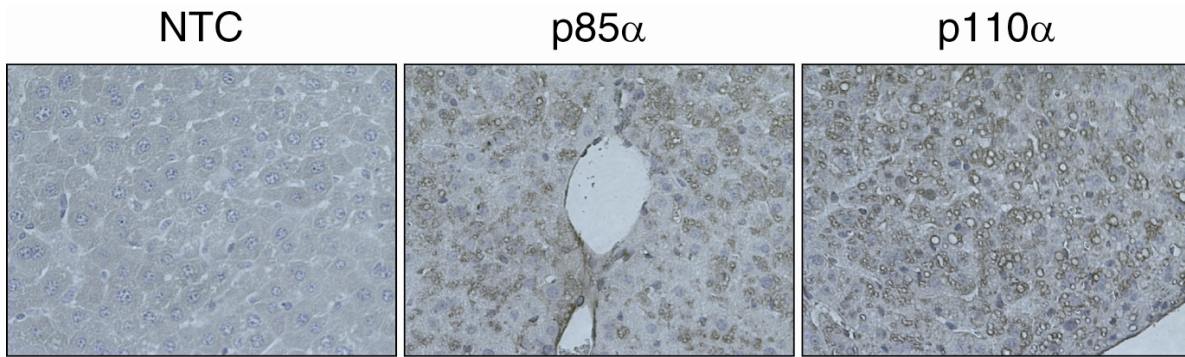


Fig. 3.17 Evidence of autophagy within the p85 α and p110 α siRNA-treated regenerating liver. LC3 staining was performed on paraffin-embedded, sectioned liver samples. Representative sections are shown for NTC-, p85 α -, and p110 α siRNA-treated mice sacrificed at the 48 h time point.

conglomerations of positively-staining cells, as illustrated in the middle and right panels below. To further explore the possibility that p85 α and p110 α siRNA treatment may stimulate an autophagic response, transmission electron microscopy (TEM) was performed on a representative formalin-fixed, paraffin-embedded sample from a mouse undergoing

liver resection and treated with p85 α siRNA, sacrificed 72 h following resection. While large vacuoles, abundant mitochondria and accumulation of endoplasmic reticulum (ER) were clearly visualized, with lipid present within the vacuoles, no autophagic vacuoles were clearly identified within the section examined (Fig. 3.18).

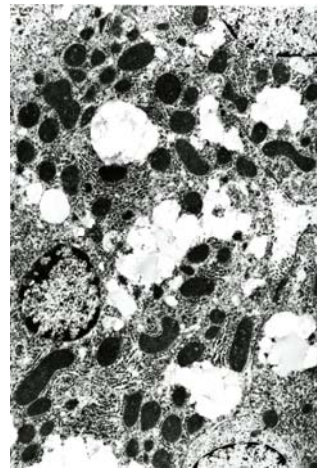


Fig. 3.18 Large vacuoles, abundant mitochondria and accumulation of endoplasmic reticulum (ER) within a hepatocyte of p85 α siRNA-treated mouse. Electron microscopy was performed on a frozen-sectioned specimen of mouse liver 72h following liver resection and p85 α siRNA treatment.

3.4 DISCUSSION

Class I PI3Ks are heterodimers composed of a regulatory (p85) and catalytic (p110) subunit; the regulatory p85 subunit is essential for the stability of the p110 catalytic subunit and for its recruitment to activated receptor tyrosine kinases or G-protein-coupled receptors. Although PI3K has been shown to be important for the proliferation of various cell types, including intestinal epithelial cells, pancreatic acinar cells, and vascular endothelial cells (70, 72, 99) and important for leukocyte trafficking, signaling, and phagocytosis (107) its role in hepatic regeneration is not known. In our present study, we demonstrate these major findings: (1) selective inhibition of the PI3K subunits p85 α and p110 α using siRNA markedly decreases the regenerative response of the liver after resection, and leads to vacuolar architectural changes with glycogen and lipid deposition; and (2) total or selective PI3K inhibition leads to a decreased number of Kupffer cells and infiltrating macrophages, with concomitant decrease in cytokine expression, within the regenerating liver.

The recruitment of leukocytes to sites of inflammation or regeneration relies on their ability to recognize chemoattractants, reorganize their cytoskeleton and membrane structure in response to such stimulants, undergo transendothelial cell migration, and interact with adhesion molecules expressed at sites of inflammation (66). The PI3K pathway plays a pivotal role in each step of this process, and studies have suggested differential roles for the various catalytic subunits of class I PI3Ks based on cell type. One study found that p110 α inhibition leads to complete inhibition of macrophage

colony stimulating factor (M-CSF)-mediated DNA synthesis in a macrophage cell line, and p110 β or p110 δ isoform inhibition leads to impaired lamellipodia formation and macrophage migration (73). Another study utilizing p85 $\alpha^{-/-}$ murine bone-marrow derived macrophages concluded that the p85 α subunit is required for the regulation of multiple actin-based functions in these cells, including adhesion, migration, wound healing, and phagocytosis (112). A third study found that p110 γ or p110 δ deficiency results in defective selectin-mediated adhesion of neutrophils, and a failure of accumulation of these leukocytes in an acute lung injury model (66). Thus, PI3K-mediated regulation of leukocyte activation and migration is complex and still poorly understood. In our present study, we identified preferential uptake of labeled siRNA into the reticuloendothelial system, including Kupffer cells and F4/80+ cells within the bone marrow, and hypothesize that total or selective PI3K inhibition leads to decreased Kupffer cell hyperplasia and hypertrophy, as well as decreased mobilization of bone marrow progenitor cells and circulating macrophages into the regenerating liver.

Circulating macrophages and resident Kupffer cells play a critical role in hepatic regeneration following resection. Aldeguer et al (46) utilized a murine model of bone marrow transplantation coupled with 70% hepatectomy to determine the contribution of bone-marrow derived cells to liver regeneration and found that complete replacement of IL-6 $^{+/+}$ bone marrow into IL-6 $^{-/-}$ irradiated mice restored regeneration after partial hepatectomy. However, complete replacement of IL-6 $^{-/-}$ bone marrow into IL-6 $^{+/+}$ irradiated mice significantly inhibited liver regeneration; regeneration can be restored in this case by administration of IL-6. Similarly, experiments utilizing GFP-labeled bone

marrow cells have demonstrated an important role for the bone marrow in repopulation of the resected liver, where a majority of cells (70%) commit to an endothelial cell lineage and others (28%) to a Kupffer cell lineage (47). Other studies have used models of Kupffer cell depletion (liposome-encapsulated dichloromethylene-diphosphonate [Cl_2MDP], gadolinium chloride [GdCl_3], or pentoxifylline) to demonstrate that a >90% reduction in Kupffer cells leads to significantly impaired liver regeneration following 70% hepatectomy in mice or rats; this response is attributed to a significant decrease in $\text{TNF}\alpha$ production (48-50). Additionally, utilizing the GdCl_3 model of Kupffer cell depletion, another group confirmed that Kupffer cell depletion significantly decreased liver regeneration and abolished hepatic expression of IL-6, HGF, and $\text{TNF}\alpha$; (119) similarly, the administration of $\text{TNF}\alpha$ antibody to mice following hepatectomy significantly inhibited regeneration (27). Given the known importance of IL-6 and $\text{TNF}\alpha$ to the priming of quiescent hepatocytes to enter the cell cycle, it is clear that macrophages and Kupffer cells are central to the early regenerative response of the liver, and that the bone marrow does contribute, in part, to the increase in Kupffer cell number following hepatectomy. In our current study, we found that there were significantly fewer F4/80 positive cells present in the regenerating livers of mice treated with total or selective PI3K inhibitors; this correlated with a decrease in cytokine production, as reflected by decreased tissue IL-6 and $\text{TNF}\alpha$ cytokine levels. Therefore, we propose that PI3K inhibition leads not only to decreased Kupffer cells and macrophages within the regenerating liver, but secretory dysfunction of Kupffer cells and macrophages present, resulting in decreased cytokine production and reduced hepatocyte priming. This leads to

decreased liver regeneration in wortmannin, p85 α , or p110 α siRNA-treated mice following resection.

In addition to its role in leukocyte trafficking, signaling, and phagocytosis, class I PI3Ks play an important role in cell survival and proliferation. The growth factors HGF, EGF, and TGF α , responsible for the progression of hepatocytes from the G₁ to S phase of the cell cycle after priming by IL-6 and TNF α , signal through receptor tyrosine kinases which, in the activated state, associate with cytosolic proteins rich in Src-homologies, such as PI3K (14, 36). Downstream signaling leads to the activation of MAPK cascades, ultimately leading to cell proliferation (36). Therefore, it can be assumed that PI3K inhibition in this setting would lead to altered growth factor signaling; alternate pathways likely compensate over time, such that late liver regeneration may be possible. Given its solubility and wide volume of distribution, treatment with wortmannin is likely to inhibit all cell types present within the liver and likely alters hepatocyte PI3K response to growth factors and cytokines in addition to its action on macrophages and Kupffer cells (120). However, we did not identify significantly higher attenuation of regeneration in wortmannin-treated mice relative to mice treated with p85 α or p110 α siRNA. Thus, we propose that decreased hepatocyte priming via decreased cytokine production is the primary mechanism of regeneration attenuation with PI3K inhibition.

Additionally, PI3K inhibition and attenuation of regeneration leads to a widespread panlobular hydropic vacuolization, with accumulation of mitochondria and ER, which may be characteristic of a nonspecific hepatocellular injury response. In this setting, we noticed an accumulation of glycogen and lipid. We hypothesized that the

vacuolization present in these samples may represent an autophagic response to injury. We based this on several facts: (1) Autophagy within hepatocytes is characterized by an accumulation of lipid, secondary to decreased protein synthesis and subsequent utilization of lipid for lipid-protein conjugation (117), and (2) there is evidence that glycogen accumulation is associated with autophagy (121, 122). Therefore, we stained with LC3, a known marker of autophagosomes, and identified patchy positivity within the regenerating liver of mice treated with p85 α and p110 α siRNA, suggesting that within certain portions of the liver, an autophagic response was indeed induced. We propose that with PI3K inhibition and decreased priming of hepatocytes to enter the cell cycle, the cells sense an accumulation of reactive oxygen species (ROS) and other toxic hepatocellular metabolites which normally drives the proliferative response (12), but are unable to respond with cell cycle entry; instead, these cells induce a survival pathway--in this case, autophagy--in an effort to evade apoptosis. Interestingly, knockout of all isoforms of p85 α in mice leads to perinatal death secondary to extensive hepatocyte necrosis and chylous ascites (113); however, the etiology of liver injury in these knockout mice has not yet been described.

We conclude that the PI3K pathway is an important early regulator of hepatic regeneration following partial hepatectomy. We suggest a dual mechanism of action in this case: (1) PI3K is important for the migration of macrophages to the site of regeneration; inhibition leads to decreased IL-6 and TNF α expression and, ultimately, a lack in the priming mechanism central to early regeneration; this appears to be the central mechanism by which PI3K inhibition leads to attenuation of regeneration; and (2) PI3K

plays an important role in HGF, EGF, and TGF α -induced hepatocyte survival, DNA synthesis, and cell division.

3.5 CONCLUSIONS

Selective PI3K inhibition with both p85 α and p110 α siRNA led to significantly decreased liver regeneration and altered architecture of the regenerating liver, especially at the earliest time points, reminiscent of findings from our studies with wortmannin. Additionally, we found that PI3K inhibition led to a significantly reduced number of Kupffer cells present within the regenerating liver relative to mice treated with vehicle, suggesting that PI3K inhibition in this setting leads to decreased phagocytic cell migration and/or replication. We also describe significant aberrations in the architecture of the regenerating livers of mice treated with PI3K inhibitors, including the accumulation of lipids and glycogen with widespread vacuolization. We conclude that the PI3K pathway signaling is essential for ordered regeneration following liver resection; major roles include hepatocyte priming and cell cycle regulation following growth factor stimulation.

CHAPTER 4

SUMMARY AND FUTURE DIRECTIONS

4.1 Summary

Our lab has previously demonstrated that pancreatic regeneration is dependent on PI3K/Akt activation (72). This is consistent with findings that PI3K activation (i) is important for immediate remodeling and cell survival following myocardial infarction (98), (ii) mediates proliferative signals in intestinal epithelial cells *in vitro* and *in vivo* (69), and (iii) modulates vascular regeneration following insult (99). Although PI3K has been shown to be important for the proliferation of various cell types, including intestinal epithelial cells, pancreatic acinar cells, and vascular endothelial cells, and important for leukocyte trafficking, signaling, and phagocytosis, its specific role in hepatic regeneration has not been previously addressed. Here, we have described for the first time the following novel findings: (1) PI3K is activated following partial hepatectomy in mice, especially at the earliest timepoints; (2) total PI3K inhibition with the pharmacologic inhibitor wortmannin, or selective inhibition of the PI3K subunits p85 α and p110 α using siRNA, markedly decreases the regenerative response of the liver after resection; (3) PI3K inhibition leads to vacuolar architectural changes with glycogen and lipid deposition, with evidence of autophagy; (4) delayed administration of PI3K inhibitors leads to full liver regeneration, suggesting an early role for PI3K in the priming of subsequent regeneration; and (5) total or selective PI3K inhibition leads to decreased Kupffer cells and infiltrating macrophages, with concomitant decrease in cytokine expression, within the regenerating liver.

4.2 **Future directions**

Several important questions remain regarding the mechanism of action of PI3K inhibition in our studies, ie, specifically which cell type is predominantly affected. In an effort to address this question, the following experiment has been proposed to determine the role of the PI3K pathway in macrophage migration and secretion.

To further confirm that PI3K inhibition decreases cytokine expression and migration in macrophages, we will culture the mouse macrophage cell line RAW 264.7 and transfect cells with wortmannin or vehicle, or NTC, p85 α , or p110 α siRNA using DOTAP liposomal transfection reagent. Following 24h of treatment, cells will be stimulated with lipopolysaccharide (LPS), and cell supernatant will be harvested for TNF- α and IL-6 ELISA. In addition, we will perform a migration study on RAW cells treated with wortmannin or vehicle, or NTC, p85 α , or p110 α siRNA, utilizing the QCM Chemotaxis 5 μ m Cell Migration assay from Chemicon, with monocyte chemoattractant protein-1 (MCP-1) as a stimulant for migration. This will allow us to confirm that PI3K inhibition leads to decreased activation of macrophages, leading to decreased cytokine production and decreased migration *in vitro*.

BIBLIOGRAPHY

1. Sabiston's Textbook of Surgery: eds: Townsend, Jr, Beauchamp, Evers and Mattox; Philadelphia, PA: Elsevier; 2008.
2. Michalopoulos GK, DeFrances MC. Liver regeneration. *Science* 1997; 276:60-66.
3. McClusky DA, 3rd, Skandalakis LJ, Colborn GL, Skandalakis JE. Hepatic surgery and hepatic surgical anatomy: historical partners in progress. *World J Surg* 1997; 21:330-342.
4. Galen. Galen on the Usefulness of the Parts of the Body. Ithaca, NY: Cornell University Press; 1968.
5. Rutkauskas S, Gedrimas V, Pundzius J, Barauskas G, Basevicius A. Clinical and anatomical basis for the classification of the structural parts of liver. *Medicina (Kaunas)* 2006; 42:98-106.
6. da Carpi B. A Short Introduction to Anatomy. New York, NY: Kraus Reprint Co.; 1969
7. Lind LR. Studies in Pre-Vesalian Anatomy. Philadelphia, PA: American Philosophical Society; 1975.
8. da Vinci L. Leonardo da Vinci on the Human Body: The Anatomical, Physiological, and Embryological Drawings of Leonardo da Vinci. New York, NY: Crown Publishers; 1982.
9. Glisson F. *Anatomia hepatis*. Amstelaedami: Sumptibus Joannis Ravesteinii; 1654.
10. Fausto N, Campbell JS. The role of hepatocytes and oval cells in liver regeneration and repopulation. *Mech Dev* 2003; 120:117-130.
11. Fausto N. Liver regeneration and repair: hepatocytes, progenitor cells, and stem cells. *Hepatology* 2004; 39:1477-1487.
12. Fausto N, Campbell JS, Riehle KJ. Liver regeneration. *Hepatology* 2006; 43:S45-53.

13. Fausto N, Riehle KJ. Mechanisms of liver regeneration and their clinical implications. *J Hepatobiliary Pancreat Surg* 2005; 12:181-189.
14. Koniaris LG, McKillop IH, Schwartz SI, Zimmers TA. Liver regeneration. *J Am Coll Surg* 2003; 197:634-659.
15. Nikfarjam M, Malcontenti-Wilson C, Fanartzis M, Daruwalla J, Christophi C. A model of partial hepatectomy in mice. *J Invest Surg* 2004; 17:291-294.
16. Michalopoulos GK. Liver regeneration. *J Cell Physiol* 2007; 17:286-300.
17. Marubashi S, Sakon M, Nagano H, Gotoh K, Hashimoto K, Kubota M, Kobayashi S, Yamamoto S, Miyamoto A, Dono K, et al. Effect of portal hemodynamics on liver regeneration studied in a novel portohepatic shunt rat model. *Surgery* 2004; 136:1028-1037.
18. Taub R. Liver regeneration 4: transcriptional control of liver regeneration. *FASEB J* 1996; 10:413-427.
19. Taub R. Liver regeneration: from myth to mechanism. *Nat Rev Mol Cell Biol* 2004; 5:836-847.
20. Mars WM, Liu ML, Kitson RP, Goldfarb RH, Gabauer MK, Michalopoulos GK. Immediate early detection of urokinase receptor after partial hepatectomy and its implications for initiation of liver regeneration. *Hepatology* 1995; 21:1695-1701.
21. Sokabe T, Yamamoto K, Ohura N, Nakatsuka H, Qin K, Obi S, Kamiya A, Ando J. Differential regulation of urokinase-type plasminogen activator expression by fluid shear stress in human coronary artery endothelial cells. *Am J Physiol Heart Circ Physiol* 2004; 287:H2027-2034.
22. Masumoto A, Yamamoto N. Sequestration of a hepatocyte growth factor in extracellular matrix in normal adult rat liver. *Biochem Biophys Res Commun* 1991; 174:90-95.

23. Masumoto A, Yamamoto N. Stimulation of DNA synthesis in hepatocytes by hepatocyte growth factor bound to extracellular matrix. *Biochem Biophys Res Commun* 1993; 191:1218-1223.
24. Diehl A. The role of cytokines in hepatic regeneration. *Curr Opin in Gastroenterol* 1997; 13:525-533.
25. Kirillova I, Chaisson M, Fausto N. Tumor necrosis factor induces DNA replication in hepatic cells through nuclear factor kappaB activation. *Cell Growth Differ* 1999; 10:819-828.
26. Iimuro Y, Nishiura T, Hellerbrand C, Behrns KE, Schoonhoven R, Grisham JW, Brenner DA. NFkappaB prevents apoptosis and liver dysfunction during liver regeneration. *J Clin Invest* 1998; 101:802-811.
27. Akerman P, Cote P, Yang SQ, McClain C, Nelson S, Bagby GJ, Diehl AM. Antibodies to tumor necrosis factor-alpha inhibit liver regeneration after partial hepatectomy. *Am J Physiol* 1992; 263:G579-585.
28. Yamada Y, Fausto N. Deficient liver regeneration after carbon tetrachloride injury in mice lacking type 1 but not type 2 tumor necrosis factor receptor. *Am J Pathol* 1998; 152:1577-1589.
29. Yamada Y, Kirillova I, Peschon JJ, Fausto N. Initiation of liver growth by tumor necrosis factor: deficient liver regeneration in mice lacking type I tumor necrosis factor receptor. *Proc Natl Acad Sci U S A* 1997; 94:1441-1446.
30. Yamada Y, Webber EM, Kirillova I, Peschon JJ, Fausto N. Analysis of liver regeneration in mice lacking type 1 or type 2 tumor necrosis factor receptor: requirement for type 1 but not type 2 receptor. *Hepatology* 1998; 28:959-970.
31. Diehl AM, Yin M, Fleckenstein J, Yang SQ, Lin HZ, Brenner DA, Westwick J, Bagby G, Nelson S. Tumor necrosis factor-alpha induces c-jun during the regenerative response to liver injury. *Am J Physiol* 1994; 267:G552-561.

32. Rai RM, Yang SQ, McClain C, Karp CL, Klein AS, Diehl AM. Kupffer cell depletion by gadolinium chloride enhances liver regeneration after partial hepatectomy in rats. *Am J Physiol* 1996; 270:G909-918.
33. Cressman DE, Greenbaum LE, DeAngelis RA, Ciliberto G, Furth EE, Poli V, Taub R. Liver failure and defective hepatocyte regeneration in interleukin-6-deficient mice. *Science* 1996; 274:1379-1383.
34. Sakamoto T, Liu Z, Murase N, Ezure T, Yokomuro S, Poli V, Demetris AJ. Mitosis and apoptosis in the liver of interleukin-6-deficient mice after partial hepatectomy. *Hepatology* 1999; 29:403-411.
35. Maione D, Di Carlo E, Li W, Musiani P, Modesti A, Peters M, Rose-John S, Della Rocca C, Tripodi M, Lazzaro D, et al. Coexpression of IL-6 and soluble IL-6R causes nodular regenerative hyperplasia and adenomas of the liver. *EMBO J* 1998; 17:5588-5597.
36. Borowiak M, Garratt AN, Wustefeld T, Strehle M, Trautwein C, Birchmeier C. Met provides essential signals for liver regeneration. *Proc Natl Acad Sci U S A* 2004; 101:10608-10613.
37. Matsumoto K, Nakamura T. Emerging multipotent aspects of hepatocyte growth factor. *J Biochem* 1996; 119:591-600.
38. Wang X, DeFrances MC, Dai Y, Padiaditakis P, Johnson C, Bell A, Michalopoulos GK, Zarnegar R. A mechanism of cell survival: sequestration of Fas by the HGF receptor Met. *Mol Cell* 2002; 9:411-421.
39. Block GD, Locker J, Bowen WC, Petersen BE, Katyal S, Strom SC, Riley T, Howard TA, Michalopoulos GK. Population expansion, clonal growth, and specific differentiation patterns in primary cultures of hepatocytes induced by HGF/SF, EGF and TGF alpha in a chemically defined (HGM) medium. *J Cell Biol* 1996; 132:1133-1149.

40. Liu ML, Mars WM, Zarnegar R, Michalopoulos GK. Collagenase pretreatment and the mitogenic effects of hepatocyte growth factor and transforming growth factor-alpha in adult rat liver. *Hepatology* 1994; 19:1521-1527.
41. Patijn GA, Lieber A, Schowalter DB, Schwall R, Kay MA. Hepatocyte growth factor induces hepatocyte proliferation in vivo and allows for efficient retroviral-mediated gene transfer in mice. *Hepatology* 1998; 19:707-716.
42. Russell WE, Kaufmann WK, Sitaric S, Luetkeke NC, Lee DC. Liver regeneration and hepatocarcinogenesis in transforming growth factor-alpha-targeted mice. *Mol Carcinog* 1996; 15:183-189.
43. Bucher NL, Patel U, Cohen S. Hormonal factors concerned with liver regeneration. *Ciba Found Symp* 1977; 95-107.
44. Mitchell C, Nivison M, Jackson LF, Fox R, Lee DC, Campbell JS, Fausto N. Heparin-binding epidermal growth factor-like growth factor links hepatocyte priming with cell cycle progression during liver regeneration. *J Biol Chem* 2005; 280:2562-2568.
45. Fausto N. Liver regeneration. *J Hepatol* 2000; 32:19-31.
46. Aldeguer X, Debonera F, Shaked A, Krasinkas AM, Gelman AE, Que X, Zamir GA, Hiroyasu S, Kovalovich KK, Taub R, et al. Interleukin-6 from intrahepatic cells of bone marrow origin is required for normal murine liver regeneration. *Hepatology* 2002; 35:40-48.
47. Fujii H, Hirose T, Oe S, Yasuchika K, Azuma H, Fujikawa T, Nagao M, Yamaoka Y. Contribution of bone marrow cells to liver regeneration after partial hepatectomy in mice. *J Hepatol* 2002; 36:653-659.
48. Selzner N, Selzner M, Odermatt B, Tian Y, Van Rooijen N, Clavien PA. ICAM-1 triggers liver regeneration through leukocyte recruitment and Kupffer cell-dependent release of TNF-alpha/IL-6 in mice. *Gastroenterology* 2003; 124:692-700.

49. Boulton RA, Alison MR, Golding M, Selden C, Hodgson HJ. Augmentation of the early phase of liver regeneration after 70% partial hepatectomy in rats following selective Kupffer cell depletion. *J Hepatol* 1998; 29:271-280.
50. Duffield JS, Forbes SJ, Constandinou CM, Clay S, Partolina M, Vuthoori S, Wu S, Lang R, Iredale JP. Selective depletion of macrophages reveals distinct, opposing roles during liver injury and repair. *J Clin Invest* 2005; 115:56-65.
51. Meijer C, Wiezer MJ, Diehl AM, Schouten HJ, Meijer S, van Rooijen N, van Lambalgen AA, Dijkstra CD, van Leeuwen PA. Kupffer cell depletion by CI2MDP-liposomes alters hepatic cytokine expression and delays liver regeneration after partial hepatectomy. *Liver* 2000; 20:66-77.
52. Starzl TE, Fung J, Tzakis A, Todo S, Demetris AJ, Marino IR, Doyle H, Zeevi A, Warty V, Michaels M, et al. Baboon-to-human liver transplantation. *Lancet* 1993; 341:65-71.
53. Wymann MP, Pirola L. Structure and function of phosphoinositide 3-kinases. *Biochim Biophys Acta* 1998; 1436:127-150.
54. Kaplan DR, Whitman M, Schaffhausen B, Pallas DC, White M, Cantley L, Roberts TM. Common elements in growth factor stimulation and oncogenic transformation: 85 kd phosphoprotein and phosphatidylinositol kinase activity. *Cell* 1987; 50:1021-1029.
55. Traynor-Kaplan AE, Harris AL, Thompson BL, Taylor P, Sklar LA. An inositol tetrakisphosphate-containing phospholipid in activated neutrophils. *Nature* 1988; 334:353-356.
56. Whitman M, Downes CP, Keeler M, Keller T, Cantley L. Type I phosphatidylinositol kinase makes a novel inositol phospholipid, phosphatidylinositol-3-phosphate. *Nature* 1988; 332:644-646.
57. Auger KR, Serunian LA, Soltoff SP, Libby P, Cantley LC. PDGF-dependent tyrosine phosphorylation stimulates production of novel polyphosphoinositides in intact cells. *Cell* 1989; 57:167-175.

58. Fukui Y, Hanafusa H. Phosphatidylinositol kinase activity associates with viral p60src protein. *Mol Cell Biol* 1989; 9:1651-1658.
59. Escobedo JA, Navankasattusas S, Kavanaugh WM, Milfay D, Fried VA, Williams LT. cDNA cloning of a novel 85 kd protein that has SH2 domains and regulates binding of PI3-kinase to the PDGF beta-receptor. *Cell* 1991; 65:75-82.
60. Skolnik EY, Margolis B, Mohammadi M, Lowenstein E, Fischer R, Drepps A, Ullrich A, Schlessinger J. Cloning of PI3 kinase-associated p85 utilizing a novel method for expression/cloning of target proteins for receptor tyrosine kinases. *Cell* 1991; 65:83-90.
61. Hiles ID, Otsu M, Volinia S, Fry MJ, Gout I, Dhand R, Panayotou G, Ruiz-Larrea F, Thompson A, Totty NF, et al. Phosphatidylinositol 3-kinase: structure and expression of the 110 kd catalytic subunit. *Cell* 1992; 70:419-429.
62. Hawkins PT, Anderson KE, Davidson K, Stephens LR. Signalling through Class I PI3Ks in mammalian cells. *Biochem Soc Trans* 2006; 34:647-662.
63. Amzel LM, Huang CH, Mandelker D, Lengauer C, Gabelli SB, Vogelstein B. Structural comparisons of class I phosphoinositide 3-kinases. *Nat Rev Cancer* 2008; 9:665-669.
64. Marone R, Cmiljanovic V, Giese B, Wymann MP. Targeting phosphoinositide 3-kinase: moving towards therapy. *Biochim Biophys Acta* 2008; 1784:159-185.
65. Osawa Y, Banno Y, Nagaki M, Brenner DA, Naiki T, Nozawa Y, Nakashima S, Moriwaki H. TNF-alpha-induced sphingosine 1-phosphate inhibits apoptosis through a phosphatidylinositol 3-kinase/Akt pathway in human hepatocytes. *J Immunol* 2001; 167:173-180.
66. Puri KD, Doggett TA, Huang CY, Douangpanya J, Hayflick JS, Turner M, Penninger J, Diacovo TG. The role of endothelial PI3Kgamma activity in neutrophil trafficking. *Blood* 2005; 106:150-157.

67. Desmots F, Rissel M, Gilot D, Lagadic-Gossmann D, Morel F, Guguen-Guillouzo C, Guillouzo A, Loyer P. Pro-inflammatory cytokines tumor necrosis factor alpha and interleukin-6 and survival factor epidermal growth factor positively regulate the murine GSTA4 enzyme in hepatocytes. *J Biol Chem* 2002; 277:17892-17900.
68. Okano J, Shiota G, Matsumoto K, Yasui S, Kurimasa A, Hisatome I, Steinberg P, Murawaki Y. Hepatocyte growth factor exerts a proliferative effect on oval cells through the PI3K/AKT signaling pathway. *Biochem Biophys Res Commun* 2003; 309:298-304.
69. Munugalavadla V, Borneo J, Ingram DA, Kapur R. p85alpha subunit of class IA PI-3 kinase is crucial for macrophage growth and migration. *Blood* 2005; 106:103-109.
70. Sheng H, Shao J, Townsend CM, Jr., Evers BM. Phosphatidylinositol 3-kinase mediates proliferative signals in intestinal epithelial cells. *Gut* 2003; 52:1472-1478.
71. Cantley LC. The phosphoinositide 3-kinase pathway. *Science* 2002; 296:1655-1657.
72. Watanabe H, Saito H, Rychahou PG, Uchida T, Evers BM. Aging is associated with decreased pancreatic acinar cell regeneration and phosphatidylinositol 3-kinase/Akt activation. *Gastroenterology* 2005; 128:1391-1404.
73. Vanhaesebroeck B, Jones GE, Allen WE, Zicha D, Hooshmand-Rad R, Sawyer C, Wells C, Waterfield MD, Ridley AJ. Distinct PI(3)Ks mediate mitogenic signalling and cell migration in macrophages. *Nat Cell Biol* 1999; 1:69-71.
74. Donahue AC, Hess KL, Ng KL, Fruman DA. Altered splenic B cell subset development in mice lacking phosphoinositide 3-kinase p85alpha. *Int Immunol* 2004; 16:1789-1798.
75. Sugatani T, Hruska KA. Akt1/Akt2 and mammalian target of rapamycin/Bim play critical roles in osteoclast differentiation and survival, respectively, whereas Akt is dispensable for cell survival in isolated osteoclast precursors. *J Biol Chem* 2005; 280:3583-3589.

76. Ihara-Watanabe M, Uchihashi T, Miyauchi Y, Sakai N, Yamagata M, Ozono K, Michigami T. Involvement of phosphoinositide 3-kinase signaling pathway in chondrocytic differentiation of ATDC5 cells: application of a gene-trap mutagenesis. *J Cell Biochem* 2004; 93:418-426.
77. Magun R, Burgering BM, Coffey PJ, Pardasani D, Lin Y, Chabot J, Sorisky A. Expression of a constitutively activated form of protein kinase B (c-Akt) in 3T3-L1 preadipose cells causes spontaneous differentiation. *Endocrinology* 1996; 137:3590-3593.
78. Watanabe H, Saito H, Ueda J, Evers BM. Regulation of pancreatic duct cell differentiation by phosphatidylinositol-3 kinase. *Biochem Biophys Res Commun* 2008; 370:33-37.
79. Wang Q, Li N, Wang X, Kim MM, Evers BM. Augmentation of sodium butyrate-induced apoptosis by phosphatidylinositol 3'-kinase inhibition in the KM20 human colon cancer cell line. *Clin Cancer Res* 2002; 8:1940-1947.
80. Park BK, Zeng X, Glazer RI. Akt1 induces extracellular matrix invasion and matrix metalloproteinase-2 activity in mouse mammary epithelial cells. *Cancer Res* 2001; 61:7647-7653.
81. Ha HY, Moon HB, Nam MS, Lee JW, Ryoo ZY, Lee TH, Lee KK, So BJ, Sato H, Seiki M, et al. Overexpression of membrane-type matrix metalloproteinase-1 gene induces mammary gland abnormalities and adenocarcinoma in transgenic mice. *Cancer Res* 2001; 61:984-990.
82. Nagakawa O, Murakami K, Yamaura T, Fujiuchi Y, Murata J, Fuse H, Saiki I. Expression of membrane-type 1 matrix metalloproteinase (MT1-MMP) on prostate cancer cell lines. *Cancer Lett* 2000; 155:173-179.
83. Zhang D, Brodt P. Type 1 insulin-like growth factor regulates MT1-MMP synthesis and tumor invasion via PI 3-kinase/Akt signaling. *Oncogene* 2003; 22:974-982.

84. Ridley AJ, Schwartz MA, Burridge K, Firtel RA, Ginsberg MH, Borisy G, Parsons JT, Horwitz AR. Cell migration: integrating signals from front to back. *Science* 2003; 302:1704-1709.
85. Chung CY, Potikyan G, Firtel RA. Control of cell polarity and chemotaxis by Akt/PKB and PI3 kinase through the regulation of PAKa. *Mol Cell* 2001; 141: 5:937-947.
86. Merlot S, Firtel RA. Leading the way: Directional sensing through phosphatidylinositol 3-kinase and other signaling pathways. *J Cell Sci* 2003; 116:3471-3478.
87. Ueki K, Fruman DA, Yballe CM, Fasshauer M, Klein J, Asano T, Cantley LC, Kahn CR. Positive and negative roles of p85 alpha and p85 beta regulatory subunits of phosphoinositide 3-kinase in insulin signaling. *J Biol Chem* 2003; 278:48453-48466.
88. Withers DJ, White M. Perspective: The insulin signaling system--a common link in the pathogenesis of type 2 diabetes. *Endocrinology* 2000; 141:1917-1921.
89. Koyasu S. The role of PI3K in immune cells. *Nat Immunol* 2003; 4:313-319.
90. Sakai K, Suzuki H, Oda H, Akaike T, Azuma Y, Murakami T, Sugi K, Ito T, Ichinose H, Koyasu S, et al. Phosphoinositide 3-kinase in nitric oxide synthesis in macrophage: critical dimerization of inducible nitric-oxide synthase. *J Biol Chem* 2006; 281:17736-17742.
91. Suzuki M, Satoh A, Ide H, Tamura K. Transgenic *Xenopus* with prx1 limb enhancer reveals crucial contribution of MEK/ERK and PI3K/AKT pathways in blastema formation during limb regeneration. *Dev Biol* 2007; 304:675-686.
92. Kanayama M, Takahara T, Yata Y, Xue F, Shinno E, Nonome K, Kudo H, Kawai K, Kudo T, Tabuchi Y, et al. Hepatocyte growth factor promotes colonic epithelial regeneration via Akt signaling. *Am J Physiol Gastrointest Liver Physiol* 2007; 293:G230-239.

93. Eickholt BJ, Ahmed AI, Davies M, Papakonstanti EA, Pearce W, Starkey ML, Bilancio A, Need AC, Smith AJ, Hall SM, et al. Control of axonal growth and regeneration of sensory neurons by the p110delta PI 3-kinase. *PLoS ONE* 2007; 2:e869.
94. Tetreault MP, Chailier P, Beaulieu JF, Rivard N, Menard D. Epidermal growth factor receptor-dependent PI3K-activation promotes restitution of wounded human gastric epithelial monolayers. *J Cell Physiol* 2008; 214:545-557.
95. Pankow S, Bamberger C, Klippel A, Werner S. Regulation of epidermal homeostasis and repair by phosphoinositide 3-kinase. *J Cell Sci* 2006; 119:4033-4046.
96. El-Assal ON, Besner GE. HB-EGF enhances restitution after intestinal ischemia/reperfusion via PI3K/Akt and MEK/ERK1/2 activation. *Gastroenterology* 2005; 129:609-625.
97. Haga S, Ogawa W, Inoue H, Terui K, Ogino T, Igarashi R, Takeda K, Akira S, Enosawa S, Furukawa H, et al. Compensatory recovery of liver mass by Akt-mediated hepatocellular hypertrophy in liver-specific STAT3-deficient mice. *J Hepatol* 2005; 43:799-807.
98. Hausenloy DJ, Yellon DM. Survival kinases in ischemic preconditioning and postconditioning. *Cardiovasc Res* 2006; 70:240-253.
99. Miyashita K, Itoh H, Sawada N, Fukunaga Y, Sone M, Yamahara K, Yurugi-Kobayashi T, Park K, Nakao K. Adrenomedullin provokes endothelial Akt activation and promotes vascular regeneration both in vitro and in vivo. *FEBS Lett* 2003; 544:86-92.
100. Higgins G, Anderson R. Experimental pathology of the liver: restoration of liver of the white rat following partial surgical removal. *Arch Path* 1931; 365:179-183.
101. Ueda J, Saito H, Watanabe H, Evers BM. Novel and quantitative DNA dot-blotting method for assessment of in vivo proliferation. *Am J Physiol Gastrointest Liver Physiol* 2005; 288:G842-847.

102. Rychahou PG, Jackson LN, Silva SR, Rajaraman S, Evers BM. Targeted molecular therapy of the PI3K pathway: therapeutic significance of PI3K subunit targeting in colorectal carcinoma. *Ann Surg* 2006; 243:833-842; discussion 843-834.
103. Larson SD, Jackson LN, Riall TS, Uchida T, Thomas RP, Qiu S, Evers BM. Increased incidence of well-differentiated thyroid cancer associated with Hashimoto thyroiditis and the role of the PI3k/Akt pathway. *J Am Coll Surg* 2007; 204:764-773; discussion 773-765.
104. Jackson LN, Li J, Chen LA, Townsend CM, Evers BM. Overexpression of wild-type PKD2 leads to increased proliferation and invasion of BON endocrine cells. *Biochem Biophys Res Commun* 2006; 348:945-949.
105. Jackson LN, Larson SD, Silva SR, Rychahou PG, Chen LA, Qiu S, Rajaraman S, Evers BM. PI3K/Akt activation is critical for early hepatic regeneration after partial hepatectomy. *Am J Physiol Gastrointest Liver Physiol* 2008; 294:G1401-1410.
106. Mitchell KA, Lockhart CA, Huang G, Elferink CJ. Sustained aryl hydrocarbon receptor activity attenuates liver regeneration. *Mol Pharmacol* 2006; 70:163-170.
107. Camps M, Ruckle T, Ji H, Ardisson V, Rintelen F, Shaw J, Ferrandi C, Chabert C, Gillieron C, Francon B, et al. Blockade of PI3Kgamma suppresses joint inflammation and damage in mouse models of rheumatoid arthritis. *Nat Med* 2005; 11:936-943.
108. Folli F, Alvaro D, Gigliozzi A, Bassotti C, Kahn CR, Pontiroli AE, Capocaccia L, Jezequel AM, Benedetti A. Regulation of endocytic-transcytotic pathways and bile secretion by phosphatidylinositol 3-kinase in rats. *Gastroenterology* 1997; 113:954-965.
109. Muller C, Dunschede F, Koch E, Vollmar AM, Kiemer AK. Alpha-lipoic acid preconditioning reduces ischemia-reperfusion injury of the rat liver via the PI3-kinase/Akt pathway. *Am J Physiol Gastrointest Liver Physiol* 2003; 285:G769-778.

110. Bradley EA, Clark MG, Rattigan S. Acute effects of wortmannin on insulin's hemodynamic and metabolic actions in vivo. *Am J Physiol Endocrinol Metab* 2007; 292:E779-787.
111. Diehl A. The role of cytokines in hepatic regeneration. *Curr Opin Gastro* 1997; 13:525-533.
112. Munugalavadla V, Borneo J, Ingram D, Kapur R. p85a subunit of class IA PI-3 kinase is crucial for macrophage growth and migration. *Blood* 2005; 106:103-109.
113. Fruman DA, Mauvais-Jarvis F, Pollard DA, Yballe CM, Brazil D, Bronson RT, Kahn CR, Cantley LC. Hypoglycaemia, liver necrosis and perinatal death in mice lacking all isoforms of phosphoinositide 3-kinase p85 alpha. *Nat Genet* 2000; 26:379-382.
114. Matalka KZ, Tutunji MF, Abu-Baker M, Abu Baker Y. Measurement of protein cytokines in tissue extracts by enzyme-linked immunosorbent assays: application to lipopolysaccharide-induced differential milieu of cytokines. *Neuro Endocrinol Lett* 2005; 26:231-236.
115. Rosengren S, Firestein GS, Boyle DL. Measurement of inflammatory biomarkers in synovial tissue extracts by enzyme-linked immunosorbent assay. *Clin Diagn Lab Immunol* 2003; 10:1002-1010.
116. Larson S, Jackson L, Chen L, Rychahou P, Evers B. Effectiveness of siRNA uptake in target tissues by various delivery methods. *Surgery* 2007; 142:262-269.
117. Martinet W, De Meyer GR, Andries L, Herman AG, Kockx MM. In situ detection of starvation-induced autophagy. *J Histochem Cytochem* 2006; 54:85-96.
118. Watanabe K, Ishidoh K, Ueno T, Sato N, Kominami E. Suppression of lysosomal proteolysis at three different steps in regenerating rat liver. *J Biochem (Tokyo)* 1998; 124:947-956.

119. Meijer C, Wiezer MJ, Diehl AM, Schouten HJ, Schouten HJ, Meijer S, van Rooijen N, van Lambalgen AA, Dijkstra CD, van Leeuwen PA. Kupffer cell depletion by CI2MDP-liposomes alters hepatic cytokine expression and delays liver regeneration after partial hepatectomy. *Liver* 2000; 20:66-77.
120. Arcaro A, Wymann MP. Wortmannin is a potent phosphatidylinositol 3-kinase inhibitor: the role of phosphatidylinositol 3,4,5-trisphosphate in neutrophil responses. *Biochem J* 1993; 296:297-301.
121. Wang Z, Wilson WA, Fujino MA, Roach PJ. Antagonistic controls of autophagy and glycogen accumulation by Snf1p, the yeast homolog of AMP-activated protein kinase, and the cyclin-dependent kinase Pho85p. *Mol Cell Biol* 2001; 21:5742-5752.
122. Kotoulas OB, Kalamidas SA, Kondomerkos DJ. Glycogen autophagy. *Microsc Res Tech* 2004; 64:10-20.

VITA

Lindsey Nicole Herman was born on May 13, 1976 in Greenville, TX, to Michael and Mary J. Herman. She was married on May 13, 2001 to James M. Jackson and changed her name to Lindsey Nicole Jackson at that time. After graduating third in her class from Wylie High School in Wylie, TX in 1994, Lindsey attended college at Texas A&M University in College Station, TX and graduated magna cum laude as a biotechnology major with a minor in English in 1998. She worked as a technical illustrator, tutor, and research technician throughout college; she was nominated to the Texas Guild of Pianists and enjoyed the arts, music, hockey, camping, and other outdoor activities while at Texas A&M.

Following college, Lindsey attended medical school at UT Southwestern Medical School in Dallas, TX. During medical school, Lindsey developed an interest in surgery and surgical oncology and held several research positions in physiology and biomedical engineering laboratories. After graduating magna cum laude at the top of her class in 2003, Lindsey began her general surgical training at the University of Texas Medical Branch in Galveston, TX. Following her intern year, Lindsey was accepted as a research fellow in gastrointestinal physiology working under the guidance of Dr. B. Mark Evers. She was awarded the Jeane B. Kempner Postdoctoral Scholar Award in 2005 in support of her studies on the role of the phosphatidylinositol 3-kinase (PI3K) pathway in colonic inflammation and carcinogenesis, and received the American College of Surgeons (ACS) Resident Excellence in Research Award 2005. She earned a Masters of Medical Science degree in December of 2006 following publication of her research article, "Targeted molecular therapy of the PI3K pathway: Therapeutic significance of PI3K subunit targeting in colorectal carcinoma" in the *Annals of Surgery* in June 2006. Additional honors included second place, Singleton Surgical Society, basic science research 2006; Houston Surgical Society Excellence in Research Award 2006; first place, Singleton Surgical Society, basic science research 2007; and the Society of University Surgeons (SUS) Excellence in Resident Research travel award February 2007.

Lindsey and Jimmy became parents to triplet girls on March 26, 2007, and Lindsey returned to clinical service in July of 2007. She was nominated to receive the Gold Foundation's Humanism and Excellence in Teaching Award in July 2008. Lindsey returned to the laboratory of Dr. B. Mark Evers in July 2008 to complete work that will culminate in this thesis and plans to return to clinical service in July 2009 for completion of her general surgical residency. She plans for a career in academic general surgery with an emphasis on surgical oncology.

Education

B.S., May 1998, Texas A&M University, College Station, Texas
M.D., May 2003, University of Texas Southwestern Medical School, Dallas, Texas
M.M.S., December 2006, University of Texas Medical Branch, Galveston, Texas

Publications

1. Jackson LN, Larson SD, Silva SR, Rajaraman R, Evers BM. PI3K/AKT activation is critical for hepatic regeneration after partial hepatectomy. *Am J Physiol Gastrointest Liver Physiol* (2008), Epub ahead of print.
2. Jackson LN, Wang QD, Zhou Y, Qiu S, Evers BM. Alternative medicine products as a novel treatment strategy for inflammatory bowel disease. *Am J Chinese Med* (in press).
3. Liu H, Weiss HL, Rychahou PG, Jackson LJ, Evers BM, Gao T. Loss of PHLPP expression in colon cancer: Role in proliferation and tumorigenesis *Cancer Res* (submitted 4/4/08).
4. Jackson LN, Chen LA, Larson SD, Rychahou PG, Boor P, Li J, DeFreitas G, Townsend CM, Evers BM. Development and characterization of a novel in vivo model of carcinoid syndrome. *Cancer Res* (submitted 8/2008).
5. Jackson LN, Li J, Chen LA, Townsend CM, Evers BM. Overexpression of Wild-Type PKD2 leads to increased proliferation and invasion of BON endocrine cells. *Biochem Biophys Res Comm* **348** (2006): 945-949.
6. Rychahou PG, Jackson LN (co-first authorship), Rajaraman S, Evers BM. Targeted molecular therapy of the PI3K pathway: Therapeutic significance of PI3K subunit downregulation in colorectal carcinoma, *Ann Surg* **243** (2006): 833-844.
7. Rychahou PG, Jackson LN, Evers BM. RNA interference: Mechanisms of Action and Therapeutic Consideration. *Surgery* **140** (2006), 719-25.
8. Larson SD, Jackson LN, Riall TS, Uchida T, Thomas RP, Qiu S, Evers BM. Increased incidence of well-differentiated thyroid cancer associated with Hashimoto thyroiditis and the role of the PI3k/Akt pathway. *J Am Coll Surg* **204** (2007), p. 764-73.
9. Larson SD, Jackson LN, Rychahou PG, Chen AL, Evers BM. Effectiveness of siRNA uptake in target tissues by various delivery methods. *Surgery* **293** (2007), G1262-71.
10. Jackson LN, Evers BM. Chapter 2—Chronic inflammation and pathogenesis of GI and pancreatic cancers. *Cancer Treatment and Research Series: The Link Between Inflammation and Cancer*, Angus G. Dalgleish and Burkhard Haefner, Springer, 2005.
11. Jackson LN, Evers BM. Chapter 80—Gastrointestinal lymphomas. *Shackelford's Surgery of the Alimentary Tract*, 5th edition, Richard T. Shackelford and George D. Zuidema, WB Saunders Co, 2007.
12. Jackson LN, Evers BM. Small bowel carcinoid tumors. *Current Surgical Therapy*, 9th edition, John L. Cameron, CV Mosby, 2007.

13. Murillo CA, Woodside KJ, Jackson LN, Evers BM. Neoplastic disorders of the gastrointestinal tract. *Modern Surgical Care: Physiologic Foundations and Clinical Applications*, 3rd Edition, Thomas Miller, Marcel Dekker Inc, New York, NY, *in press*

Accepted Abstracts:

1. Jackson LN, Evers BM. The role of PI3K activation in hepatic regeneration. Singleton Surgical Society, oral presentation, May 2005.
2. Jackson LN, Rychahou PG, Evers BM. Targeted RNA interference of PI3K pathway components confers survival benefit in a mouse model of inflammatory bowel disease. American College of Surgeons Surgical Forum, oral presentation, won Excellence in Research Award for GI tract research, October 2005.
3. Rychahou PG, Jackson LN, (co-first authorship), Evers BM. Targeted molecular therapy of the PI3K pathway: Therapeutic significance of PI3K subunit downregulation in colorectal carcinoma. Southern Surgical Association, oral presentation, December 2005.
4. Jackson LN, Rychahou PG, Silva SR, Evers BM. The role of PI3K in colonic inflammation. McLaughlin Colloquium, poster presentation, January 2006.
5. Jackson LN, Larson SD, Chen A, Silva SR, Ueda J, Evers BM. PI3K/Akt activation is critical for hepatic regeneration following partial hepatectomy. Society of University Surgeons, Academic Surgical Congress, poster presentation, February 2006.
6. Rychahou PG, Jackson LN, Evers BM. RNAi directed to the PI3K p85 α subunit attenuates inflammatory changes associated with DSS-induced colitis. Society of University Surgeons, Academic Surgical Congress, oral presentation, February 2006.
7. Jackson LN, Li J, Chen A, Townsend CM, Evers BM. Overexpression of wild-type PKD2 leads to increased proliferation and invasion of BON endocrine cells. American Gastroenterology Association, Digestive Disease Week, May 2006.
8. Jackson LN, Rychahou PG, Silva SR, Evers BM. Differential Effects of Selective or Complete PI3K Inhibition in a Murine Inflammatory Bowel Disease Model. American Gastroenterology Association, Digestive Disease Week, May 2006.
9. Jackson LN, Larson SD, Silva SR, Ueda J, Chen A, Evers BM. siRNA interference of the PI3K/Akt pathway leads to decreased regeneration following 70% partial hepatectomy in mice. American College of Surgeons, November 2006.
10. Jackson LN, Larson SD, Chen A, Rychahou PG, Silva SR, Ueda J, Evers BM. PI3K activation is critical for hepatic regeneration following hepatectomy. Society of University Surgeons, Academic Surgical Congress, oral presentation, plenary session, February 2006.

11. Jackson LN, Chen A, Larson SD, Rychahou PG, Silva SR, Boor P, Evers BM. Development of a novel in vivo model of carcinoid syndrome. American Gastroenterology Association, Digestive Disease Week, oral presentation, May 2007.
12. Jackson LN, Larson SD, Chen A, Rychahou PG, Silva SR, Ueda J, Evers BM. PI3K activation is critical for hepatic regeneration following hepatectomy. SARS, Birmingham, England, oral presentation, presented by invitation of SUS with travel award, January 2008.

Summary of Dissertation

Hepatic resection is associated with rapid proliferation and regeneration of the remnant liver. Phosphatidylinositol 3-kinase (PI3K), composed of a p85 α regulatory and a p110 α catalytic subunit, participates in multiple cellular processes, including cell growth and survival; however, the role of PI3K in liver regeneration has not been clearly delineated. In these studies, we used the potent PI3K inhibitor, wortmannin, and small-interfering RNA (siRNA) targeting the p85 α and p110 α subunits to determine if total or selective PI3K inhibition would abrogate the proliferative response of the liver following resection. After partial hepatectomy in mice, there is an increase in PI3K activity; total PI3K blockade with wortmannin, and selective inhibition of p85 α or p110 α with siRNA resulted in a significant decrease in hepatocyte proliferation, especially at the earliest timepoints (ie, 48h and 72h). Fewer macrophages and Kupffer cells were present in the regenerating liver of mice treated with wortmannin or siRNA to p85 α or p110 α , as reflected by a paucity of F4/80+ cells present by immunohistochemistry (IHC). Additionally, PI3K inhibition led to an aberrant hepatocyte architecture characterized by vacuolization, lipid deposition, and glycogen accumulation. Our data demonstrate that PI3K/Akt pathway activation plays a critical role in the early regenerative response of the liver after resection; inhibition of this pathway markedly abrogates the normal hepatic regenerative response, perhaps by inhibiting macrophage infiltration and cytokine elaboration and thus hepatocyte priming for replication.

Permanent address: 318 Winding Oak Lane South
League City, TX 77573

This dissertation was typed by Lindsey N. Jackson, M.D., with manuscript preparation assistance by Karen K. Martin.